M.J. de Hoon

Air Tightness

Predicting the performance of a building envelope

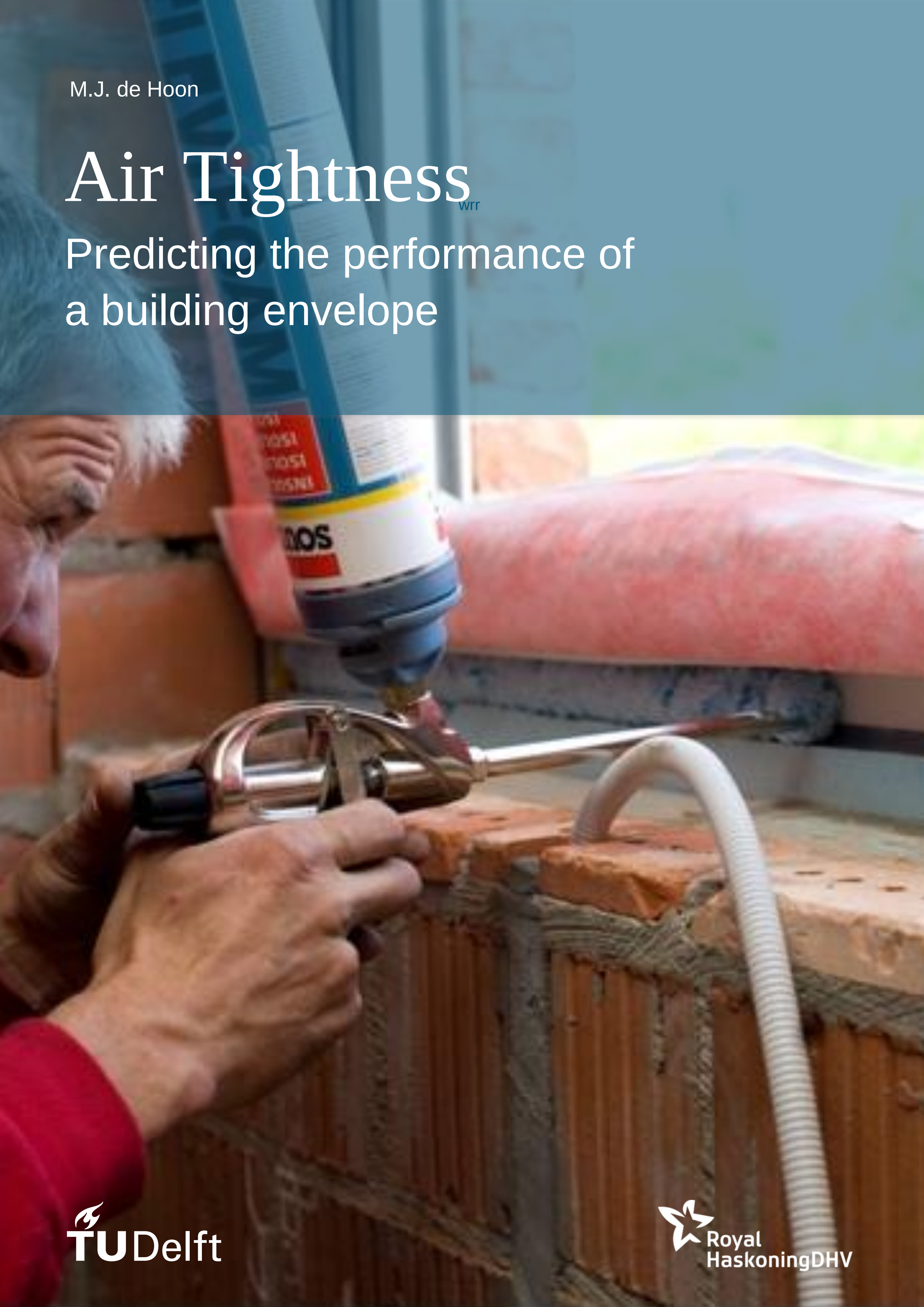

TU Delft

Royal HaskoningDHV

Technische Universiteit Delft

Air Tightness

Predicting the performance of a building envelope

By: Maartje de Hoon
Number: 1302922

Thesis: In partial fulfilment of the requirements for the degree of Master of Science at Delft University of Technology
Faculty: Civil Engineering
Track: Building Engineering
Specialisation: Building Technology & Physics

To be defended publicly on Friday November 25, 2016 at 4:00 PM

Supervisor: Prof. ir. P. G. Luscuere
Committee: Dr. ir. P. van den Engel
Dr.ir. H.R. Schipper
Ing. E. Smits
Company: Royal HaskoningDHV
Larixplein 1
Eindhoven

An electronic version of this thesis is available at http://repository.tudelft.nl/

Technische Universiteit Delft

Preface

While finishing my bachelor at the Faculty of Architecture, I realized that I wanted to develop more knowledge on the technical aspects of the building design. That is why I made the transition to the Faculty of Civil Engineering. Throughout my Master Degree course, I specialized in Building Physics. My interest mainly focuses on the integration of design and technology and on solving problems that arise during construction or commissioning of a building.
Since 2009 in addition to my studies, I am working for “Meetbureau Bijleveld” (MbB), where I gained a lot of knowledge on the air permeability of buildings. Within MbB we work according to the ASTM standard E799 "Standard Test Method for Determining Air Leakage Rate by Fan pressurization", in order to test the air permeability of rooms that are fire protected with an oxygen displacement gas.
For my Master’s thesis I hoped to apply the knowledge that I gained on air permeability in a, for me, new perspective. Through Peter Luscuere, professor at TU Delft, I got in contact with Royal HaskoningDHV. They were interested in this topic because of their involvement in the design and realization of cleanrooms and other spaces with a controlled atmosphere. Less air leakage means less necessary air flow and thus lowers the investment and operational costs for the air conditioning systems.

Based on my experiences within MbB, the available calculation values for the flow characteristics, specifically the flow exponent most guidelines are based on, seems to be too optimistic. Since no exact data is available on the air permeability in practice, I will use my Master’s thesis to deepen my knowledge on this topic. I will try to find out which factors are important during the design, to make a realistic assessment of the expected air leakage of a building envelope.

After nine intensive, but most of all interesting months, I can finally wind-up tis thesis. I could not have reached the results without the assistance and support of many persons and companies, which I hereby would like to give an acknowledgement.
First of all I would like to thank Ko Bijleveld, my tutor in the field of air tightness, always willing to give a detailed explanation. He has been a great example to leave nothing unexplained and to keep exploring until observations can be logical founded. Also he has been a great sponsor for my thesis by providing the necessary equipment needed for my experiments. For that purpose I would also like to thank Niek-Jan Bink of Acin Instruments, for visiting my measurement setup with his FlowFinder to provide in a validation method for my measurements.
Furthermore thanks is given to Harry Nieman, Philip Dobbels en Hans Phaff for their personal time to discuss my thesis and the extra information they provided. To Henry den Bok for his support during the execution of my measurements. To Erwin Smits for his personal guidance within RHDHV and his interest in my thesis, while he had never heard of the topic prior to my arrival and to Vivian Timmermans for sharing her insights and experiences on the subject and her critical questions on my findings and conclusions.
Thanks to the commitment of my graduation committee it became possible to dedicate my Master’s thesis to air tightness concerns, a topic that has is rarely discussed within the context of my education, but which has a strong personal interest for me.
Lastly off course I could not have accomplished finishing my Master’s degree without my friends and family, who kept supporting me even during the times I lost my focus and needed help to get back on track. Hopefully you are as proud of the end result as I do!

M.J. de Hoon
Eindhoven, November 2016

Technische Universiteit Delft

Abstract

In the field of building physics the performance of the building envelope is a highly studied topic. Heat, light, sound and humidity are common topics to include in design requirements. Air tightness is becoming increasingly common in this list, but it still lacks for detailed information on performance requirements or calculation methods.
When communicating on air tightness, a large variability in units is used. Flow rates are expressed in liters or cubic meters, per second or per hour. Reference pressure ranges from 4 to 50 Pa or higher and for some regulations a correction to building volume is applied. Lastly there are some publications that provide in air tightness coefficients for common building joints, to calculate on expected flow losses. These coefficients are given per meter, square meter, or per product. No wonder engineers get lost when working on this subject.
This Master's thesis is intended to draft a uniform calculation method for determination of the air permeability in the design phase of a building.

Next to providing in an overview of the above mentioned standards and regulations, research has been performed on calculation methods that are currently used for determination of air tightness. These can be identified as the power law ($q_v = C \cdot \Delta P^n$) which is most common in practice, the quadratic formula ($\Delta P = AQ + BQ^2$) and formulas which determine the volumetric air flow by geometric proportions of the opening, using the Reynolds number and loss coefficients analogue with ducts and material properties of air.

The literature study showed that most documents in use are based on the power law formula, using a standard value for the flow exponent originating from an old dataset, whose collector did not mean to provide in a mean value. The flow exponent is an indication for the development of turbulent or laminar flow and has a great influence on the calculated volumetric air flow when using the power law. In order to test this standard value and to gain more insight in the development of turbulence through openings, a measurement setup is made. Different shaped openings, cross sections, diameters and flow lengths have been tested. Unfortunately the equipment used appeared to be insufficiently precise. Therefor the absolute values of the results cannot be used to base any sounds conclusions on, but some trends have been made visible. Most importantly it is proven that the assumed standard value for the flow exponent is too high and extrapolation of air tightness data outside of the measured range induces large deviations from real occurring flows.

Lastly the influence of edge effects on the measurements is tested by the use of a numerical model using CFD. Due to difficulties with the mesh that could not be resolved within the program available, the absolute values of these results are questionable too, but it is shown that the effect of sharp edges cannot be ignored. Therefor the results of the physical measurements cannot be corrected with this model to base conclusions on the geometries tested.

Table of Contents

Technische Universiteit Delft

1 Framework

1.1 Introduction

1.1.1 Air tightness of the building envelope

The indoor environment is a well-studied topic within building physics. The avoidance of moisture penetration, thermal and acoustic comfort and complaints with respect to the indoor qualities set requirements for the building envelope. The quality of this envelope as a whole and of construction components in particular is increasingly specified in documentation and certificates. Simultaneously tightening of requirements such as the energy performance coefficient (EPC) and the development of the Passive house leads to higher demands of the envelope.
Good ventilation is required based on health and comfort for the users and energy efficiency. Sufficient air change rate can reduce energy demands for heating or cooling, while maintaining the indoor air quality, loss of air due to unexpected leakage points may result in poor building performance which is only revealed when construction has been finished. During the design phase a correct computer model or calculation method to asses these air flow could prevent this. This Master's thesis is intended to better assess these losses in the early design phase.

1.1.2 Nature and relevance

When air unwantedly flows from outside of an envelope to the inside, this is called infiltration. Exfiltration is meant when air undesirably escapes. By building airtight, this uncontrolled air flow can be prevented. In practice, due to movable components, connections and ducts, it is never possible to build completely airtight. That is why air permeability would be a better formulation of the subject.

Nature
Low air permeability has many advantages, but in itself is not (yet) an objective in the design of a building. However other perspectives with demands can indirectly have low air permeability as a requirement. These demands can be categorised as follows:

- Building Physical reasons
  The Dutch Building regulation (Bouwbesluit) lays down requirements for the maximum infiltration in rooms, in order to guarantee a healthy indoor air quality. In the European directive "Energy Performance of Buildings Directive" (EPBD) energy labels are provided, which are based on a calculation method for energy performance that can be used for both existing buildings and new constructions. Regulations for new constructions are in line with the Energy Performance Coefficient (EPC) (NEN 7120 + C2 2012). The air permeability from this perspective is often referred to as q_{v10}, which is a characteristic value for the volumetric flow (q_v) that occurs through the cracks and seams of the envelope, at a pressure difference of 10 Pascal.
- Energy management
  Starting point in the calculation of mechanical and balanced ventilation is the volume of the rooms to be treated. This volume, combined with the desired (often by legislation imposed) ventilation rate determines necessary flow rate of the air conditioning installations. Loss of heated/cooled air means loss of energy. The losses through the envelope (the air permeability) are represented as standard values. After completion, through an air permeability test, one may examine whether the space (and therefore the installation) complies with the principles set out in the design.
- Rooms with a controlled atmosphere
  One may think of a cleanroom or isolation room. Such areas are often built for medical, technical or chemical sensitive activities. There is a strict boundary between the controlled atmosphere and its surroundings. A pressure difference is maintained with their surroundings, in order to keep harmful

substances in (under pressure), or pollution out (over pressure). The conditioning of air in these areas is much more intensive and therefore more expensive, than for example, a residence or office. The above-mentioned argument of energy loss for this kind of spaces is therefore even more important.

- Leakage from crawl space (radon gas)
  The flow of air through leaks in the partition between the crawl space and the residential part of a dwelling carries water vapour with it, coming from the crawl space. When there is a stone underground, this water vapour is often contaminated with harmful substances such as radon gas. To minimize the supply of this unwanted water vapour to the residential area the Dutch building regulation (Bouwbesluit) sets a limit to this leakage. A structure that separates a residential area, a toilet or a bath room from a crawl space should hold a maximum air flow of up to $20 \cdot 10^{-6}$ $m^3/(m^2.s)$.
- Pollutant gasses and particulate matter (PM)
  For the limitation of pollutant gas concentrations such as NO_x, CO_2 and $PM_{2.5}$ in indoor air there are regulations that prescribe the air exchange rate. Indoor air pollution associated with combustion (smoke in particular) has a long history. CO, CO_2, NO_x and SO_2 which are easily measured have received the most attention (Godish 1989).
  Despite people spend on average 80% of their time indoors, a publication of the Worlds Health Organization (WHO) showed that there are no legal limits established for the indoor concentration of fine particles. Since there is no evidence that the origin of indoor particulate matter differs from that of fine dust in the outdoors, the WHO concludes that the guidelines they set in 2005 for air quality can also be applied to the indoor climate (WHO 2010). Recent studies by TNO have shown that ventilation rate, air permeability and filter quality of the air conditioning system are indicative factors for the PM2.5 concentration in offices and schools. Since such buildings have relatively low ventilation rates, improvement of the air permeability will have a great impact on air quality (Jacobs and Borsboom 2015).
- Acoustics
  Noise pollution is a major factor in the comfort of a building. The soundproofing of frames and rotating parts in the façade is crucial to the final sound insulation of a building. The dimensions of slits and holes, along with the frequency of the sound, will have great effect on the sound insulation of a plane (Martin 2007).
- Water leakage
  The water tightness of a building, on the level of detail, is mainly dependent on the air permeability of the skin. An airtight detail is a watertight detail. When this is not the case, especially under high wind loads, moisture may enter the building. In addition, air flow escaping from the inside to the outside may cause condensation within the structure.

Relevance

When being able to make a reliable calculation method on air permeability that can be ruled before construction of a building / space this has many advantages:

- ✓ Possible design flaws come to light. As a result, the design can be adjusted at an early stage. This prevents failure costs and undesirable solutions with polyurethane, sealants and tape.
- ✓ Preventing unnecessary oversizing of ventilation systems to ensure sufficient pressure. This will save investment costs.
- ✓ The User Requirement Specifications (URS) and technical specifications will contain realistic, substantiated requirements.
- ✓ Contractors can be better informed in advance about the extent to which the air permeability is critical and what measures should be taken.
- ✓ When it is possible to make a good prediction in advance, one can focus on better alternatives before the works start.
- ✓ Focus on airtight construction is a focus on the energy consumption; with demands for building energy neutral by 2020 air tightness can't be ignored.

1.1.3 Scope and limitations

In the current standards and regulations there is a variety of available units and quantities. In practice, these units and quantities are used interchangeably, leading to confusion and discussions. This is reflected in multiple specification texts and official publications, such as the “Stichting BouwResearch / Civieltechnisch Centrum Uitvoering Research en Regelgeving” (SBR CUR) publication on building airtight and the directive for office buildings of the “Nederlands-Vlaamse Bouwfysica Vereniging” (NVBV).
In addition, there is no calculation method available, which enables a good prediction of the air permeability in the design process (in advance) of a building. Specifically it lacks in clear indicators for structural cracks and crevices, and there is no calculation method to make the translation between different parameters (e.g. the air permeability requirements in accordance with Building Regulations 2012 and the directive for seam and gap seals in SBR publications). Also a manner to include wind pressure in the design analysis is unclear.
In practice, this makes it almost impossible to provide potential customers in advance with a founded advice. In order to cope with uncertainties, designers will fall back to over-dimensioning of installations and making double constructions. Only after completion of a project, an actual assessment of the air tightness can be made.

It is clear that there is a need to set a limit to this air-permeability, and the possibility to determine in advance whether this limit is structurally feasible:
To connect with the increasingly stringent demands which are made on the energy performance of buildings (energy-0 in the future), it is necessary to limit the losses. This is impossible without a good airtightness.
Also within controlled rooms, such as operating rooms, laboratories and clean rooms, it is necessary that the required pressure hierarchy can be maintained. In practice, it appears in some cases that these pressure levels are not met. This leads to additional costs and delays in delivery, or worse to possible contamination and non-performance.

Within this graduation thesis a firm start will be made to collect available research numbers from the past, to frame and value the current database. In addition with the use of a test setup the relation between different parameters will be captured. Based on this framework and dataset a conclusion can be formed on which data should be known in the design phase to form a good prediction on the air permeability.

1.2 Aim and objectives

The aim of this thesis is not a quest to provide in a set of calculation parameters, but an attempt to correlate all decisions in the design phase that have an impact on the final air permeability.

The current rules and regulations dictate standardised permeability coefficient for known leakage points, or a maximum allowable volume flow for a given reference pressure. In order to design a well-founded calculation method, the variation in these default values needs to be mapped. Since this variety exists in both quantities and in units, all values must be converted in order to compare them with each other.

Current standards are mostly concerned about guidelines and calculation methods on measurements procedures. Standards that concern the desired or maximum air tightness of an envelope translate air leakage into an acceptable loss of air volume or a maximum envelope opening.
However none of these provide any knowledge to the contractor: What does he have to do in order to pass given rules?
Therefor the main problem definition is:

To draft a uniform calculation method
for determination of the air permeability in the design phase.

1.2.1 Hypotheses

The following hypotheses have been postulated:

- The ratio between the area and perimeter of a leakage opening are determinative for the degree of turbulence of the resulting air flow through this opening.
- There is a limit to the diameter of an opening in order for laminar air flow to occur

Most Dutch regulations are based on the Power Law (see Section 2.2.1). This method defines the flow characteristics of a building envelope in its flow exponent and coefficient. When calculating on an envelope based on theoretical values, the flow exponent is prescribed to have a fixed value of 0,625 (to 0,66). This thesis proposes that:

- It is impossible to define one standard flow exponent that will accurately predict the air leakage of any building envelope.
- Since the exponent is an indication for the type of air flow (laminar, turbulent, transitional), it can be expressed in variables found in flow dynamics.

While the first set of measurement results was analysed, an additional hypothesis has been formulated:

- Sharp edges of an opening will introduce turbulent flows which highly determine the flow characteristics according to power law of the opening itself.

1.3 Approach

1.3.1 Analysis current standards and regulations

Since most designers which are faced with air tightness concerns will work according to current building standards and regulations, an evaluation has been made of the codes that are available. Safety codes, building regulations, inspection reports and others from the Netherlands and other European countries are consulted. A distinction will be made between regulations concerning measurement procedures and standards that dictate the building performance.

1.3.2 Evaluation calculation methods

Since there is a difference in both quantity and unity recorded in the scope of available documents, a calculation method should be used to connect all mentioned default values, in order to achieve a complete framework. Current known methods are evaluated to determine the most appropriate ones.

1.3.3 Evaluating comparable research

Air tightness of buildings has been a research topic since the beginnings of the 20th century. Both the impact of high and low air tightness on the building climate as the variables within fluid dynamics that lie on the base of each leakage are studied before. The amount of air flowing in and out of an enclosure is known to be the result of a pressure difference over its envelope. What the influence is of the size and distribution of the openings over this envelope is a less studied topic.
A survey is made considering studied topics which are related to air tightness.

1.3.4 Collecting measurement data

Since most research only publishes conclusions and the available data coming from “Meetbureau Bijleveld” (MbB) is not representative to form conclusions on buildings in general, some additional measurements are executed. The aim of these measurements is to form a conclusion on the value for the flow exponent, and to investigate whether the geometrical proportions of openings can indicate the flow characteristics of the leakage flow.

A first set of measurements is executed on openings with the same leakage area to test the hypothesis that there is a correlation between the openings geometry and the flow exponent. Since observed values of the flow exponent fall outside of the theoretical framework a second set of measurements is executed to investigate openings of circular shapes and slits in with gradually increasing diameter.

1.3.5 Developing computational model

The data collected with both measurement sets did not provide a base solid enough to ground incontrovertible conclusions on. To investigate the influence of edge effects due to the squared corners of the test openings a simplified model is generated using Comsol, an interactive environment for modelling and simulating using computational fluid designs.

1.3.6 Sources

The documents that are mentioned in the reference list at the end of this document form the largest part of all which are read during the process of this thesis. They are considered important for further research on the topic. This certainly does not mean that it forms a total overview of the available knowledge. There is a vast and ever expanding library available in many different languages. This thesis is mainly based on Dutch and English documents.
After the measurements within this research were completed the results caused a new flood of information and associated corresponding literature. Undoubtedly further research into the topic will reveal an even larger body of work which is ignored in this thesis. Particularly sources in different languages then English, German and Dutch miss out and documents that could not be consulted without an investment or donation.

1.3.7 Outline

This thesis can be subdivided into three sections:
The Problem definition which starts with *Chapter 1* (the present chapter), introducing the problem and framework which lies at the base of the research. *Chapter 2* continues with listing the state of the art of both measurement procedures and calculation methods which relate to air tightness.
The Procedure consists of data collecting through measurements *(Chapter 3)* and further verification of hypotheses by a numerical model in *Chapter 4.*
Final remarks can be found in *Chapter 5*, divided in conclusions on the hypotheses, interpretation of the results of the procedure and recommendations for further research.

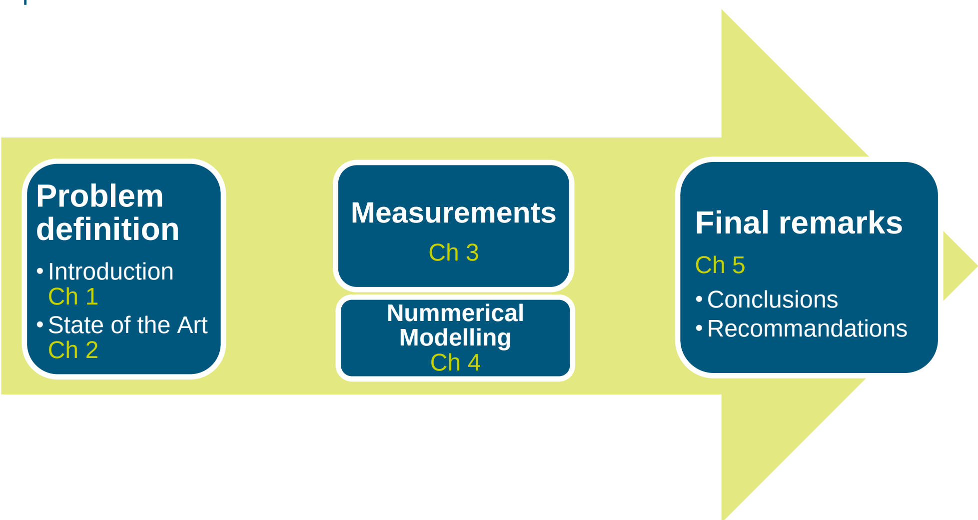

Figure 1.1 - Main outline of this thesis

2 State of the art

2.1 Standards and regulations

2.1.1 Regarding to building performance

- “Building Research Establishment Environmental Assessment Method” (BREEAM) is an international assessment method for sustainability of the built environment based on a scoring system for several subjects such as management, energy, materials and use. In the Netherlands a derivation is made (BREEAM-NL) that makes a distinction between new buildings, renovations, masterplanning projects and demolitions. The directive for new buildings and renovation projects has the criteria that the building needs an air tightness assessment based on NEN-EN 13829 (method A) in order to score points on the energy label for the thermal quality of the envelope.
- NEN 8088 describes the method used in the Netherlands to determine the EPC (Energie Prestation Coefficient) of a building. Within this EPC the air tightness of the concerned is of the matter. Based on the age, type and height of the building, a theoretical value can be determined.
- NEN 7120 is the regulation in which the modus to replace the theoretical value with a measurement. It is expressed as a q_{v10} value, which is corrected to the amount of flour surface.

Rooms with a controlled atmosphere

- Directive 10 of the VCCN gives a classification and measurement method for cleanrooms, in order to determine the degree of air permeability in a simple and reliable method (VCCN Projectgroep 15 2015). Within this directive the classes are defined by a leakage factor. With this factor *f* the cumulative air permeability coefficient of all leakages is determined. Then, using the power law (see Section 2.2.1) the maximum allowable volume of air flow through these leakage points is calculated. Based on the determined leakage class one will find the permissible air leakage, per square meter of skin surface, at a given pressure difference.

2.1.2 Measurement procedures

- NEN-EN 13829 "*Thermal performance of buildings - Determination of air permeability of buildings - Fan pressurization method*" - describes the measurement of the resulting air flow rates over a range of indoor-outdoor static pressure differences. This standard is intended for the measurement of the air leakage of building envelopes of single-zone buildings. For the purpose of this standard, many multi-zone buildings can be treated as single-zone buildings by opening interior doors or by inducing equal pressures in adjacent zones. The standard is withdrawn and replaced by NEN 2686
- NEN 2686 (2008) *“Air leakage of buildings - Method of measurement”* - Important updates to NEN_EN13829 are the set point of the minimal pressure reading of 15 Pa and a maximum interval of 8 to 15 Pa between two readings, up to 100 Pa. The data points need to be drawn in a pressure/flow graph and the result of the experiment is a reading of $q_{v;10}$ from this graph.
  Building volumes that exceed 500 m^3 need to be tested in sections of 3000 m^3 at most and the result is the highest of these sections, after the value is corrected to the loss of a corresponding volume of 500 m^3:

$$q_{v;10} = \frac{q_{v10;measured}}{V_{netto}} * 500 \qquad [1]$$

  Where:

$q_{v;10}$	volumetric air flow at 10 Pa	m^3/s
V_{netto}	Volume of tested section	m^3

- NEN-EN 15004-1 (2008) “*Fixed firefighting systems - Gas extinguishing systems - Part 1: Design, installation and maintenance, Annex E: Door fan test for determination of minimum hold time”* – In order to calculate the time an envelope is protected to fire by the extinguishing gas, the equivalent leakage are is calculated based on a doorfan test. This standard requires testing in the range of 10 – 60 Pa. This standard also prescribes a field calibration check for the measurement set. A result of this test performed on the equipment used for this research can be found in Appendix B4.

2.1.3 Information on current calculation method

SBR CUR published a document for “Building air tight”, which provides in a set of standardized values for most building materials and construction methods common in the Netherlands. This dataset is mostly based on measurements of housing dwellings, executed by Nieman Groep and complemented with data from the Air Infiltration and Ventilation Centre (AIVC). There are three quality levels defined: basic, good and excellent.

2.2 Available calculation methods

Remarkable is that the only formula that is found in any standard or regulation is the so called “power law” which gives a dependency of the volumetric flow (Q) on the pressure difference (ΔP), using a factor (C) and exponent n that indicates whether the flow is turbulent (n=0,5) to laminar (n=1,0).
However there is also a method know that expresses the pressure difference as a quadratic formula of Q. This equation gives an indication of the contribution of fully developed laminar and turbulent flows. Earlier scientists have tried to link those two calculation methods using a S-factor that correlates the flow exponent from the power law with the factors of the quadratic formula.
On the scale of a single opening this S-factor can also be calculated using the dimensions of the considered opening and the physics of the air flowing. These parameters are highly studied within fluid dynamics, but no clear link seems to exist concerning air tightness of whole rooms/buildings. Within fluid dynamics openings are usually arranged by their Reynolds number, a dimensionless quantity that indicates whether the flow pattern will be turbulent or laminar.

2.2.1 Power law

The calculating formula with which a link has been established between the air flow volume as a result of an air pressure differential across a building envelope and the flow characteristic of this shell is well known commonly expressed as:

$$q_v = C \cdot \Delta P^n \qquad \text{(NEN 1087 2001)} \qquad [2]$$

Where:

q_v	volumetric air flow	m^3/s
C	air permeability coefficient	$m^3/(s\cdot Pa^n)$
ΔP	pressure difference	Pa
n	flow exponent	-

The result of this method is a description of the flow characteristics in the permeability coefficient and the flow exponent. The last of these two is critical for extrapolating the measured data to the pressure regime of interest. Theoretically the flow exponent lies between the 0,5 for fully developed turbulent air flow and the 1,0 for fully developed laminar air flow (Walker, Wilson, and Sherman 1998; Urquhart and Richman 2015; Sherman 1992; Orme, Liddament, and Wilsom 1998; Santamouris and Wouters 2006).

This makes the flow exponent a good indicator for the type of flow and thus it provides an indication of the relative size of the dominant leaks. Also, changes in the flow exponent of a second measurement after a retrofit or sealing operation of an envelope will indicate the effect of the taken measures.

Theoretical limiting range of exponent
The values mentioned as boundaries for turbulent flow (n = 0,5) and laminar flow (n = 1,0) are a result of Bernoulli's equation:

$$p_1 + \frac{1}{2}\rho \cdot v_1^2 + \rho g z_1 = p_2 + \frac{1}{2}\rho \cdot v_2^2 + \rho g z_2 + \Delta p_f$$ (Knoll, Wagenaar, and Weele 2002) [3]

Where:

p	bias pressure	Pa
ρ	density	kg/m^3
v	velocity	m/s
g	gravitational acceleration	m/s^2
z	elevation	m
p_f	pressure loss due to friction	Pa

Strictly this equation only holds for inviscid flow, but since shear stresses are negligible due to very small velocities gradients, it can be applied for the still-air discharge of orifices due to pressure differences over this opening (Etheridge 2012).

Since the atmospheric pressure of air (p) changes simultaneously with a change in height (z), the static part of Bernoulli's equation ($\rho g z$) can be neglected. If we take p_1 = 0 and v_1= 0 and pressure losses due to friction are neglected, we can express the maximum velocity in terms of air flow volume and the area of the opening ($v = q/A$) this results in:

$$\Delta p = \frac{1}{2}\rho \cdot \left(\frac{q_v}{A}\right)^2$$ [4]

Rewriting: $$q_v = C \cdot \Delta p^{0,5}$$ [5]

Where:

Δp	pressure difference	Pa
C	constant	-
q_v	volumetric air flow	m^3/s

From this expression we can read that 0,5 is a limiting value for the flow exponent, since a lower value would indicate that energy "appears" and the principle of energy conservation wouldn't hold.
For a more detailed calculation the pressure loss due to friction is taken into account (Kula and Sharples 1994).

$$\Delta p_f = \lambda \cdot \frac{l}{D} \cdot \frac{1}{2}\rho \cdot v^2$$ (Knoll, Wagenaar, and Weele 2002) [6]

Where:

p_f	pressure loss due to friction	Pa
λ	friction coefficient	-
l	length of opening in flow direction	m
D	Diameter	m
ρ	density	kg/m^3
v	velocity	m/s

For this method an extra parameter needs to be introduced: the Reynolds number, a dimensionless quantity that indicates the occurring of laminar/turbulent flow development through an opening:

$$Re_o \equiv \frac{\rho u_m d_h}{\mu} = C \cdot u_m$$ (Etheridge 2012) [7]

Where:

Re_o	openings Reynolds number	-
ρ	density	kg/m^3
u_m	mean velocity	m/s
d_h	hydraulic diameter $= 4\frac{A}{perimeter}$	m d_h = *d* for circle d_h = *2*d* for rectangular duct (w >> d)
μ	dynamic viscosity $\mu = \rho \cdot \eta$	Pa/s
η	Kinematic viscosity	m^2/s
C	constant	-

Many researches has been performed on this number, stating that high values indicate turbulent air flow and low values laminar air flow, with a turning point around 2300. This Re <2300 indicates laminar flow (Etheridge 2012; Sherman and Chan 2003).

Now, the Reynolds number can be used to determine the friction coefficient (λ), for laminar flow we know:

Laminar flow: $$\lambda = \frac{64}{Re} = \frac{64\mu}{\rho \boldsymbol{v} D} = C \cdot v^{-1}$$ (Bejan 2013; Etheridge and Sandberg 1996; Duncan, Thom, and Young 1960) [8]

Where:

λ	friction coefficient	-
Re	Reynolds number	-
μ	dynamic viscosity	Pa/s
ρ	density	kg/m^3
v	velocity	m/s
D	Diameter	m
C	constant	-

When we insert formula [8] into [6] and expressing the velocity in terms of air flow volume and the area of the opening ($v = q/A$) we get for laminar flow:

$$\Delta p_f = \lambda \cdot \frac{l}{D} \cdot \frac{1}{2}\rho \cdot \left(\frac{q_v}{A}\right)^2 = C \cdot v$$ [9]

Since: $$v = \frac{q}{A}$$ [10]

We get: $$\Delta p = C \cdot q$$

And thus the theoretical limit for the flow exponent of fully developed laminar flow equals 1,0.

2.2.2 Quadratic formula

Although the power law has been proven to fit the results of any pressure test, or air tightness test quite well, there is no link with any physical paradigm. When test results are split up for fully developed turbulent and fully developed laminar flow, these correspond to an exponent of 0,5 respectively 1,0 (Sherman and Chan 2003).
The relationship between pressure and flow for a single crack are given for both fully developed turbulent flow and fully developed laminar flow:

$$q_{v;turbulent} = C \cdot \Delta P^{0,5}$$ [11]
$$q_{v;laminar} = C \cdot \Delta P$$ [12]
(Etheridge 2012; Sherman, Wilson, and Kiel 1984)

If we combine these two into one formula, this results in what is known as the quadratic formula:

$$\Delta P = AQ + BQ^2$$ (Walker, Wilson, and Sherman 1998; Baker, Sharples, and Ward 1987; Sherman 1992) [13]

Where:

$$A = \frac{12\mu Z}{Ld^3}$$ fully developed laminar friction losses coefficient [14]

$$B = \frac{\rho Y}{2d^2L^2}$$ entry, exit and turbulent friction losses coefficient [15]

And:

μ	dynamic viscosity	Pa/s
Z	length of opening in flow direction	m
L	width of the opening	m
d	thickness of opening	m
ρ	density	kg/m^3
Y	1,5 + n_b	n_b = number of bends within the crack/opening

This combined equation makes it possible to vary the flow from laminar to turbulent over a range of flows. However, due to the combination of fully developed laminar and turbulent flows and entry and exit losses, this is a physically unrealistic approach to be applied in building air tightness. The convoluted crack geometries that are common in building leaks are rarely fully developed and in addition wind turbulence may cause the pressures across building leaks to be unsteady (Walker, Wilson, and Sherman 1998).

Since not all openings are expressible in geometrical dimensions as width, length or a given diameter, the hydraulic diameter is introduced as a factor of the area and the perimeter:

$$d_h = 4\frac{A}{perimeter}$$ [16]

Where:

d_h	hydraulic diameter	m
	$d_h = d$ for circle	
	$d_h = 2*d$ for rectangular duct (w >> d)	
A	area	m^2

Although the quadratic formula disregards the existence of transition between streamline and turbulent flow, the advantage of this formula is that the coefficients are independent of the flow rate. Unlike the power law, the coefficients in the quadratic formula can be linked directly to the openings parameters.

David Etheridge: More accurate at lower pressure values. Air tightness tests are executed at high pressures, in the range of 50 Pa, while common building pressures are more in the range of 4 – 10 Pa.

Mathematically, the solution to the quadratic equation [4] is:

$$Q = \frac{-A \pm \sqrt{A^2 + 4B\Delta P}}{2B}$$ [17]

The negative root is neglected since all real flows are positive.

2.2.3 Other methods

While researching the topic of air tightness the power law and quadratic formulation are interchangeably, depending on the author of a specific reading. The forms of the determination of the coefficients in the quadratic formula denote the importance of the properties of air in understanding the behaviour of leakages. Deeper knowledge of fluid dynamics is necessary to understand the dependence of the different variables that are mentioned. A detailed but clear explanation can be found in the work of Duncan, Thom and Young (Duncan, Thom, and Young 1960).

Multiple sources have stated that the extent in which a flow through an opening is turbulent depends on its geometry. The similarity between the before mentioned methods is that it treats the air permeability of an envelope, or a system, as a whole, without defining the leakages itself. It is clear that the result of this system is a summation of all individual leaks, but since we are only interested in the system response (and not in the exact openings geometry), this system can be represented by equivalent parameters of a single opening.
Although arbitrary, the choice for a circular geometry is most logical, since this is a well-studied form in fluid dynamics and the cross-section is defined by a single parameter. The most common form to treat the problem of laminar flow in short, circular pipes is by linearizing the Navier-Stokes equation which gives:

$$\Delta P = \frac{32\mu l u}{d^2} + m\frac{1}{2}\rho u^2 \qquad \text{(Sherman 1992)} \qquad [18]$$

Where:

ΔP	pressure difference	Pa
μ	dynamic viscosity	Pa/s
l	length of opening in flow direction	m
u	air velocity	m/s
d	thickness of opening	m
m	constant depended on linearization	approx. 2,8
ρ	density	kg/m^3

The mean velocity (u_m) of an opening can be determined if the flow rate and the openings area areknown:

$$u_m = \frac{q}{A} \qquad [19]$$

Given a flow through a pipe, resistance due to friction and components such as valves, bends and tees will cause a pressure drop. Many experiments have been performed in the past, building a large database of known loss coefficients, which are split into the pressure loss due to friction (ξ_F) and due to components (C_L):

$$\xi_{12} = \xi_F + C_L = \frac{\Delta P}{\frac{1}{2}\rho u_m^2} \qquad [20]$$

Where:

ξ_{12}		= ζ (Knoll, Wagenaar, and Weele 2002)
ξ_F	Friction loss coefficient	-
C_L	components loss coefficient	-
ΔP	pressure difference	Pa
ρ	density	kg/m^3
u_m	mean air velocity	m/s

These coefficients are used when the dimensions of air ducts needs to be determined based on desired air flow volumes. The coefficients represent the pressure loss due to duct length and amount and type of bends (Knoll, Wagenaar, and Weele 2002).
This equation only holds if the flow is fully developed, that is if the pipes (or ducts) are long enough. That is why it causes a lot of difficulties when it is applied to ventilation openings (Etheridge and Sandberg 1996), let alone leakage openings of unknown geometry.

The flow through an envelope, given an applied pressure, is the result of the combination of all openings in this envelope. For relatively large openings this flow is sometimes represented by an equivalent flow through a flat plate orifice. The orifice flow equation is formulated as:

$$q = C_d * A * \sqrt{\frac{2}{\rho}\Delta P}$$ (Orme, Liddament, and Wilsom 1998) [21]

Where:

C_D	discharge coeffcient	- $\left(\frac{Actual\ mass\ flow\ rate}{Ideal\ mass\ flow\ rate}\right)$
q	air flow	m^3/s
ΔP	pressure difference	Pa
ρ	density	kg/m^3
ΔP	pressure difference	Pa

The same formula can also be found in David Etheridge's work. He however uses $C_{d;still\text{-}air}$, which is the discharge coefficient of an opening in a surface separating two much larger spaces, with nominally still-air conditions and with uniform and equal densities.

For known geometries, Etheridge uses the analogue with ducts, and considers a building envelope as a number of ducts and components where the same loss coefficients can be used. The cumulative of this series results in the overall resistance called the discharge coefficient C_d.
The discharge coefficient of an opening between two regions of stationary air is then defined by:

$$C_D = \frac{q}{A}\sqrt{\frac{\rho}{2\Delta P}} \qquad [22]$$

Where:

C_D	discharge coeffcient	-
q	air flow	m^3/s
ΔP	pressure difference	Pa
ρ	density	kg/m^3
ΔP	pressure difference	Pa

When interested in the dimensional component of the opening causing pressure loss, by rewriting equation [21] we get:

$$C_{LO} = \frac{\Delta P}{\frac{1}{2}\rho u_m^2} - \xi_F \qquad [23]$$

David Etheridge uses this to determine an expression for the friction loss coefficient. He concludes that for fully developed flow, using the wall shear stress Fanning friction factor ($c_f = 2\tau_0/\rho u_m^2$) inside the momentum equation

$$\Delta P = \left(\frac{4\tau_0(\Delta x)}{d_h}\right) \qquad [24]$$

which defines

$$\Delta P = 4\left(\frac{\rho u_m^2}{2} * c_f \frac{L}{d_h}\right) \qquad [25]$$

We can read

$$\xi_F = \frac{4Lc_f}{d_h} \qquad [26]$$

Where:

ξ_F	Friction loss coefficient	-
L	flow length	m
c_f	wall shear stress	-
d_h	hydraulic diameter	m

2.2.4 Validity

The power law and quadratic formula are both based on a ratio between the volumetric flow rate and the pressure difference. So, using a dimensionless pressure it is possible to manipulate the quadratic expression into a power-law formulation or vice versa (Sherman and Chan 2003):

$$S = \frac{m \rho d^4}{4096 \mu^2 l^2} \cdot \Delta P \qquad [27]$$

Where:

m	constant depended on linearization	approx. 2,8
ρ	density	kg/m^3
d	diameter of opening	m
μ	dynamic viscosity	Pa/s
l	length of opening in flow direction	m
ΔP	pressure difference	Pa

This pressure S can be used to determine the flow exponent:

$$n = \frac{1}{2}(1 + (1 + 8S)^{-\frac{1}{2}}) \qquad [28]$$

These derivations could be used to determine the dimension of a leakage based on the flow regime. However they only hold for single leaks. Walker, Wilson and Sherman (1998) have issued the problem of leaks which are in series or parallel in the envelope and expanded this derivation. It is still only possible to base a conclusion on this data when the distribution of the leaks over the envelope is known.
The benefit of this model is not so much to provide a possibility to determine the geometrics of leakage openings based on air tightness measurements, but to confirm the robustness of the power law. It also tells us that the exponent is pressure dependent. This dependency is low, so that over a narrow range of pressures the exponent can be assumed to be fixed (Sherman and Chan 2006). However this means that extrapolating to a pressure of interest, outside the range of measurements one cannot just assume it is a constant.

David Etheridge already concluded that if all openings in an envelope are known, meaning all areas, discharge coefficients and positions, the sum of all these single flows will form the envelopes flow.
The relation between all individual flows is in the conservation of mass.
In other words: all changes in flow rate, due to a change of wind speed or opening/closing of adjacent rooms will result in a change of internal pressure to re-establish the mass balance (Etheridge 2010).

To conclude we can say that both the power law and the quadratic formula are valid in order to describe the air tightness of an envelope.

2.3 Comparable research data

2.3.1 Flow exponent

A lot of research has been done to fully developed (laminar) flow. These leaks typically are found to have low Reynolds numbers and the flow will be dominated by laminar friction losses and will be linearly proportional to the pressure drop.
With very short leaks on the other hand friction losses cannot be ignored. These types of leaks can be treated as sharp edged orifice in which the flow is proportional to the square of the pressure drop (Sherman and Chan 2006), as with fully developed turbulent flow.

Extensive literature agrees that n has the limiting values of 0,5 (for orifice flow) and 1,0 (for fully developed / long pipe flow). However with pressurization measurements occasional flow exponents below 0,5 are found with a power law correlation. Earlier research has shown that it is in fact physically possible for such low exponents to occur, without having the environment change due to the pressure gradient of the measurements. When Reynolds number of openings gets greater than 1000, orifice coefficients will decrease with Reynolds number, leading to a flow exponent of less than 0,5 (Sherman, Wilson, and Kiel 1984).

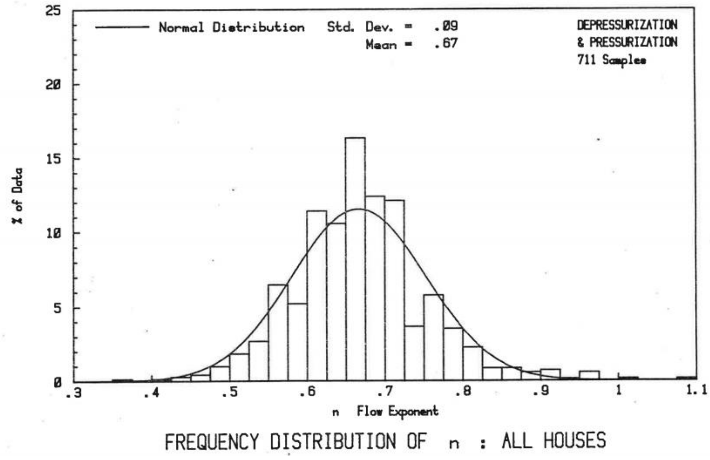

Figure 2.1 - Frequency distribution of flow exponent by Orme et all (1998)

Orme concludes there is no good correlation, but a normal distribution to recognize, with a mean value of 0,65. This document is referenced when this value is used as good indicator for the flow exponent (Orme, Liddament, and Wilsom 1998)

The data Orme based his conclusions on, was gathered in the 17 years that air tightness measurements where performed prior to his publication. Unfortunately the data was unavailable for this thesis, but the indexes show that the largest share of data was originated from housing dwellings in foreign countries. As a reference test results of MbB are used, which consisted of 123 sets of measurements. Although this sample size is remarkable smaller, the graphical representation of both datasets shows a clear difference.

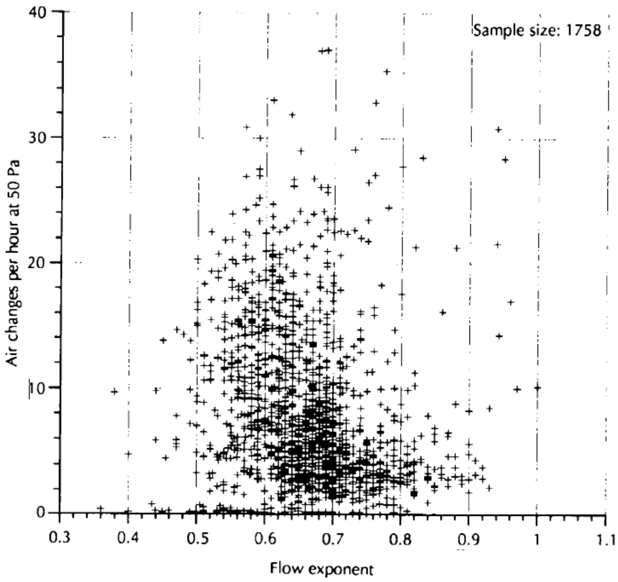

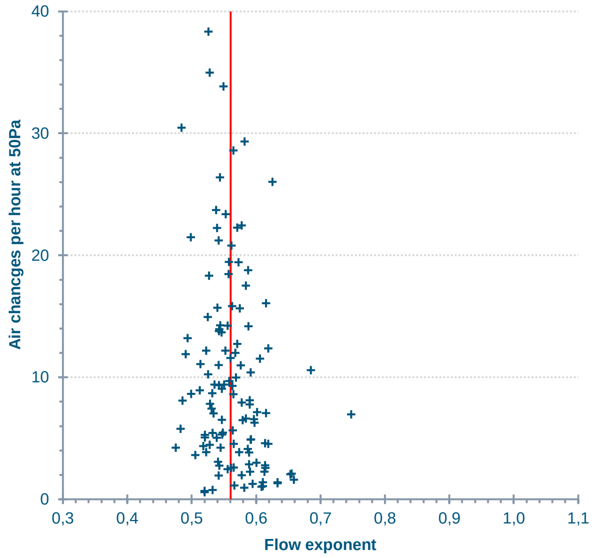

Figure 2.2 - Orme combined data sets from 13 countries to evaluate the flow exponent and ACH_{50}

Figure 2.3 - Dataset based on MbB measurements (2015)

Technische Universiteit Delft

Royal HaskoningDHV

This different mean value is probably the result of the different type of buildings that are used for the tests in each dataset. It is most likely that the dataset that Orme used to base his conclusion on contained a large percentage of timber frame constructions, whose leakage openings typically consist of elongated slits. On the other hand there is the dataset of MbB, which contained mostly concrete constructions or steel constructions whose walls were erected out of large, closed, sheets. This cannot be determined with certainty, but it notes that we should be careful in making assumptions for a fixed value for the flow exponent.

Usually when a pressurization measurement is performed also the R-squared values over the datapoints is calculated. After the measurements within this study where completed further literature review revealed that recent study has shown that these values cannot be trusted as single indicator for accuracy. It is possible to have a varying flow exponent, while R-squared values remain nearly perfect.
The higher or lower the flow exponent becomes, the greater effect it will have on extrapolating of the data. Therefor a theoretical substitution of a flow exponent is very difficult. For the same reason it cannot be justified to apply any extrapolation when flow exponents outside of the theoretical frame of 0,5 – 1,0 are found (Urquhart and Richman 2015).

2.3.2 Interpreting data from pressurization measurements

Due to unavoidable measurement uncertainties these pressurization tests are usually executed at higher pressures (10 – 50 Pa) and extrapolated back to more typical pressures inside buildings (1 -5 Pa).
Even when a measurement has been performed, any extrapolation of this data to occurring building pressures will cause an uncertainty of unknown magnitude (Urquhart and Richman 2015). Therefor it can be more important to test the building at the desired pressure level then to achieve a linear relationship over the data points.
However when comparing enclosure leakage values of the same envelope pre- and post-retrofit, this linear relationship will help to understand the changing of leakage path geometry. In order to interpret the date from pressurization measurements many users algebraically determine the physical parameter A_e: Effective leakage area. It is defined by assuming Bernoulli equation approximation:

$$A_e = C * \sqrt{\left(\frac{\rho}{2}\right)} * \Delta P_{ref}^{n-0,5} \qquad \text{(Santamouris and Wouters 2006)} \qquad [29]$$

Where:

A_e	effective leakage area	m^2
C	air permeability coefficient	$m^3/(s \cdot Pa^n)$
ρ	density	kg/m^3
ΔP_{ref}	reference pressure difference	Pa
n	flow exponent	n

Leakage area

Since the A_e is an extensive property of a building envelope, it needs to be normalized in order to compare the values for different envelopes. This can be done by correcting the A_e by the envelopes volume, by envelope area or by floor are. While current building standards use the specific effective leakage area as a function of the envelope area (NEN-EN-ISO 9972-2015); Sherman et all have introduced the specific leakage as a ratio of A_e and the floor area since this is the most commonly quoted building characteristic and for single-family buildings floor area and envelope area should correlate rather well. It is most likely that there is a correlation between the flow exponent and this specific leakage. As they concluded there is a slight trend visible in their data of lower exponents for higher specific leakages (Sherman, Wilson, and Kiel 1984):

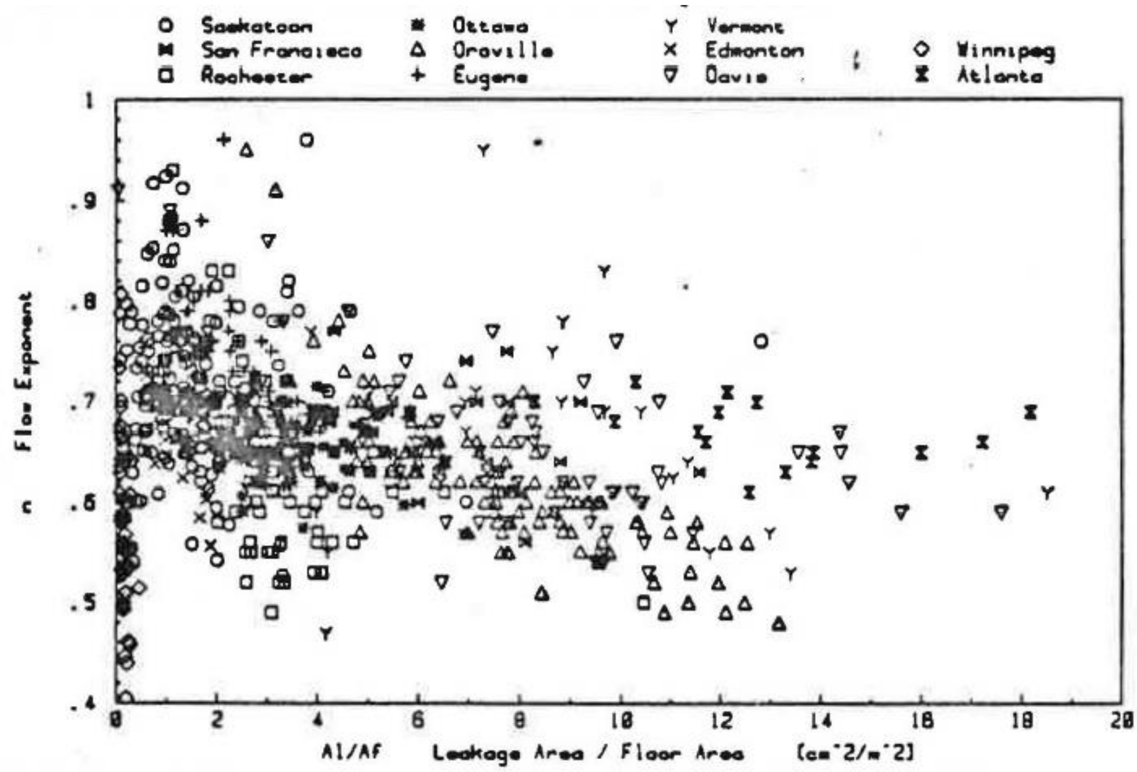

Figure 2.4 - Variability of flow exponent with specific leakage

In the Dutch regulations a calculation independent of the reference pressure is found:

$$A_e = \frac{C * \sqrt{\rho}}{1000 * 2^n} \qquad \text{(NEN 2686 2008)} \qquad [30]$$

Where:

A_e	effective leakage area	m^2
C	air permeability coefficient	$m^3/(s \cdot Pa^n)$
ρ	density	kg/m^3
n	flow exponent	n

The document notes that this conversion only applies theoretical for fully turbulent flow, n = 0,5. From experiments it has been found in practice that this relationship is also used for other values of n.

Another common parameter used to express the amount of leakage is the equivalent leakage area, or ELA:

$$ELA = \frac{A_e}{0{,}61} \qquad \text{(NEN-EN 15004 2006)} \qquad [31]$$

Where:

ELA	equivalent leakage area	m^2
A_e	effective leakage area	m^2

This is the cross-sectional area of an orifice hole (shaped like the blower door hole) that would have the same leakage flow rate as the building if both were subjected to a 4 pascal indoor/outdoor pressure difference. The ELA is used for fan calibration checks and for identification of actual leaks.

Norms and normalization
In order to compare different buildings or envelopes with each other, the metrics used in air tightness calculations need to be scaled to a normalized value.
In mechanical engineering it is most common to use a reference building volume. The ACH_{50} (Air Changes per Hour at 50 Pa) is the most common metric to quote the infiltration and ventilation rates.
Most standards use the floor area, since this is the most easiest to determine from a practical standpoint. The A_e or q_{v10} is set to boundaries for a reference area.
However the envelope area would be a more significant value to express air tightness since in practice all leaks will be distributed over all surfaces that form the envelope.

2.4 Key leakage pathways

Most typical leakage paths that are found during leakage detections by MbB consist of connections between different building components, movable components in the envelope such as doors and windows and the feed of cables or ducts to adjacent rooms. Especially rooms with great height often have slits in corners or cracks in the walls due to setting of the materials under the influence of temperature fluctuations. The types of leakage problems have much to do with the construction of the dwellings.

The effectiveness of various retrofitting strategies has been studied before. Lowe et al. found that one of the most important factors is the method used to construct the walls (Lowe, Johnston, and Bell 1997).
In a research project which goal was to give guidance in choosing appropriate materials for air barrier system, 36 common building materials were tested and ranked for air leakage using laboratory test chamber experimental setup (Air-Ins Inc. 1998).

As mentioned in section 2.1.3 SBR CUR prescribes three performance levels:
- Basic (1), which corresponds with the Dutch Building Regulation (Bouwbesluit)
- Good (2), which should represent the current standard
- Excellent (3), can be used when extra tightening measures are taken.

The values for the basic level are found by using data from the AIVC and by an inventory of all potential leakage pathways in tested dwellings. After deduction of known leakage values, acquired from manufacturers of the building components used, the remaining leakage measured is allocated to the inventoried components (H.M. (Harry) Nieman, personal communication, May 16, 2016).

2.5 Current work procedure

Although there is general agreement that the power law is a good descriptor of air tightness data, there is no real agreement on the best metrics to use in quoting air tightness data. The best way to quote air tightness data will depend on what you plan to use it for. Issues such as how many parameters to be used in quoting air tightness data and whether or not air tightness data should be normalized by the size of the building are important when deciding upon the optimal metric (Sherman and Chan 2003).
The current rules and regulations often give standardised permeability coefficient C for known leakage points, or a maximum allowable volume flow $_{qv\ for}$ a given reference pressure and an assumed value for the flow exponent n.

The C and n and can only be determined experimentally. Since a judgement should be rendered about the desired / permitted air permeability of an envelope in the design phase assumptions should be made.
This assumption can be made in several ways (SBR CUR):
- A (standard) determination method in accordance with NEN 8088-1;
- Input data based on previously completed projects;
- A calculation based on the length and quality of the connection.

Assumptions for utility buildings based on any of these methods are often of a complete different scale then the result of construction.

A common expression for the air tightness of an envelope is the single parameter A_e, the effective leakage area (see section 2.3.2). The risk of expressing the air tightness property in such a dependent variable is that one easily forgets which data lies in the base of the expression and is communication as if the A_e is a physically existing opening in the envelope that needs to be closed.

In the Netherlands, the flow rate at 10 Pa ($q_{v,10}$) is a new expression for the air losses of an envelope. This value is introduced in the EPC calculations which is set to boundaries to provide for new completed buildings to be more energy efficient (NEN-EN-ISO 9972-2015).

Based on conversations with various persons at measurement locations and within Royal HaskoningDHV it seems that design principles and requirements are set based on poor information and mentioned standards. These requirements are not translated to a specific design. Designers and contractors have no grip on the effect of detailing and execution of the works.
After completion, when a test is required for completion, a measurement company will come by to do an air tightness test. In most cases the set requirements are not met. Since failing this test is not an option, the contractor will have to add tape, kit and PUR on leakage points until the room or building passes the test.

2.6 Remarks

A large variety of leakage coefficients is made available. To calculate using these coefficients the power law is used with a standard value for the flow exponent of around 0,65. By examination of this power law we see that these flow coefficients are represented by the volumetric air flow at 1 Pascal. The standard value of the flow exponent is based on a database of measurements up to 1995 (Orme, Liddament, and Wilsom 1998), while the authors of this database conclude themselves that 0,65 is the mean value of the flow exponents collected, but there is no correlation to be found between this value and the entire database. The magnitude of the error as a result of extrapolation by a standard flow exponent is not taken into account by any publication of standard flow coefficients.

Besides the power law also the quadratic formula has proven to form a good fit on datasets of volumetric air flow and pressure differences over a building envelope. The quadratic formula provides in two loss coefficients, one for the fully developed laminar friction losses and one for the entry, exit and turbulent friction losses. There is no index found of representative values for these loss coefficients.

3 Measurements

3.1 Theoretical background

The blower door got its name from the fact that in most cases a fan would be mounted inside a door frame, or optional in a window frame or other convenient envelope opening. It was first used in Sweden in 1977 and gained ground quickly as a method to determine the tightness of building envelopes (Kronvall 1980). While equipment has developed a lot since, the measurement procedure hasn't changed a lot: The steady-state flow through the fan is measured at various steady pressure differences across the envelope.
Due to unavoidable measurement uncertainties these pressurization tests are usually executed at higher pressures (10 – 50 Pa), at which pressure noise and zero drifts caused by wind or stack effects are also reduced. The results are extrapolated back to more typical pressures inside buildings (1 -5 Pa).

As seen in paragraph 2.1 all regulations with prescriptions for air tightness measurements are based on the power law.

3.2 Research design

Since test results of MbB showed a complete different mean value for the flow characteristics as found in various literature, a test setup is designed to provide a better view of the relationship between the various parameters. A measurement window is created in a controlled environment (laboratory, in which panels with known leakage openings can be mounted. The aim of this test setup is to investigate the correlation between the coefficient C and the exponent n in the power law. This information would be very useful to interpret the available databases such as the catalogues of SBR CUR / NVBV.

3.2.1 Test room

A transmission room at the TU Delft, designed to perform acoustic measurements is found to be suitable for air tightness measurements. The room is located on the first floor of the faculty of Applied Sciences and labelled as D163/D165 (see figure 6). Together with another transmission room on the ground floor of the faculty, these rooms are built as a separate box inside the faculty. This box is founded on rubber blocks, so there is as little influence from the rest of the building as possible. For the air tightness test part D165 will be used. All adjacent rooms are opened, so air can flow unimpeded and a stable situation is ensured. The basic geometrics of room D165 are recorderd:
Volume of enclosure : 99,1 m^3 Average height of enclosure: 4,57 m
Surface area envelope: 128,3 m^2

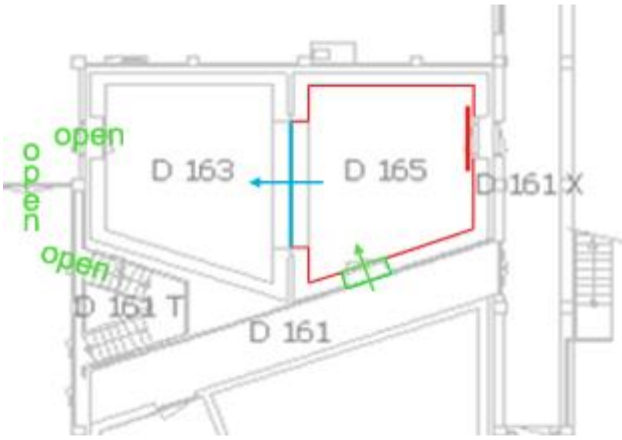

Figure 3.1 - Floorplan Test room

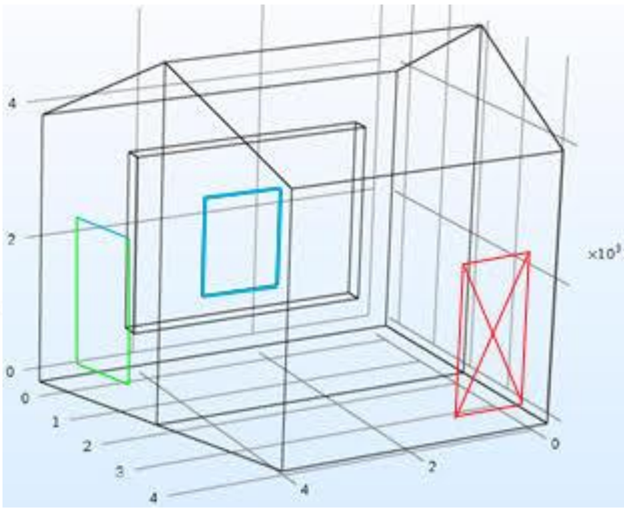

Figure 3.2 - Computer model Test room D165

As can be seen the floorplan has a tapered form. The room also has a gabled roof. These irregular forms are designed because of the acoustic purpose of the room. This form has no advantage for testing of air tightness, but no disadvantage either

The door leading to D161X is closed with tape. A measuring door is built in the door frame towards D161. This way room D165 can be pressurized. In the wall between D163 and D165 a window frame is deposited in the concrete, which will be used as measuring window. Perpendicular to the frame some U-profiles are also deposited in the concrete. Along the periphery of the frame, with the use of T-bolts and wing nuts, four wooden beams can be pressed against the frame. Both sides of the interface of the frame and the beams are provided with illmod.

3.2.2 Premeditation

Dataset 1: Fixed leakage area

The first set of leakage openings to be tested consists of different shaped openings with a similar leakage area A_e. The openings vary in their perimeter, hydraulic diameter and the amount of corners. All openings are cut into a sheet of MDF (12 mm thick):

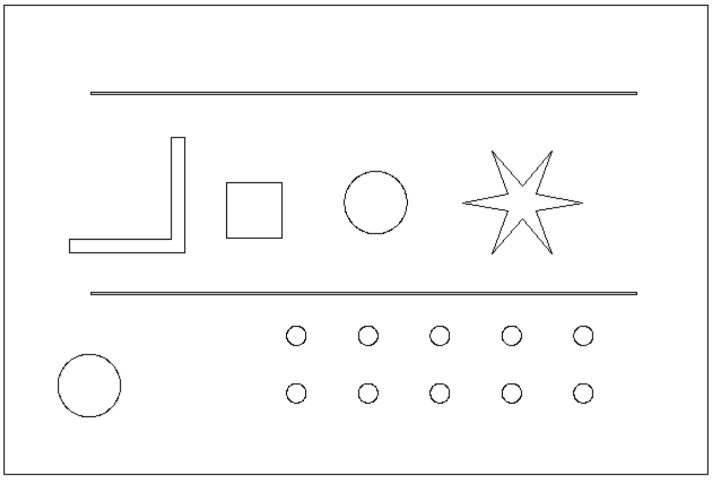

Dimensions: 1225 x 815 mm
All openings are 9500 mm^2
Two slits together
10 small openings together

Figure 3.3 - Lay-out measuring panel 1

The following measurements will be performed on this panel:

Table 1 - Index measurement dataset 1

Shape	Measurement (#)	A (mm^2)	Perimeter (mm)	d_h (mm)	Corners (#)
Large circle (center)	1.1	9500	345,52	54,99	0
Large circle (corner)	1.2	9500	345,52	54,99	0
Star	1.3	9500	989,17	38,42	12
Square	1.4	9500	389,87	97,47	4
L-shape	1.5	9500	810,00	46,91	6
Slits (2)	1.6	9500	3820,00	9,95	8
Small circles (1)	1.7	950	109,26	34,78	0
Small circles (10)	1.8	9500	1092,62	34,78	0
Small circles (4)	1.9	3800	437,05	34,78	0

Dataset 2: Gradually growing slits and holes

In contrast with the first dataset, the second group of measurements is based on a fixed form. Since the literature study provided most information on circular shaped openings and the slit is best representative for a crack or joint in buildings, these are the forms that will be studied.

Gradually the hydraulic diameter is enlarged, in order to investigate the influence on the flow characteristics.

Last, the circular openings will be provided with a metal pipe, in order to enlarge the flow length through the openings. The openings are all cut into a sheet of MDF (12mm thick):

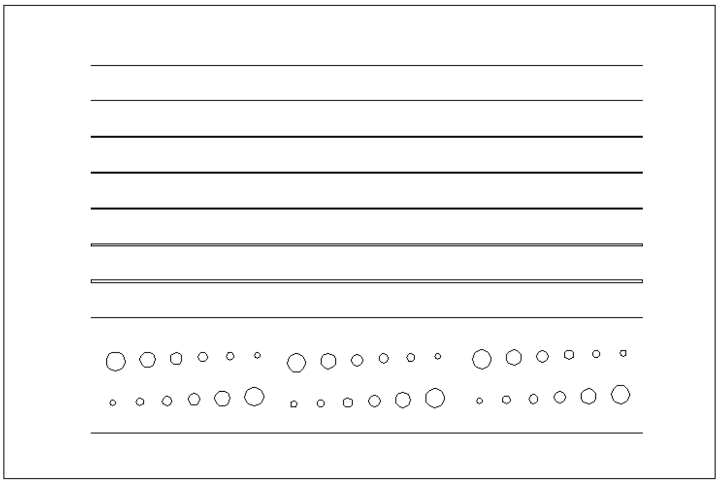

Dimensions: 1225 x 815 mm
All slits have a length of 850 mm
Slit diameter varies from 5 to 0,5 mm
There are three slits of 0,5 mm to vary in length

Openings have diameter of 10, 13, 16, 20, 26 and 32 mm.
The four smallest openings can have a pipe inserted of 16, 34 or 50 cm length

Figure 3.4 - Lay-out measuring panel 2

Since a building envelope will rarely contain only one single opening, the circular openings will be tested as group and as single opening. Like the first dataset all measurements are numbered and listed with their geometrical properties:

Table 2 - Index measurement dataset 2 - slits

Shape	Measurement (#)	A (mm^2)	Perimeter (mm)	d_h (mm)	L (mm)
Slit 0,5mm	2.01	475	1901	1,00	12
2x Slit 0,5mm	2.02	950	3802	1,00	12
3x Slit 0,5mm	2.03	1425	5703	1,00	12
Slit 1,5mm	2.04	1425	1903	3,00	12
Slit 2mm	2.05	1900	1904	3,99	12
Slit 2,5mm	2.06	2375	1905	4,99	12
Slit 3mm	2.07	2850	1906	5,98	12
Slit 4mm	2.08	3800	1908	7,97	12
Slit 5mm	2.09	4750	1910	9,95	12

Table 3 - Index measurement dataset 2 - circular openings

Shape	Measurement (#)	A (mm^2)	Perimeter (mm)	d_h (mm)	L (mm)
Circle 10mm	2.10	78,54	31,42	10,00	12
Circle 13mm	2.11	132,73	40,84	13,00	12
Circle 16mm	2.12	201,06	50,27	16,00	12
Circle 20mm	2.13	314,16	62,83	20,00	12
Circle 25mm	2.14	490,87	78,54	25,00	12
Circle 32mm	2.15	804,25	100,53	32,00	12
Circles 10mm	2.16	471,24	188,50	10,00	12
Circles 13mm	2.17	796,39	245,04	13,00	12
Circles 16mm	2.18	1206,37	301,59	16,00	12
Circles 20mm	2.19	1884,96	376,99	20,00	12
Circles 25mm	2.20	2945,24	471,24	25,00	12
Circles 32mm	2.21	4825,49	603,19	32,00	12

Table 4 - Index measurement dataset 2 - metal pipes

Shape	Measurement (#)	A (mm^2)	Perimeter (mm)	d_h (mm)	L (mm)
Pipes d10/L50	2.22	381,70	169,65	9,00	50
Pipes d13/L50	2.23	678,58	226,19	12,00	50
Pipes d16/L50	2.24	923,63	263,89	14,00	50
Pipes d20/L50	2.25	1526,81	339,29	18,00	50
Pipes d10/L34	2.26	381,70	169,65	9,00	34
Pipes d13/L34	2.27	678,58	226,19	12,00	34
Pipes d16/L34	2.28	923,63	263,89	14,00	34
Pipes d20/L34	2.29	1526,81	339,29	18,00	34
Pipes d10/L16	2.30	381,70	169,65	9,00	16
Pipes d13/L16	2.31	678,58	226,19	12,00	16
Pipes d16/L16	2.32	923,63	263,89	14,00	16
Pipes d20/L16	2.33	1526,81	339,29	18,00	16

3.3 Measurement setup

Most common blower door tests consist of a calibrated, variable-speed fan, a pressure measurement instrument, called a manometer and a framework used to mount the fan in a building opening. The setup for this test is a bit more comprehensive, to achieve more accurate results.

3.3.1 Equipment

Extendable door
The framework exists of various panels with draught strip on the sides. Two panels can extend in the horizontal direction and contain an opening that fits a ventilator. If the ventilator is absent, the opening can be closed with a sealing plate. Lastly there is one panel, extendable in two directions, to cover the height of the door. All panels are clamped in the original doorframe. As extra precaution, the entire panelled door is covered with a sheet of plastic that and sealed with duct tape to the doorframe and measuring tube.

Ventilator
On the outside of the measurement room a ventilator is placed in front of the opening in the extendable door. The ventilator is of the brand Fischbach, type D770/E 650-4, and has a maximum pressure difference of 648 Pa and a maximum air output of 1,426 m3/s. The number of revolutions of the ventilator is adjusted by means of an **autotransformer**, which is placed inside the measuring room.

Measuring tube
A PVC tubing of 30 cm in diameter is mounted on the ventilator, to guide the air flow through the extendable door, inwards the measurement room. A set of calibrated measuring flanges fit inside the tube, to reduce the section of the tube and thus increase the velocity of the air inside the tube, at equal pressure difference. Their calibration can be found in Appendix 2.1.

Digital micro fan-wheel anemometer

At 45 centimeters from the end of the PVC tube, an anemometer is placed in the center of the section of the tube. The anemometer is of the brand Thies Clima, and has serial number 0101121. The air velocity in the tube can be read off live, or integrated over a period of 26 seconds.
The digital display of the anemometer has an accuracy of 0,1 m/s.
The calibration certificate can be found in Appendix 2.2.
Based on this calibration a fourth-order polynomial formula is composed to approximate the intermediate values: $v_{corrected} = -1{,}19122872671573 \cdot 10^{-6} \cdot \mathrm{v}_{reading}^{4} + 1{,}87359890608141 \cdot 10^{-4} \cdot \mathrm{v}_{reading}^{3} - 2{,}141385101608 \cdot 10^{-3} \cdot \mathrm{v}_{reading}^{2} + 0{,}896870400814093 \cdot v_{reading} + 0{,}781625048580583$
The result is showed in the graph below.

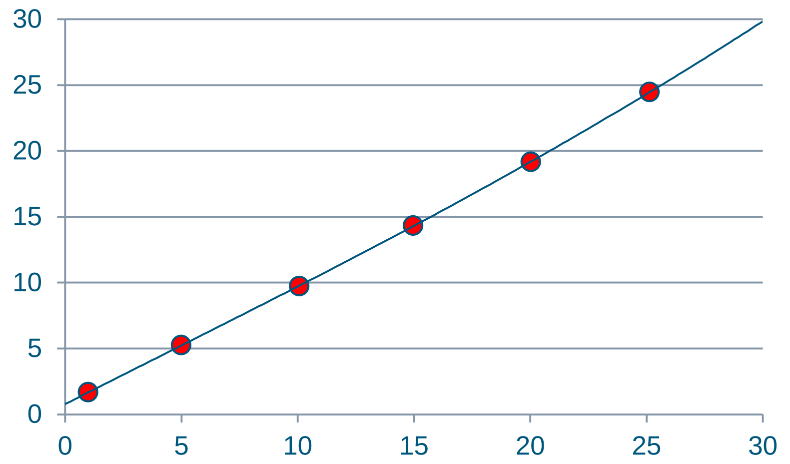

Figure 3.5 - Approximation corrected readings anemometer (x = reading, y = corrected)

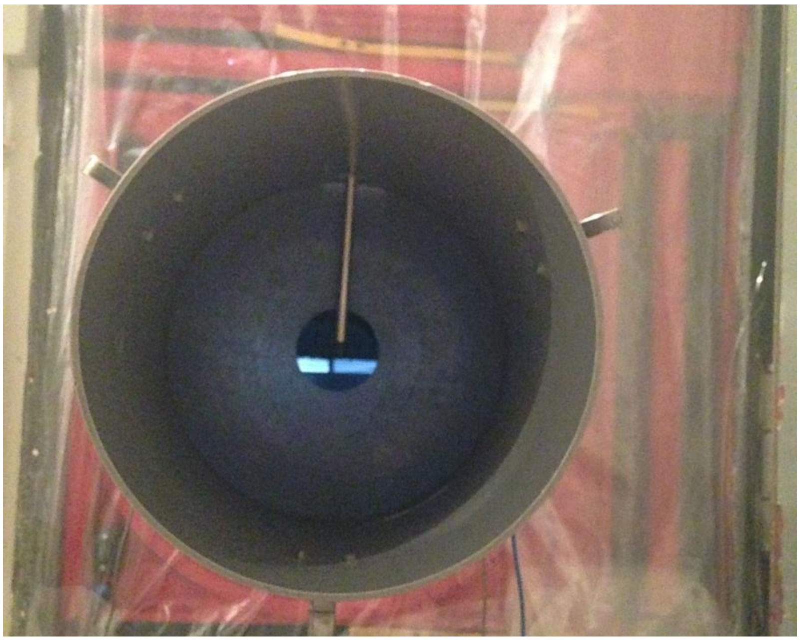

Figure 3.6 - View of flanges and anemometer inside PVC tube

Inclined well-type manometer
Lastly, a manometer is used for registering the pressure difference of the measurement room with its environment. The manometer is of the brand Airflow, type 5, serial number 99905. The manometer is levelled using the straight edges on top and placed in the horizontal position. In this position the instrument can be read in Pa with a multiplication factor of 50 and an accuracy of 0,25 Pa.
The calibration certificate can be found in Appendix 2.3.

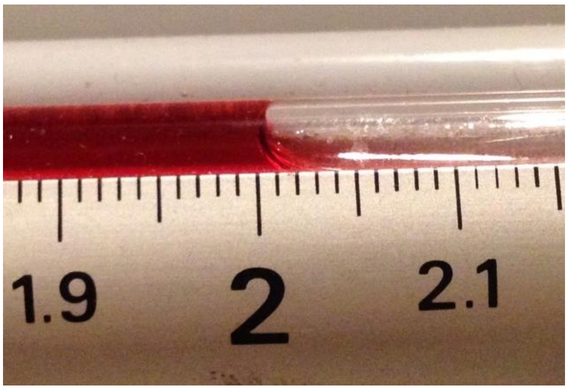

Figure 3.7 - Manometer reading of 100 Pa

3.3.2 Setup

Figure 3.8 - Measurement setup with manometer, measuring tube inside panelled door and measuring window with closed MDF

3.3.3 Measurement procedure

First all measurement conditions are checked, to ensure all environmental properties are accurate. All openings are sealed with duct tape and a baseline assessment is performed to check whether all assemblies are air tight. During measurements the ventilator blows air into the enclosure. By adjusting the number of revolutions of the ventilator with the autotransformer the required pressure difference can be maintained. After a stable situation is achieved, pressure difference and air flow are recorded.

The observed air flow is the total air flow going in and out of the measuring rooms envelope; $q_{v;total}$. Since it is not feasible to provide the entire room with an air tight sealer, it cannot be excluded that air leakage may occur besides the applied openings in the measuring window. Therefor a measurement with a closed sheet of MDF is performed, to determine the leakage of the measurement rooms envelope itself: $q_{v;testroom}$. The result of the subtraction of these two is the air flow through the impeded opening: $q_{v;opening}$.

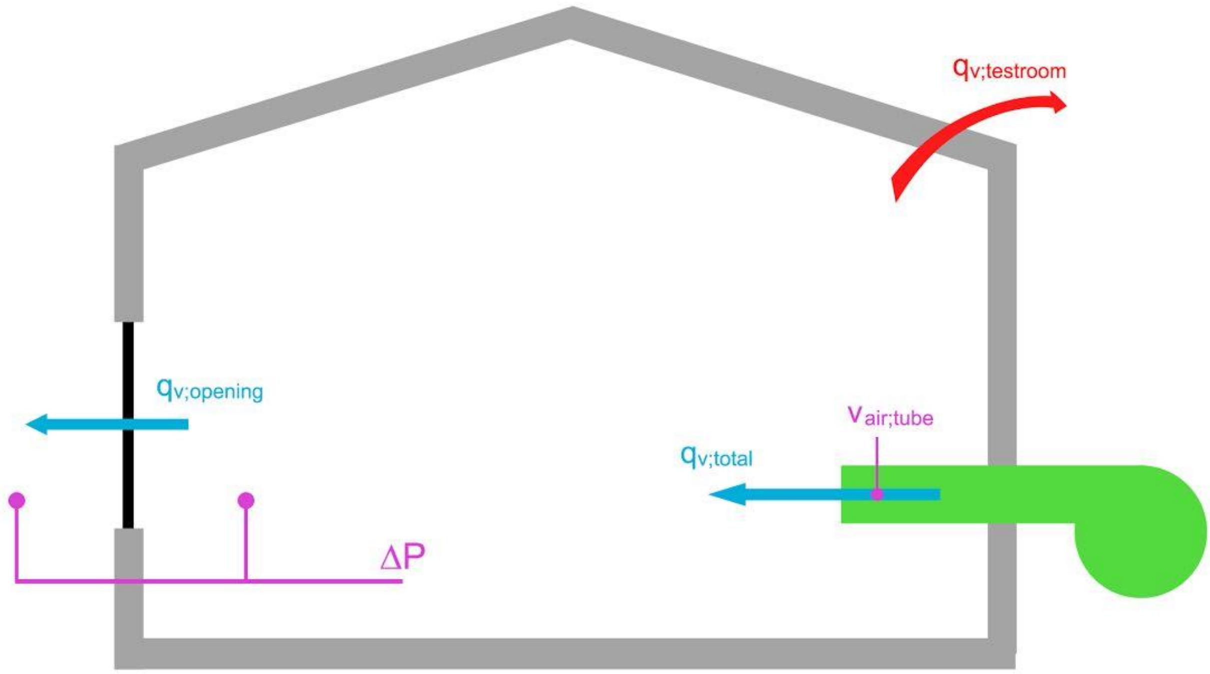

Figure 3.9 – Schematic measurement principle

Measurement conditions
In order to perform a good blower door measurement, the test room should be as independent of the rest of the building as possible. This means all surrounding rooms must be opened in order for the air to flow free from the leakage openings back to the ventilator.
High temperature differences between the test room and its surroundings must be avoided, to avoid any unwanted air flow due to convection.

Data collecting
When the pressure difference is brought to a stable level, the air velocity inside the PVC tube is measured. The accuracy of this measurement procedure is largely dependent on the instrumentation and apparatus used and on the ambient conditions under which the data are taken. Using the calibration data, the recorded readings are calculated to corrected values.

Measurements are made at six to ten pressure differences, evenly spaced over the interval between 10 Pa and the maximum obtainable pressure difference, with 100 Pa as an absolute maximum. While keeping the desired pressure difference as level as possible, the air velocity is registered and integrated for 26 seconds. In order to minimize errors each measurement is repeated at least once. When both measurements are within the range of 2 decimals the average value is taken to be true. If the difference between two readings is larger, the measurement will be repeated up to five times to get a good average.

3.4 Data collecting

The geometric definitions of the room are recorded to give an impression of the dimensions of the test room. The environmental definitions are used to correct the measured values. Besides the pressure difference and the air velocity inside the PVC tube, also the temperature both inside and outside of room D165 is monitored. Before starting and halfway each set of measurements the bias pressure is checked. A full overview of all the test results per dataset can be found in Appendix A. For this thesis only the difference between the datasets and possible correlations of the air flow rate and the openings geometry are of interest.

3.4.1 Data corrections

Pressure difference
Since the test room is built as a separate box inside the building, the air surrounding the test room can flow unimpeded and the bias pressure is recorded to be stable around zero for all datasets.
In case a bias pressure it must be noted that the average zero-flow pressure difference (offset) should be subtracted from each of the measured pressure differences, ΔP_m, to obtain the induced pressure differences, ΔP.
There is also a correction for the influence of altitude on the pressure difference, in case there is a height difference between the observation points of the manometer. During the measurements performed for this thesis this is not necessary, since the measurement locations, both inside and outside of the test room, were at the same height (floor level).

Air flow rate
The reading of the anemometer provides a value for the air velocity at the centre of the PVC tube: v_r. Using the calibration of the anemometer this reading is corrected into the measured velocity v_m. After multiplication with the section area of the flange and the calibrated coefficient of the latter, the result is a measurement of the air flow rate q_m.
A last correction needs to be performed for the temperature and pressure at the flow measuring device to convert the air flow rates, q_m, to air flow rates, q_{env}, through the building envelope for depressurization:

$$q_{env} = q_m \left(\frac{\rho_{int}}{\rho_e}\right) \approx q_m \left(\frac{T_e}{T_{int}}\right) \qquad [32]$$

Where:

q	volumetric air flow	m^3/s
ρ	density	kg/m^3
T	temperature	°C

The temperature is measured at the start, halfway and by the end of each set of data, that is per opening. Since the temperature proved to be of a constant nature, the mean of these readings is used to correct each measured dataset.

3.4.2 Baseline assessment

The leakage area of the envelope of the measurement room is assed. Because the test window is applied from the inside of the room, during the over pressure test the panel is pressed into the sealant, while it is sucked out of its sockets during the under pressure test. For this reason it is decided to only perform pressurization tests and to simulate depressurization by inversing the measuring panel inside the frame. After some extra sealing of the emergency exit and the measurement door the leakage area of the envelope is found to be about 10 cm^2. Although this is a very low value for an envelope of 128,3 m^2, compared with the affixed known openings the contribution of the rooms leakage is over 10% of the total. Since this is too high for a value to be neglected, the air flow rate of the envelope is over the interval of 10 – 100 Pa:

Table 5 - Baseline assessment 1

ΔP	$q_{testroom}$	ΔP	$q_{testroom}$
10	0,0043	60	0,0142
20	0,0069	70	0,0159
30	0,0090	80	0,0176
40	0,0109	90	0,0194
50	0,0125	100	0,0207

These values will later be subtracted from the measured values to calculate the flow through the affixed openings only:

$$q_{opening} = q_{envelope} - q_{testroom} \quad [33]$$

3.4.3 Results

The air flow rate through the building envelope will be plotted against the corresponding pressure differences. Each measured combination of Q and P will form a data point in the graph. In line with the power law theory these points adjust to a straight line when plotted on a double logarithmic scale. Using an unweighted log-linearized regression technique a value for the flow exponent can be found. Substituting this value of a single data point will algebraically determine the flow coefficient.

A lot of research has been done to the computational approach of air tightness approximations. As can be read in section 2.2 another commonly used method is the quadratic formula. For this purpose $q_{env}^2$is calculated. Based on the values of q_{env} and q_{env}^2 with their corresponding pressure differences, a quadratic regression is applied, to determine the values for A and B for each opening.

Table 6 - Results measurements dataset 1

	Power law		Quadratic formula	
Measurement (#)	c	n	A	B
1.1	0,0075	0,4806	-60	21114
1.2	0,0073	0,4924	12	18798
1.3	0,0077	0,4890	-3	17877
1.4	0,0075	0,4806	-60	21114
1.5	0,0072	0,5004	31	17588
1.6	0,0084	0,4950	5	13888
1.7	0,0011	0,4019	-4925	2493976
1.8	0,0075	0,4806	-60	21114
1.9	0,0035	0,4443	-654	153751

Table 7 - Results measurements dataset 2

	Power law		Quadratic formula	
Measurement (#)	c	n	A	B
2.01	0,0000	0,9524	54801	1737303
2.02	0,0001	0,9170	1	488509
2.03	0,0001	0,9565	20896	-58773
2.04	0,0005	0,5780	1466	1548366
2.05	0,0011	0,5232	-59	674944
2.06	0,0017	0,4927	91	340592
2.07	0,0024	0,4793	-254	220633
2.08	0,0035	0,4768	-142	103509
2.09	0,0047	0,4709	-222	64453
2.10	0,0000	1,1835	130105	-33690792
2.11	x	x	x	x
2.12	0,0002	0,5967	15120	10668389
2.13	0,0003	0,5479	6046	5919922
2.14	0,0004	0,5603	4047	2894629
2.15	0,0005	0,5967	3152	1296304
2.16	0,0005	0,5202	615	3691301
2.17	0,0010	0,4683	-1219	1597681
2.18	0,0013	0,4859	-794	788640
2.19	0,0020	0,4502	-942	445425
2.20	0,0031	0,4491	-683	190438
2.21	0,0042	0,4633	-239	83345
2.22	0,0001	0,6478	8464	17521671
2.23	0,0002	0,6349	9866	2405969
2.24	0,0005	0,5224	648	3825424
2.25	0,0010	0,4878	-287	1131416
2.26	0,0002	0,5695	12597	9889080
2.27	0,0004	0,5595	6004	2189657
2.28	0,0006	0,5122	-601	2694195
2.29	0,0011	0,4841	-786	1018778
2.30	0,0002	0,6354	12884	6634974
2.31	0,0004	0,5683	1571	2915632
2.32	0,0007	0,4930	-2084	2831417
2.33	0,0013	0,4700	-1470	937879

3.4.4 Validation

To exclude some uncertainties from the test results, three methods were used to check the correctness of both the measurement setup and the result found. Since each measuring panel was lasered with multiple openings but a measurement needs to be executed on every single opening, it is very important that the sealant of the openings that are not of concern is really air tight.
Secondly, due to the widening gradient in the wall that contains the measuring window, it was not certain that these angles would affect the air flow inside the measuring room, near the panel. If this is the case, the position of an opening in the panel would influence the results.
Lastly the robustness of the equipment used was questioned. Since the measurements would be performed on very small openings, a small deviation in the results, could have a great influence on the flow characteristic results.

Sealing material
First a baseline assessment was performed using a closed MDF panel in the measurement window. Second we placed the MDF panel with the lasered openings and closed all openings with duct tape, in order to check whether duct tape is a good material to close the openings that are not of interest during measurements.

Table 8 - Validation duct tape as sealing material

ΔP (Pa)	Q_v (m^3/s)		Deviation
	Closed MDF	Closed MDF	($Q_{v,MDF}$ / $Q_{v,duct\ tape}$)
10	**0,0043**	**0,0043**	1,56%
20	0,0069	0,0066	4,78%
30	0,009	0,0088	1,48%
40	0,0109	0,0106	2,48%
50	0,0125	0,0124	1,10%
60	0,0142	0,0142	0,00%
70	0,0159	0,0158	0,91%
80	0,0176	0,0171	2,94%
90	0,0194	0,0187	3,14%
100	0,0207	0,02	3,37%
n	**0,6781**	**0,6785**	**0,06%**
c	**0,0009**	**0,0009**	**-2,40%**

The deviation in the measurement values are all within 5% as the resulting flow characteristics conform the powerlaw is even within 2,5%. Therefor duct tape is accepted as material to temporarily close the lasered openings.

Position opening
A second validation is executed, to check whether the position of the openings within the measuring panel and window is of any influence on the resulting readings. The circular opening in the middle of panel 1 is exactly the same as the one in the corner. The readings for both openings are as follows:

Table 9 - Validation opening position

ΔP (Pa)	Q_v (m^3/s)		Deviation
	Middle	Corner	($Q_{v,middle}$ / $Q_{v,corner}$)
10	0,0273	0,0275	0,90%
20	0,0395	0,0393	-0,64%
30	0,048	0,0485	1,07%
40	0,0556	0,0564	1,42%
50	0,0626	0,0634	1,30%
60	0,069	0,0707	2,40%
70	0,0735	0,0732	-0,39%
n	**0,5176**	**0,5272**	**1,83%**
c	**0,0083**	**0,0081**	**-2,22%**

The deviation between the two measurements is assumed to be small enough to neglect any influence regarding the position of the opening inside the measurement window.

Flow rate readings

Lastly, the method used to measure the ventilation flow is checked by comparing them with the readings of a FlowFinder which is placed over opening in question. Since the presence of the FlowFinder could possibly change the flow characteristics of the opening, both readings were taken simultaneously. The flow finder has a known accuracy of +/- 3% of the reading, or at least +/- 3 m^3/hr (=0,0008 m^3/s). Using this data the accuracy range of the FlowFinder is determined for each measurement. This method is used on the circular opening, the square and on four small circles together:

Table 10 - Validation circular opening / FlowFinder

ΔP (Pa)	Q_v (m^3/s)			Deviation
	FlowFinder	Accuracy range	Anemometer	($Q_{v,anemo}$ / $Q_{v,FF}$)
10	0,0218	0,0210 – 0,0225	0,0230	-1,62%
20	0,0303	0,0294 – 0,0312	0,0317	-1,57%
30	0,0375	0,0364 – 0,0386	0,0383	0,00%
40	0,0458	0,0444 – 0,0472	0,0442	0,51%
50	0,0517	0,0501 – 0,0533	0,0499	0,50%
60	0,0571	0,0554 – 0,0588	0,0551	0,52%
70	0,0595	0,0577 – 0,0613	0,0569	1,41%

Table 11 - Validation squared opening / FlowFinder

ΔP (Pa)	Q_v (m^3/s)			Deviation
	FlowFinder	Accuracy range	Anemometer	($Q_{v,anemo}$ / $Q_{v,FF}$)
10	0,0225	0,0217 – 0,0233	0,0230	0,00%
20	0,0311	0,0302 – 0,0320	0,0317	0,00%
30	0,0383	0,0372 – 0,0394	0,0383	0,00%
40	0,0461	0,0447 – 0,0475	0,0442	1,16%
50	0,0531	0,0515 – 0,0547	0,0507	1,57%
60	0,0587	0,0569 – 0,0605	0,0548	3,76%

Table 12 - Validation 4 small circles / FlowFinder

ΔP (Pa)	Q_v (m^3/s)			Deviation
	FlowFinder	Accuracy range	Anemometer	($Q_{v,anemo}$ / $Q_{v,FF}$)
20	0,0128	0,0120 – 0,0136	0,0134	0,00%
40	0,0175	0,0167 – 0,0183	0,0187	-2,00%
60	0,0208	0,0200 – 0,0216	0,0221	-2,16%
80	0,0247	0,0239 – 0,0255	0,0250	0,00%
100	0,0264	0,0256 – 0,0272	0,0278	-2,08%

We see that the volumetric flow is decreased with 15 – 20% when the readings of the anemometer are compared with the readings of the same openings tested without FlowFinder. Therefor the readings of the FlowFinder are only compared with the anemometer readings that were taken simultaneously.
Only a third of the readings of the anemometer felt within the accuracy range of the FlowFinder. With the exception of one reading (the squared opening at highest pressure difference), all other readings were within 3% of the range of the FlowFinder.
Since the presence of the FlowFinder over the opening was of a much larger influence, at both high and low pressure differences and for the largest and smallest openings, the method with the anemometer is assumed to be more accurate for our research.

3.4.5 Edge effects

Since the results of the circular openings with a pipe inserted did not show the expected results, the hypothesis was raised that the protrusion of the pipes where of influence. To discard this prospect, the edge of the pipes needed to be in line with the surface of the panel. Due to the weight of the pipes, only the 16 centime length variants remained clamped in the openings when retracted to the edge of the panel.

Table 13 - Index measurement dataset 3

Shape	Measurement	A_e (mm^2)	Perimeter (mm)	d_h (mm)	L (mm)
Pipes d10/L16*	3.1	381,70	169,65	9,00	16
Pipes d13/L16*	3.2	678,58	226,19	12,00	16
Pipes d16/L16*	3.3	923,63	263,89	14,00	16
Pipes d20/L16*	3.4	1526,81	339,29	18,00	16

3.5 Data Analysis

3.5.1 Power law & Quadratic formula fit

The first and most striking observation is that a large amount of the flow characteristics show a flow exponent of less than the theoretical limit of 0,5. If n drops below the theoretical value of 0,5 the power law is no longer valid (ASTM E779-10), due to Bernoulli's limit (Walker, Wilson, and Sherman 1998) (see section 2.2.1).

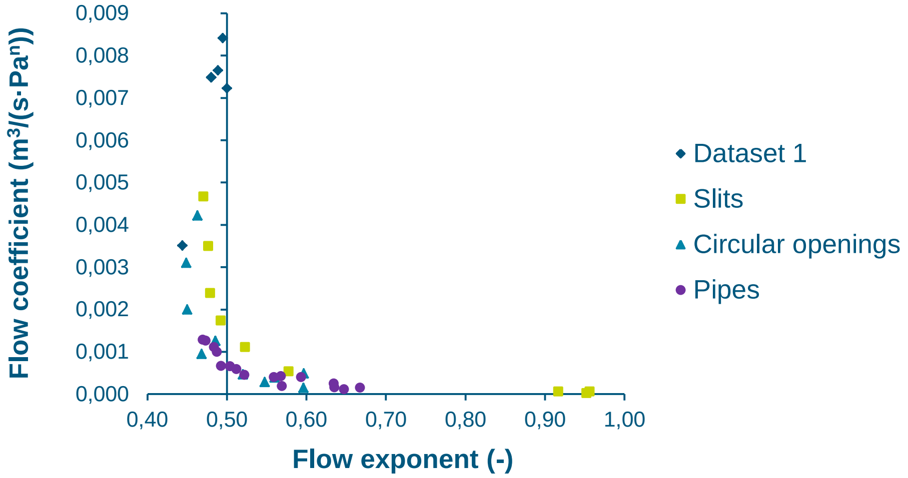

Figure 3.10 - Chart of all datasets for Power Law

Also, when we investigate the data for the quadratic formula, we can find a lot of negative values. In this equation A is the coefficient for the fully developed laminar friction losses and B indicates the entry, exit and turbulent friction losses. A negative coefficient would indicate negative losses, which by theory is also impossible (see section 2.2.2).

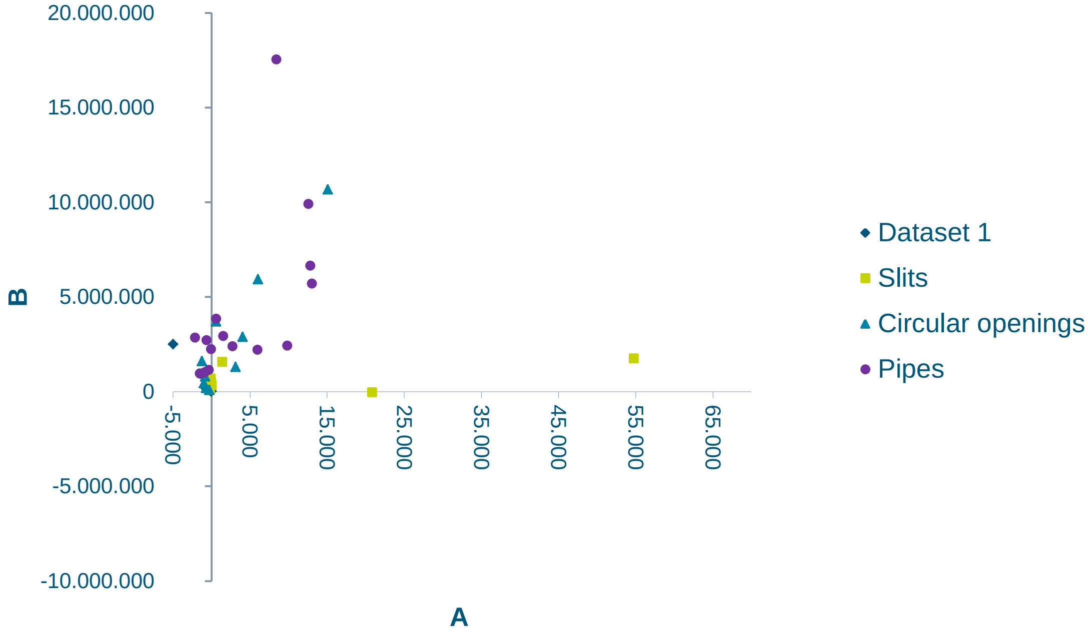

Figure 3.11 - Chart of all datasets for Quadratix Formula

Because the openings tested in these measurements all consist of openings made in an MDF sheet with a laser cutter, we assume that both the inlet and outlet of the opening have perpendicular edges. It is suspected that the influence of edge effects due to the squared corners of the test openings cannot be neglected and highly influence the flow behaviour inside the opening, which might cause these theoretically impossible values.

3.5.2 Further calculations

Based on the studied literature some other parameters outside the power law and quadratic formula are determined for each dataset.

Table 14 - Calculations on dataset 1

Meas. (#)	A (m^2)	$A_{e;50}$ (m^2)	ELA_{4Pa}	$u_{m;4}$ (m/s)	$u_{m;50}$ (m/s)	Re_4 (-)	Re_{50} (-)
1.1	0,0095	0,0054	0,0093	1,53	5,28	10164	34982
1.2	0,0095	0,0055	0,0092	1,52	5,37	10056	35557
1.3	0,0095	0,0057	0,0096	1,59	5,60	3673	12958
1.4	0,0095	0,0054	0,0093	1,53	5,28	9008	31002
1.5	0,0095	0,0056	0,0092	1,52	5,54	4302	15660
1.6	0,0095	0,0064	0,0106	1,76	6,31	1055	3782
1.7	0,00095	0,0006	0,0013	2,10	5,90	4395	12371
1.8	0,0095	0,0054	0,0093	1,53	5,28	3214	11062
1.9	0,0038	0,0022	0,0041	1,71	5,42	3585	11348

From this data we can see that the equivalent leakage area at 4 Pa a good indicator for the identification of actual leaks as mentioned in section 2.3.2, although the value is not correct, it is revealing that all the different shapes are calculated within the same area as the actual opening, while most flow exponents lie below the critical value of 0,5.
Another observation is the difference in air velocities through the openings in set 1.7, 1.8 and 1.9. Each of these measurements consisted of one or more identical small openings. As Walker, Wilson and Sherman (1998) concluded multiple openings in the same envelope will influence each other (See section 2.2.4).

Besides the observation that a high ELA indicates a low flow exponent and on the contrary a high flow exponent corresponds with a low ELA, there is no mathematical correlation to be found in order to use one of the two as an indicator for the other.

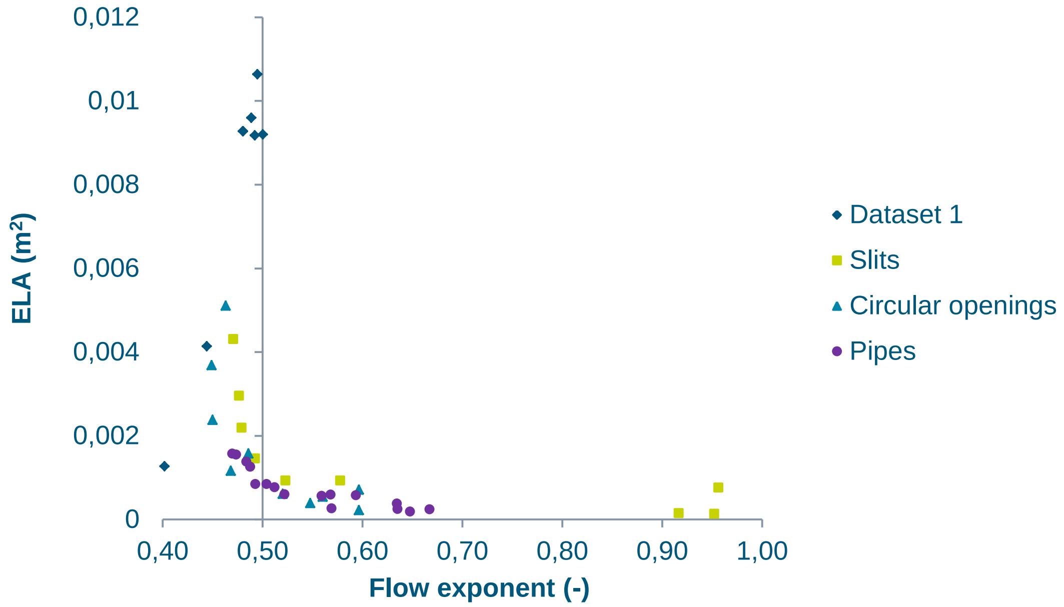

Figure 3.12 - Graphical representation of ELA and Flow exponent

When investigating the Reynolds number, we see that the threshold concerning the beginning of transition from laminar to turbulent flow which should be <2300, based on the hydraulic diameter and mean velocity (Bejan 2013; Etheridge 2012). Even when the Reynolds number becomes <2300 (red line in figure 3.13) the flow exponent can still indicate highly turbulent flow such as at measurement 2.4. Only with the elongated shaped slits a correlation between a declining Reynolds number and a rising flow exponent could be recognised.

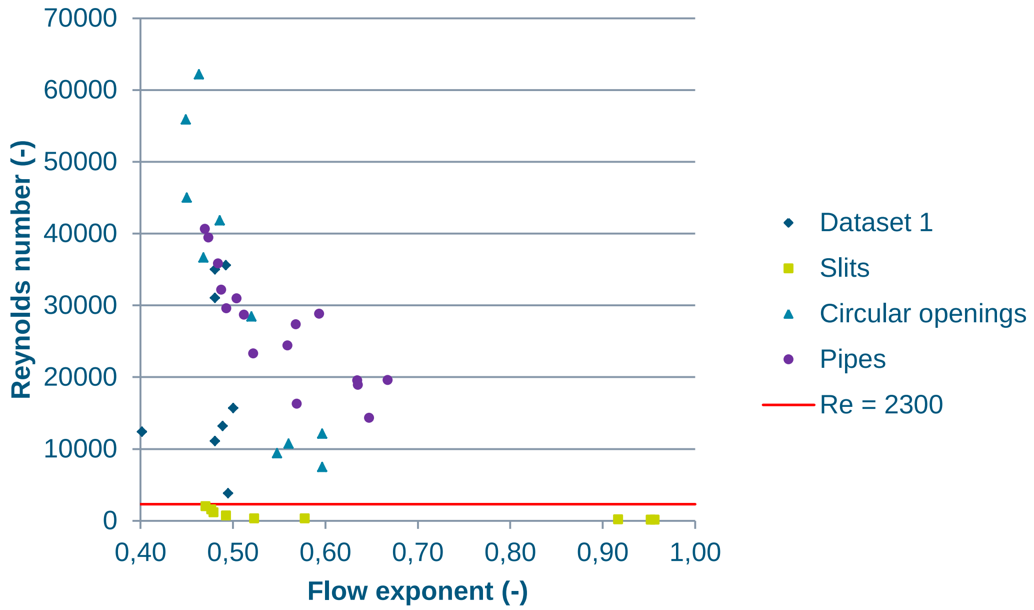

Figure 3.13 - Graphical representation of Reynolds number & Flow exponent

For the slit openings also the correlation between the depth of the slit and the flow exponent has been visualised:

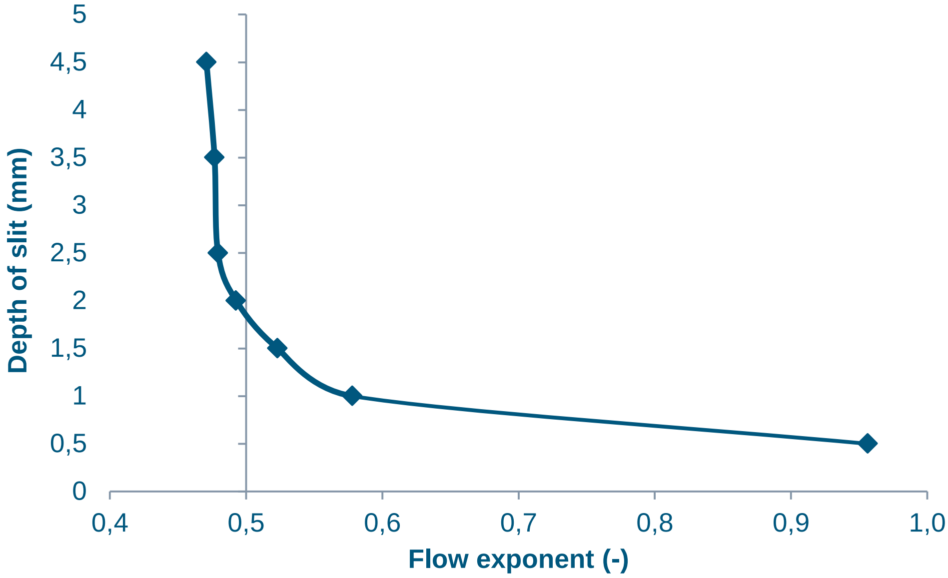

Figure 3.14 - Crack thickness : Flow Exponent

There seems to be a correlation between the depth and the flow exponent, however a more critical view explains that the range between 0,5 and 1,0 mm depth covers almost the entire theoretical range of the flow exponent (0,56 – 0,95).

To check wether the same correlation can be found all the circular openings of measuring panel 2 are also plotted for their hydraulic diameter against the flow exponent:

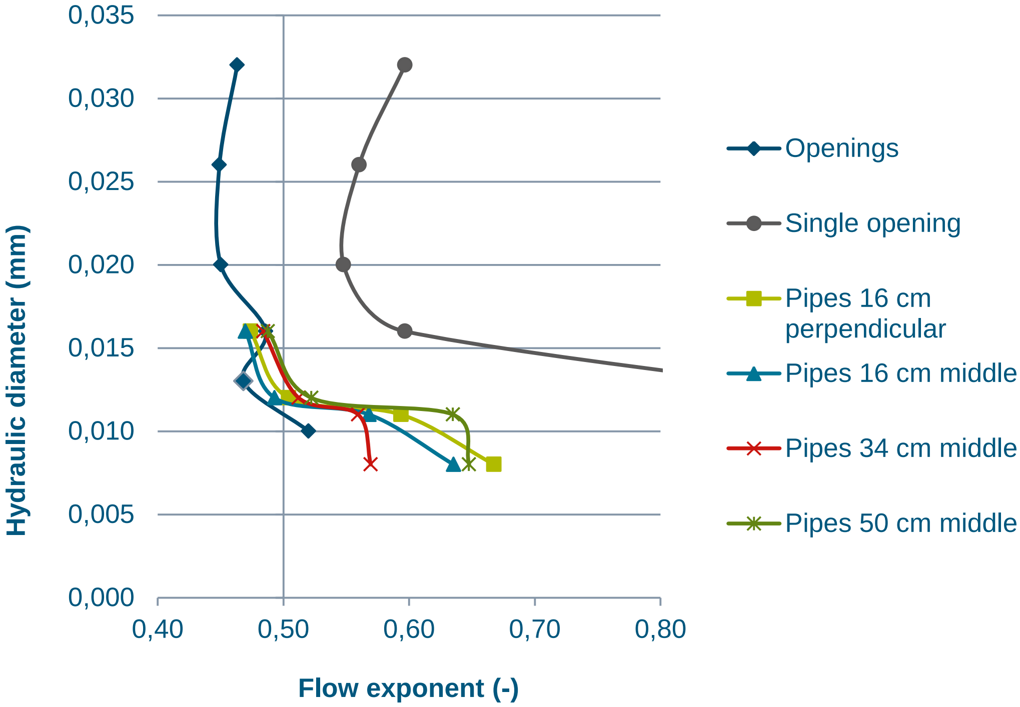

Figure 3.15 - Variability of d_h: Flow Exponent

The thing to notice in Figure 3.15 is steep change in the trend towards turbulence for each smalles openings. Also the influence of the length of the pipe could be read from this figure. Although the strange observation can be done that the line of the 34 cm pipes crosses the lines of both 16 cm pipes. This might be caused by the finish of the cutting line, which is done by hand, but this cannot be said with certainty.

David Etheridge (2012) uses the ratio between de length and width (hydraulic diameter) of the crack as indicator for the development of the flow regime. Therefor also this parameter is plotted against the flow exponent:

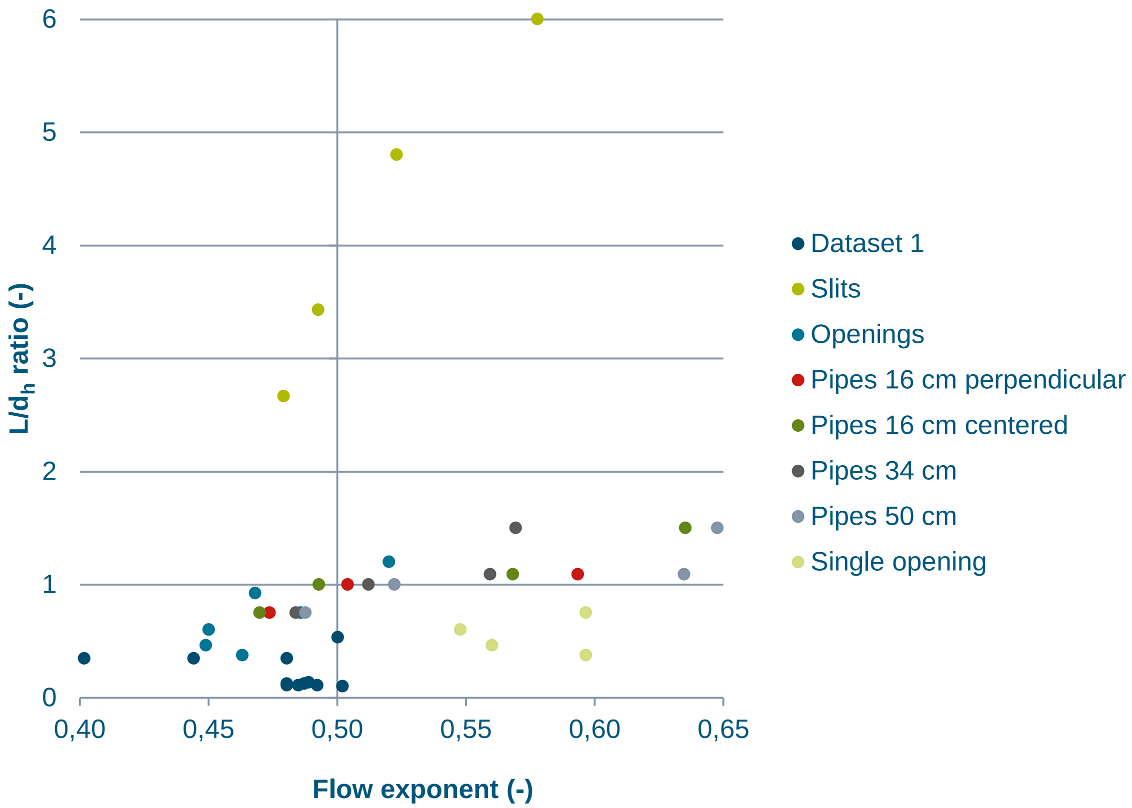

Figure 3.16 - Variability L/d ratio : flow exponent

3.6 Error Investigation

3.6.1 Precision

As mentioned in the measurement procedure all measurements are repeated at least once. If the measurement from the anemometer is within a margin of 0,2 m/s the average of both values is taken. If the difference is larger, an extra measurement is taken per 0,1 m/s difference (so measuring 7,1 and 7,7 means an extra measurement, say 7,3. Then the measurement of 7,7 is ignored and a fourth measurement is taken for control). However, in most recordings the readings where within 0,2 m/s. Since all readings are entered at rounded values of one decimal per m/s, using the calibration of the flanges we can calculate the accuracy of the air flow measurements:

Table 15 - Accuracy q_{env} (m^3/s) per flange

#1	#2	#3	#4	#5
0,00001	0,00011	0,00042	0,00187	0,00730

It appears that the volumetric air flow measured is within the size of the accuracy of the equipment. For some datasets the lowest data point is smaller than the accuracy of the flange used. (See appendix A, measurement 2.10, 2.12, 2.13, 2.22, 2.23, 2.26, 2.27, 2.30 and 2.34). Although both the power law and the quadratic formula still have a good correlation on the dataset included these lowest values, it is necessary to question the validity of the calculated coefficients. It could be that instead of the opening in the measuring panel, the characteristics of the flange are measured instead.

3.6.2 Error propagation

Because the flow through the designed leaks is calculated by the difference between the baseline-assessment and the assessment with openings, all errors induced in the measurement are doubled. Making the accuracy of the pressure reading 0,1 Pa and the accuracy of the air flow rate:

Table 16 - Accuracy of $q_{opening}$ (m^3/s) per flange

#1	#2	#3	#4	#5
0,00002	0,00022	0,00084	0,00373	0,01459

No further explanation is needed to understand that the argument of readings within the range of this accuracy now even holds for a larger section of the measured data.

3.6.3 Robustness

Although the above indicate the total error can be given a magnitude, there are more factors that influence the reading then just the accuracy and precision alone.
For instance the pressure difference is accomplished by adjusting an autotransformer. Since this device contains a copper coil, the width of the windings determines the interval with which the revolutions of the ventilator can be adjusted. Especially at the measurements of the small openings, this caused difficulties. Sometimes the autotransformer had to be kept switching in order to maintain the desired pressure level. This leads to the large suspicion that this procedure might have had an influence on the reading for the air flow rate.
Secondly the anemometer is assumed to be mounted exactly in the middle of the PVC tube. Since this placement is performed manually, it is most likely that there was a little deflection. Especially the readings with the smaller flanges might be influenced.
Another uncertainty that increases, when the size of the flange decreases, is the correctness of the flanges. Although these are calibrated, it may well be that they are slightly damaged due to the frequent transport. They show a lot of scratch marks, both on the outer and the inner rim. For the inner ring this might cause small changes in the openings surface area. For the outer ring a small damage might cause the flange to shift inside the PVC tube, causing the centre of the flange and the anemometer to be unaligned.
It is expected that errors due to robustness are of a smaller range then the errors caused by the precision and propagation, and can therefor be neglected.

3.6.4 Uncertainties

The last deviation that needs to be taken in mind is the significance of the flow coefficient. Extrapolation of the data to pressures outside of the tested range should be performed with great awareness. Specifically when the calculated flow exponent lies outside of the theoretical valid frame, it is impossible to make a statement on the geometry or area of the leakage path, as the calculated exponent implies that those leakage pathways are changing relative to pressure (Urquhart and Richman 2015).
However the calculation method used to determine the flow coefficient actually is an extrapolating of the measured data down to 1 Pa.

3.7 Findings

Although the exact values presented by the measurements are expected to be incorrect due to the errors caused by the equipment and the unknown influence edge effects might have, some trends can still be noted and there are a few remarks that can be formed based on these measurements.

- Both the power law and the Quadratic formula form a good fit for air tightness measurements. However great deflections originate for both models when it is extrapolated outside of the measured interval, which is clearly illustrated when we look at the results of one dataset (for example 1.1). Both formulas fit perfect within the range of the measurements, but the deviate increases when extrapolation continues.

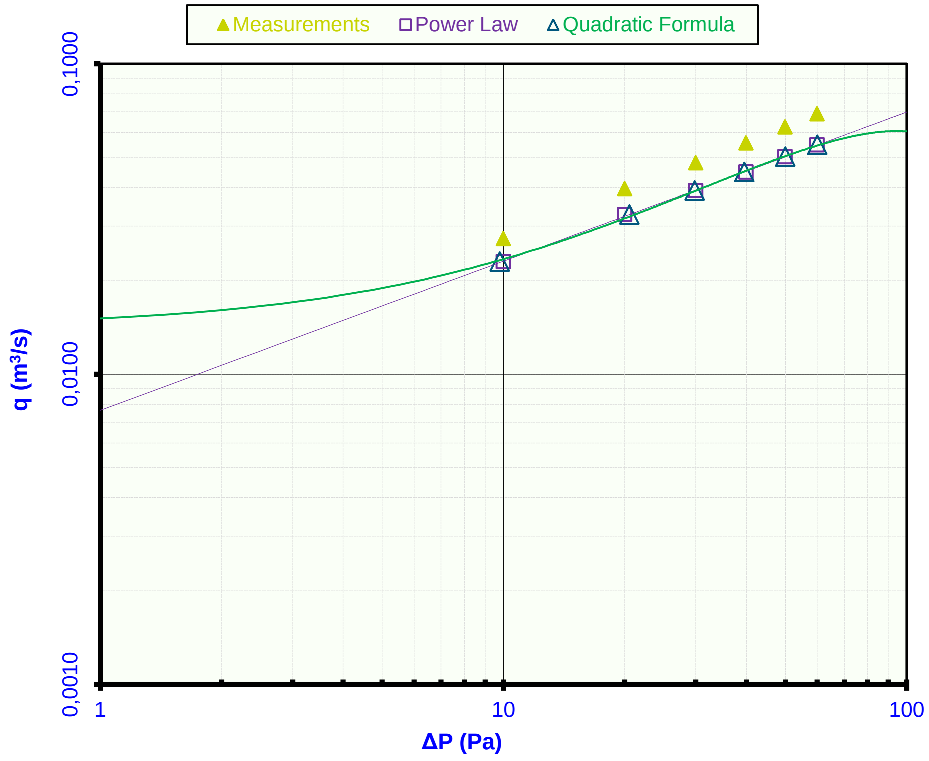

Figure 3.17 - Measurement results of 1.1 with Power Law and Quadratic Formula fitted

- Figure 3.17 also illustrates what happens if the wrong set of flow coefficient/exponent is used. A change in flow coefficient would cause a displacement along the y-axis of the entire dataset, and a change of the flow exponent causes a change in inclination with the coefficient (value for 1 Pa) as pivoting point. Since the graph is drawn with a double logarithmic scale, errors grow exponentially.
- Theory implies that the flow exponent needs to lie in between the interval of 0,5 – 1,0, actual measurement results are not uncommon to fall outside this range. Where the most accepted explanation for such values is a change in the environment such as opening valves or flaps, this test has showed that it can also occur in a fixed environment. The explanation for these observations most probably lies within the different losses that are neglected for framing the theoretical range. For example the above mentioned edge effects are suspected to play an important role by the formation of turbulence flow.
- The flow exponent from the power law is assumed to be normative for the type of flow of each measurement. This experiment is mostly focussed on the dependency of geometrical properties and in addition for the Reynolds number. Further study of fluid dynamics probably will give better understanding of the known loss coefficients within this topic and may lead to a better indicator or even better calculation method then those available with current knowledge.

4 Computational model

4.1 Research design

4.1.1 Premeditation

Based on the results of the measurements the hypothesis raised that edge effects in the setup caused turbulence in the air current. Since the measured panels were fabricated by laser cuts in MDF plates, the edges of the openings are sharp. Due to the small thickness of the panels the hypothesis raised that the influence of the geometry of the opening is overshadowed by the edge effects.

4.2 Model description

Repeating the measurements with rounded edged would be too costly and time consuming. Therefor a CFD model is made. In order to save on calculation time and since we're only interested in the effect of the sharpness of the edges, a 2D model is created with Comsol Multiphysics 5.2, a general-purpose software platform, based on advanced numerical methods, for modeling and simulating physics-based problems such as fluid flow.

4.2.1 Geometry

The measurement setup is simulated with primitive solids by two boxes (100mm width, 200mm height), connected with a centred slit of 1 mm height and 12 mm length corresponding with the thickness of the MDF sheet used.
In order to change the edges the difference of a box and a circle with a diameter of 2 mm (twice the thickness of the slit) is added, as can be seen in Figure 4.1.

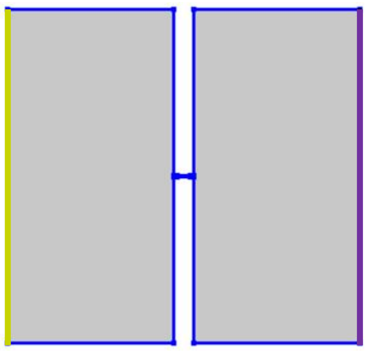
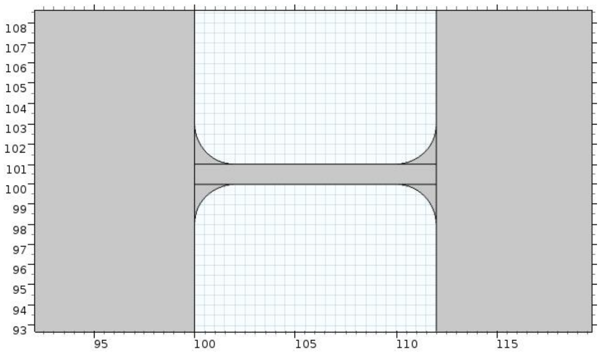

Figure 4.1 - Overview model (left) and dimensions slit (right) in Comsol

The geometry is covered with a mesh using the boundary layer option of the program and manual settings to make sure the interval between two knots on the edge of the slit is smaller than the slit itself. Therefor the settings for the element size on the edge are set to very fine. To save on calculation time the interval is accepted to grow rapidly when the knots get more distanced from the walls, so this element size is set to rough.

4.2.2 Settings

The left side wall of the left box (green line in Figure 4.1) is used as inlet and determined to be 4 or 50 Pa. The right side wall of the right box (purple line) is used as outlet. All other walls (blue) are boundaries for the flow.

All solids are recorded with the programs build in material properties for air (ρ = 1,205 kg/m^3 and μ = 0,00002 Pa/s).
For the calculation under “study” the Turbulent Flow, k-ε model is used with standard settings.
Wall roughness is eliminated from the calculation.

4.3 Results

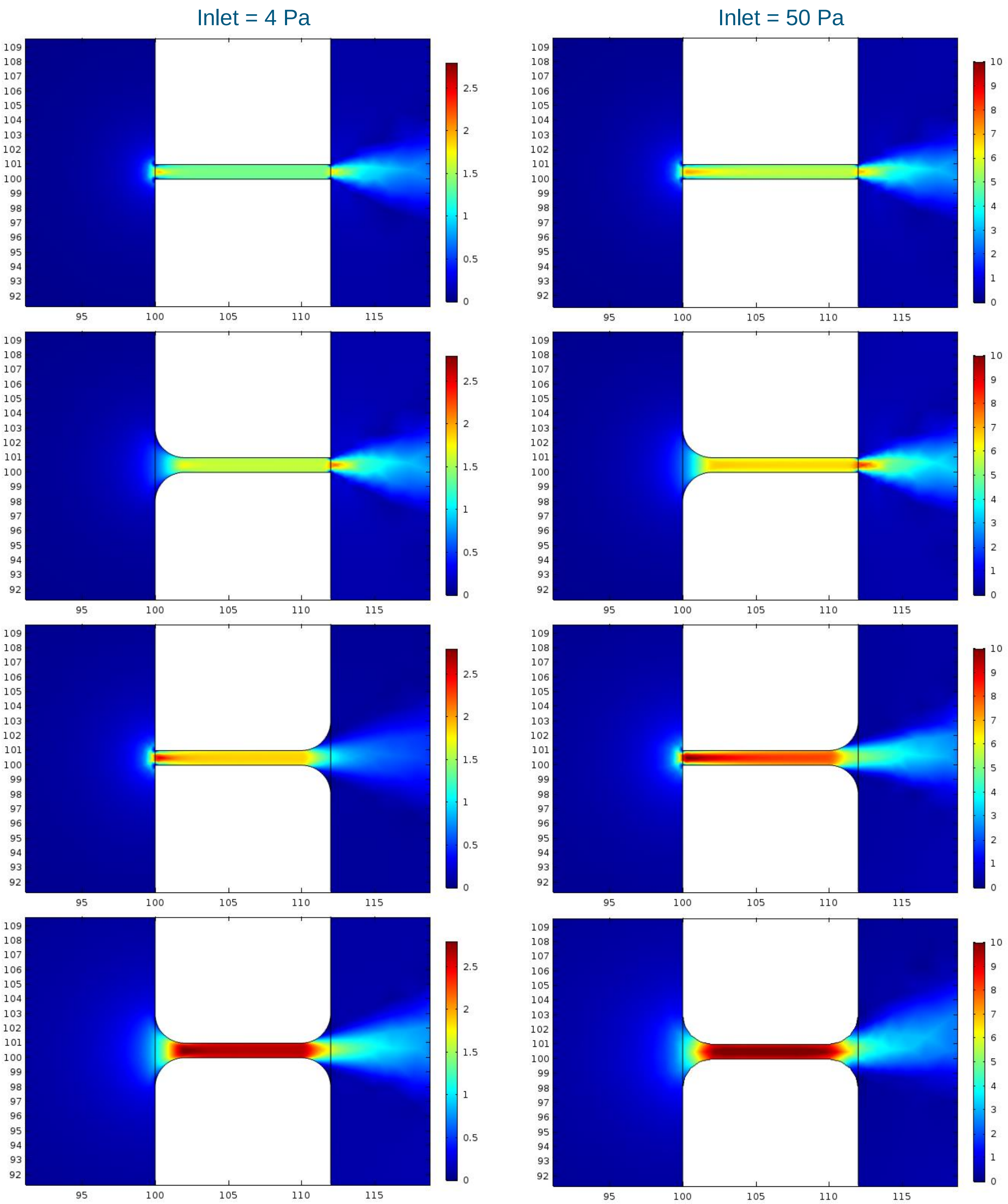

Figure 4.2 – Graphical results of air velocity (m/s)

4.4 Analysis

4.4.1 Input

When comparing the models with the same inlet pressure and same hydraulic diameter, it is very clear that there is a great effect on the air velocity at the outlet side. It seems that the effect of rounding the exit is even larger than the effect of a rounded inlet.
A remarkable observation can be made at the model with only a rounded exit. It seems that the air current is given a deviation upwards. When exploring the cause of this directional change, it appeared that the mesh that is created by the program isn't symmetrical. Since the outcome is the result of an iterative process, the little deflection could cause the remarkable result.

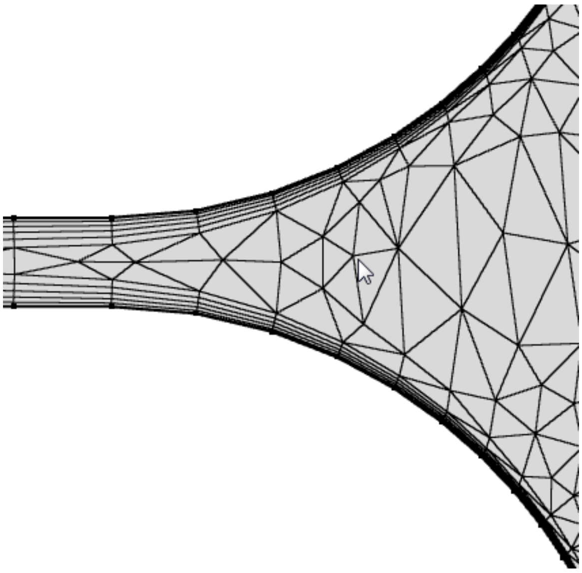

Figure 4.3 - Detail of mesh in rounded exit

4.4.2 Output

From the results it is very clear that rounding the edges of the slit has a large influence on the velocity and thus on the volumetric air flow which passes through. The influence of the rounded exit appears to be larger than the influence of a rounded inlet. Although the exact values for the velocities are incorrect due to standard settings and the problem with the mesh, the results from this model can still be seen as prove for the large influence of the edge effects of an opening.
Even more striking is the fact that the influence appears to be larger for higher pressure differences. When we look at the graphs for the 4 Pa pressure difference, we see that for the original model with sharp edges the mean air velocity inside the slit is about 1,4 m/s. With rounded edges this velocity increases to about 2,6 m/s, an increase of 85%.
The graphs for 50 Pa pressure difference show that the original model with sharp edges has a mean air velocity of 5,0 m/s. With rounded edges this velocity increases to about 10,0 m/s, an increase of 100%.
So the higher the pressure difference, the faster the velocity and thus the air flow volume will increase due to rounded edges. For the power law relationship this will cause a growth of the flow exponent (or in a $q^v/\Delta P$ graph a steeper slope). This endorses the hypothesis that sharp edges will introduce turbulent flows which determine the flow characteristics according to the power law. This means the results of the measurements in the transmission room cannot be used to base conclusions on the influence of the geometrical properties tested.

5 Conclusions and recommendations

5.1 Conlusions

This Master's thesis has investigated the air tightness of a building envelope. The scope was a quest towards a uniform calculation method for determination of the air permeability in the design phase. During the course of the research the intended problem definition proved to be too complicated. Drafting a new calculation method without a good overview of all relevant variables air tightness is concerned with, is simply not possible. Even drafting a list of necessary input that should be included in the design, based on the results of this research would lack for the same details as current standards and directives do. Still this research has added value for those interested in air tightness concerns.

5.1.1 Calculation methods

It is showed that Dutch standards are fully based on the power law expression for air flow, and prescribe an assumed flow exponent of 0,65. Based on the literature study and results from MbB it is illustrated that this value is based on information which is taken out of context. The collector of the data that is referenced as source, concluded himself that no clear correlation could be found. Also, his data came from several knowledge organisations from around the world. Worldwide there is a large variety in construction methods, making it very unlikely that there would be one parameter that describes this entire building stock.
As with the exponent, current knowledge on the power law's flow coefficient is questioned. There is a large variety in unities used in the various available documents, sometimes even within the same document. Current Dutch standards define a maximum air flow at 10 Pascal (q_{v10}) for a defined reference volume. These reference parameters are very useful to generate an index for air tightness in which different envelopes can be compared. However they do not form a guideline in the design phase since too many assumptions are included. A flow rate which is scaled to a reference volume does not provide any actual specific requirement for a certain surface or joint within the design. In addition, 10 Pascal is an arbitrary pressure and converting to the actual estimated pressure difference over the envelope would need a calculation method such as the power law, with proper characteristic values.

Still the power law is a useful tool when working on air tightness. The parameters C and n of the power law give a good correlation of measurement data, but they do not form a secure physical interpretation. Any translation of leakage geometry to flow characteristics of this calculation method will be very delicate and not applicable on other envelopes than tested.
Further, due to the transition of turbulent flow to laminar flow at low velocities, hence low pressure differences, measurement data collected in the range of 10-100 Pa is not representative for the occurring pressure differences which are in the range of 4-10 Pa. Since most buildings are subject to these lower pressure values, except for rooms with a controlled atmosphere, data gathered with current air tightness measurements do not form a solid basis for a prediction on air losses in practise.

The quadratic formula is a more fundamental model to register the air losses due to pressure differences. It represents coefficients for the laminar and turbulent contribution to the total flow, based on viscosity, density and geometrical properties of the openings.
Without exact knowledge of the geometry of leakage paths, it will be very hard to characterize the flow through these penetrations. With current knowledge the best advice would be to completely coat or wrap the envelope with an air tight layer.

5.1.2 Interpretation results

In order to test the hypotheses, measurements have been performed on openings that were cut into a sheet of 12 mm MDF by a laser. The ratio between the area and perimeter of a leakage opening is investigated to test whether there is a correlation with the formation of turbulent or laminar flow. A large section of the results showed theoretical impossible values, thus no substantive conclusions can be drawn based on this data. Due to the laser cuts the edges of the openings were perpendicular and it is expected that this caused edge effects which blurred the results. However it did appear that a very small diameter causes the development of laminar air flow, even though the tiny flow length through the MDF sheet.

The results of the numerical model just as the measurements cannot be interpreted as exact values. However the magnitude of the increase of velocity through an opening by rounding the edges was incontrovertible. Therefore, based on this model it can nevertheless be established that these edge effects induce turbulent flow which has significant effects on the flow rate of an opening.

In order to really get grip on this subject a study of the history of ventilation would make interesting reading. The development of standards and directives may be placed in context of the available knowledge when they were submitted. Eventually further research to air tightness will result in a complete set of new design rules and thus new standards. Current regulations drive the engineer or designer in a thought pattern without a grounded solution or guideline. Most engineers working on the problem of air tightness of building envelopes are not the engineers with solid knowledge of fluid mechanics. Probably the solution for predicting air tightness can only be found with a combined solid knowledge of both fluid dynamics and construction methods and detailing. Other researchers already have proven the analogue between ducts and their loss coefficients and flow through sharp edged orifices. Although the results of this research do not form a ground to determine the variables that indicate the flow exponent, the hypothesis that these can be found in flow dynamics is enlarged.

5.2 Recommendations

The outcome of this research differs completely from the initial expectations. This is partly explained by the gain of knowledge during the process and partly by the beforehand known data that appeared to be unfounded. Also the equipment used for the measurements showed to be too robust. These are lessons learned for all who will work on follow-up study.
Although a further assessment and comparison of the current building stock and their air tightness seams the first grid to found any prediction methods for future building performances, the behaviour of air flow through single openings should be understood. Only when this knowledge is mapped the mutual influence of different openings in one building envelope can be predicted.

5.2.1 Future measurements

Since most of the data available is in the form of conclusions, without publication of their core data, a lot of experiments need to be performed to gather data on the relation between volumetric air flow and pressure differences within building envelopes.
A distinction should be made between measurements on openings representative for this envelope and measurements on characteristic openings. The first can, especially in the short term, provide in a better reference frame for determination of realistic air tightness performance. The latter is necessary to gain an overview of the influence of all parameters. Only when all variables are known, a good research can be designed. Most important is to decide which parameter is of interest and to exclude all other variables in both the geometrical definitions of the opening and the environmental differences at each side.
This sounds as basic research design, but since the experiments performed for this thesis should investigate the geometrical properties of openings, but no conclusions could be drawn due to the disturbance by other coefficients, it needs extra attention.

The same holds for the equipment needed. When designing a measurement setup it is recommended that the expected air flow rates fall broadly within the equipment's reach. A good preparation contains mathematical calculations on the expected flow rates, to determine this minimal accuracy. The intervals between measurement points should be of a smaller range than the accuracy of the equipment.
The greatest added value for measurements is reached when low pressure levels, down to 1 Pascal, can be tested.
For the test room it is advised to design an apparatus which monitors both the pressure levels at each side of the considered opening and the air quantity that passes. Instead of the volumetric air flow, one may consider to monitor the mass flow instead, to eliminate changing air properties due to temperature, height or humidity differences over the opening.

5.2.2 Development computational model

To eliminate any environmental influences a computational model such as CFD can be very helpful. However these programs need a lot of variables as input and a good understanding of each of these is necessary before a reliable model can be designed. A model that contains all parameters which are present in practise probably will need an extensive computation time.

Improvement on the model to test the edge effects as done for this thesis can be performed by a more gradually decreasing diameter. When the constriction between two volumes, the slit, is more of a smooth transition, the flow characteristics will be almost fully determined by the narrowest point. When this is modelled in 3D, a good test of the geometrical properties alone can be accomplished.

The greatest added value for a CFD model can be reached when it varies in the same parameter as a physical measurement model. Usually a physical model is used to validate the CFD model. This will become difficult when parameters have been missed. When both models correspond, the computational one can be used to test any hypothesis to save on production costs for the physical model.
When better knowledge is present of flow behaviour in single leakage openings, a CFD model can come in very useful to test any combination of openings that are placed as series or parallel to each other.

Technische Universiteit Delft

6 Literature

Air-Ins Inc. 1998. 'Airtightness Tests on Components Used to Join Different or Similar Materials of the Building Envelope', *Research Highlights*, Technical Series: 98-121.

ASTM E779-10. "Standard Test Method for Determining Air Leakage Rate by Fan Pressurization." In.

Baker, P.H., S. Sharples, and I.C. Ward. 1987. 'Air flow through cracks', *Building and Environment*, 22: 293-304.

Bejan, Adrian. 2013. *Convection Heat Transfer - Fourth Edition* (John Wiley: New Yersey).

Duncan, W.J., A.S. Thom, and A.D. Young. 1960. *An Elementary Treatise on the Mechanics of Fluids* (Edward Arnold: London).

Etheridge, David. 2010. 'Ventilation, air quality and airtightness in buildings.' in Matthew R. Hall (ed.), *Materials for energy efficiency and thermal comfort in buildings* (Woodhead Publishing Limited: Cambridge).

———. 2012. *Natural Ventilation of Buildings - Theory, measurement and design* (John Wiley & Sons, Ltd.: West Sussex).

Etheridge, David, and Mats Sandberg. 1996. *Building Ventilation : Theory and Measurement* (John Wiley & Sons Ltd.: Chichester).

Godish, Thad. 1989. *Indoor air pollution control* (Lewis Publishers: Florida).

Jacobs, Piet, and Wouter Borsboom. 2015. *Effect of building and installation design on PM2.5* (TNO).

Knoll, W.H., E.J. Wagenaar, and A.M. van Weele. 2002. '2.9 Luchtkanaalberekening.' in, *Handboek Installatietechniek* (ISSO: Rotterdam).

Kronvall, J. 1980. *Air Tightness Measurements and Measurement Methods* (Swedish Council for Building Research: Stockholm).

Kula, H.G., and S. Sharples. 1994. 'Air Flow Through Smooth and Rough Cracks', *The Role of Ventilation, 15th AIVC Conference*, 27-30 September: 710-17.

Lowe, R.J., D. Johnston, and M. Bell. 1997. 'Airtightness in UK Dwellings: A Review of Some Recent Measurements.' in, *The Second International Conference on Buildings and the Environment* (Paris).

Martin, dr. ir. H.J. 2007. 'H6 Geluidlekken.' in TUe (ed.), *Geluidisolatie* (TUe: Eindhoven).

NEN-EN-ISO 9972-2015. "Thermal performance of buildings - Determination of air permeability of buildings - Fan pressurization method." In.

NEN-EN 15004. 2006. "Fixed firefighting systems - Gas extinguishing systems - Part 1: Design, installation and maintenance." In.

NEN 1087. 2001. "Ventilatie van gebouwen - Bepalingsmethoden voor nieuwbouw." In.

NEN 2686. 2008. "Air leakage of buildings - Method of measurement." In.

NEN 7120 + C2. 2012. "Energieprestatie van gebouwen - Bepalingsmethode." In.

Orme, Malcolm, Martin W. Liddament, and Andrew Wilsom. 1998. "Numerical Data for Air Infiltration and Natural Ventilation Calculations." In.: International Energy Agency - Air Infiltration and Ventilation Centre.

Santamouris, Matt, and Peter Wouters. 2006. *Building Ventilation: The State of the Art* (Earthscan: London).

Technische Universiteit Delft

SBR CUR. 'Bepaling invoerwaarde luchtdoorlatendheid voor EPC-berekening', *Infoblad 012*.

Sherman, M. 1992. 'A Power-law Formulation of Laminar Flow in Short Pipes', *Journal of Fluids Engineering*, 114: 601-05.

Sherman, M.H., and Rengie Chan. 2003. "Building Airtightness: Research and Practice." In. Berkeley: Lawrence Berkeley National Laboratory.

Sherman, M.H., and W.R. Chan. 2006. 'Building Air Tightness: Research and Practice.' in Peter Wouters; (ed.), *Building Ventilation - The State of the Art* (Earthscan: UK).

Sherman, M.H., D.J. Wilson, and D.E. Kiel. 1984. *ASTM Symposium on Measured Air Leakage Performance of Buildings* (AIC: Philadelphia).

Urquhart, Robin, and Russell Richman. 2015. 'The Relationship between Flow Exponents and Flow Values and Associated Implifications for Air Leakage Testing using Fan (De)Pressurization Methodology.' in, *Making Buildings Better* (Noord-Amerika).

VCCN Projectgroep 15. 2015. "Richtlijn voor het classificeren en testen van luchtdoorlatendheid van de schil van schone ruimten en gelijksoortige gecontroleerde omgevingen." In.

Walker, Ian S., David J. Wilson, and Max H. Sherman. 1998. 'A comparison of the power law to quadratic formulations for air infiltration calculations', *Energy and Buildings*, 27: 293-99.

WHO. 2010. "WHO guidelines for indoor air quality: selected pollutants." In.: World Health Organization,.

Appendices

A. Measurement readings

1. Dataset 1

Measurement 1.1 — Large circle (center)

ΔP_{Bias} (Pa)	0
ΔT_{int} (°C)	27,7
ΔT_{e} (°C)	25
Flange #	3
μ	0,00002
ρ	1,205

Openings geometrics

L (m)	0,012	**A (m^2)**	0,0095
w (m)	na	**Peri (m)**	0,346
d (m)	na	**P/A**	36,370
Ø (m)	0,110	**L/d_h**	0,109
d_h (m)	0,110		

ΔP_m (Pa)	v_r (m/s)	q_m (m^3/s)	q_{open} (m^3/s)	q_{open}^2 (m^3/s)	ΔP_{QF} (Pa)
10	9,4	0,0273	0,0230	0,0005	9,80
20	14,3	0,0396	0,0327	0,0011	20,56
30	17,6	0,0480	0,0390	0,0015	29,82
40	20,5	0,0556	0,0448	0,0020	39,62
50	23,1	0,0626	0,0502	0,0025	50,09
60	25,4	0,0690	0,0548	0,0030	60,11

Power Law

c	n	r
0,0075	0,4806	0,9996

Quadratic Formula

A	B	r
-60	21114	0,9999

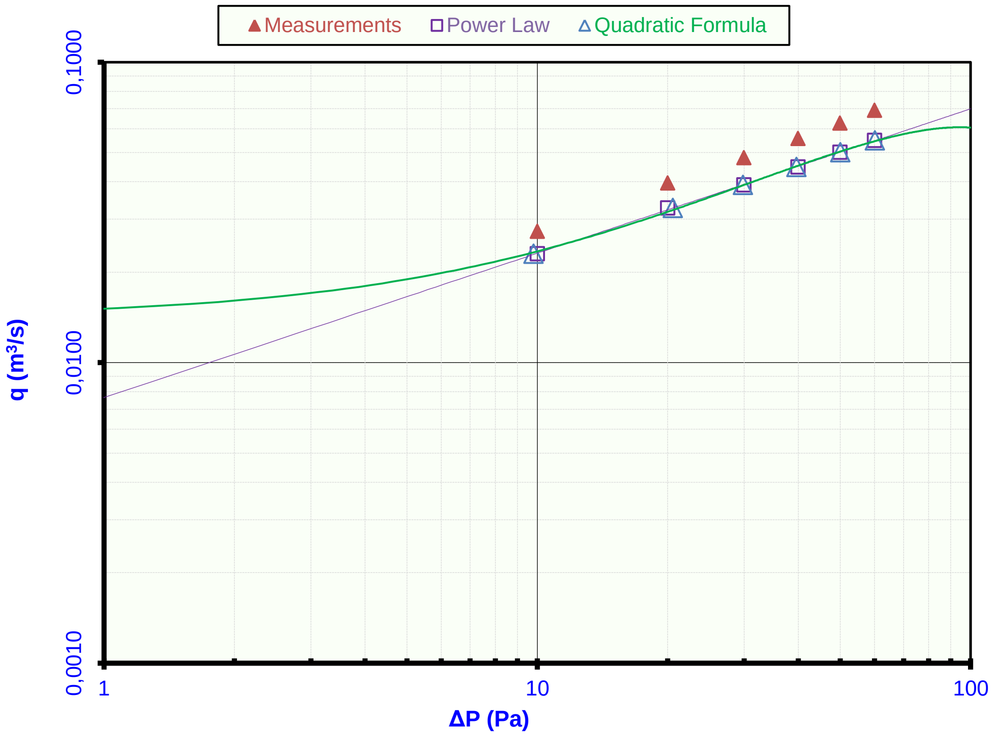

$A_{e;50}$ (m^2)	0,0054	**$u_{v;4}$ (m/s)**	1,53	**Re_4**	10164
ELA_4 (m^2)	0,0093	**$u_{v;50}$ (m/s)**	5,28	**Re_{50}**	34982

Measurement 1.2 Large circle (corner)

ΔP_{Bias} (Pa)	0
ΔT_{int} (ºC)	27,7
ΔT_e (ºC)	25
Flange #	3
μ	0,00002
ρ	1,205

Openings geometrics

L (m)	0,01	**A (m^2)**	0,0095
w (m)	na	**Peri (m)**	0,989
d (m)	na	**P/A**	104,13
Ø (m)	0,11	**L/d_h**	0,11
d_h (m)	0,11		

ΔP_m (Pa)	v_r (m/s)	q_m (m^3/s)	q_{open} (m^3/s)	q_{open}^2 (m^3/s)	ΔP_{QF} (Pa)
10	9,5	0,0276	0,0233	0,0005	10,45
20	14,2	0,0393	0,0324	0,0011	20,13
30	17,8	0,0485	0,0396	0,0016	29,88
40	20,8	0,0564	0,0456	0,0021	39,57
50	23,4	0,0635	0,0510	0,0026	49,45
60	26	0,0707	0,0565	0,0032	60,67

Power Law

c	n	r
0,0073	0,4924	0,9996

Quadratic Formula

A	B	r
12	18798	0,9999

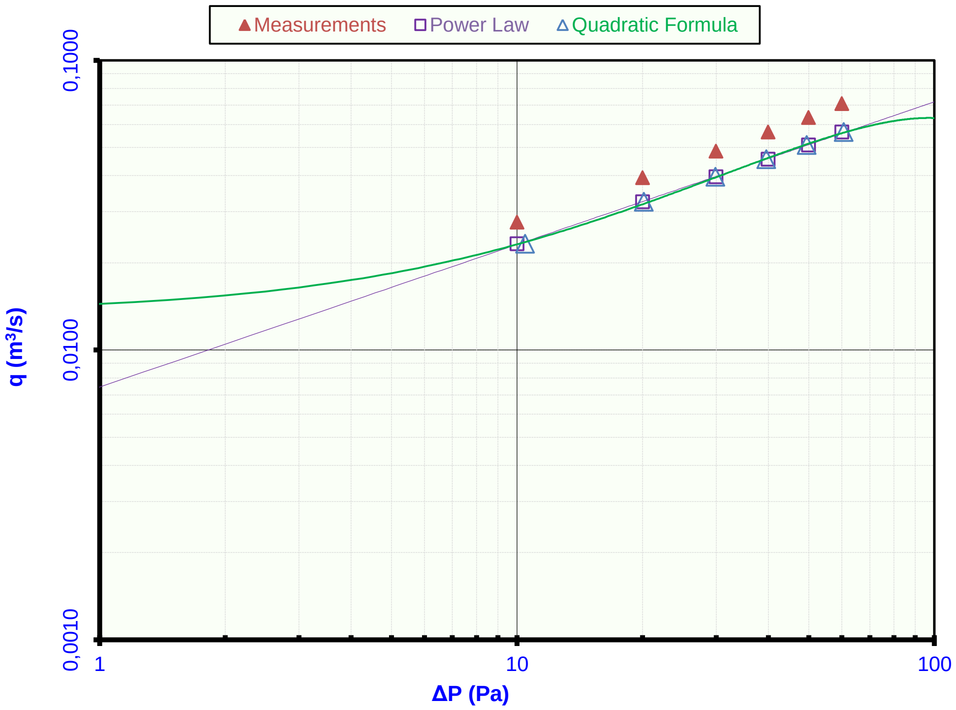

$A_{e;50}$ (m^2)	0,0055	$u_{v;4}$ (m/s)	1,52	Re_4	10056
ELA_4 (m^2)	0,0092	$u_{v;50}$ (m/s)	5,37	Re_{50}	35557

Measurement 1.3 Star

ΔP_{Bias} (Pa)	0
ΔT_{int} (°C)	26,2
ΔT_e (°C)	25
Flange #	3
μ	0,00002
ρ	1,205

Openings geometrics

L (m)	0,01	**A (m^2)**	0,0095
w (m)	0,12	**Peri (m)**	0,989
d (m)	0,09	**P/A**	104,13
Ø (m)	0,06	**L/d_h**	0,31
d_h (m)	0,04		

ΔP_m (Pa)	v_r (m/s)	q_m (m^3/s)	q_{open} (m^3/s)	q_{open}^2 (m^3/s)	ΔP_{QF} (Pa)
10	9,9	0,0286	0,0243	0,0006	10,46
20	14,8	0,0409	0,0339	0,0012	20,49
30	18,4	0,0501	0,0411	0,0017	30,11
40	21,7	0,0588	0,0480	0,0023	41,04
50	24,5	0,0665	0,0540	0,0029	52,03
60	27,2	0,0742	0,0599	0,0036	64,05

Power Law

c	n	r
0,0077	0,4890	0,9992

Quadratic Formula

A	B	r
-3	17877	0,9998

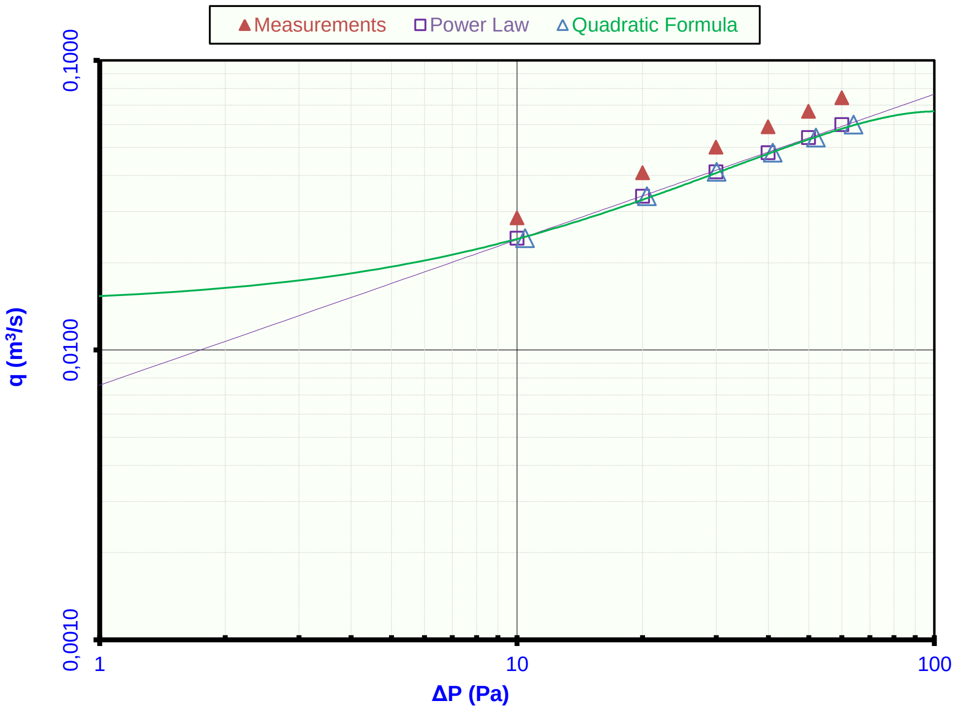

$A_{e;50}$ (m^2)	0,0057	**$u_{v;4}$ (m/s)**	1,59	**Re_4**	3673
ELA_4 (m^2)	0,0096	**$u_{v;50}$ (m/s)**	5,69	**Re_{50}**	13161

Measurement 1.4 Square

ΔP_{Bias} (Pa)	0
ΔT_{int} (°C)	27,7
ΔT_e (°C)	25
Flange #	3
μ	0,00002
ρ	1,205

Openings geometrics

L (m)	0,01	**A (m^2)**	0,0095
w (m)	0,10	**Peri (m)**	0,390
d (m)	0,10	**P/A**	41,04
Ø (m)	na	**L/d_h**	0,12
d_h (m)	0,10		

ΔP_m (Pa)	v_r (m/s)	q_m (m^3/s)	q_{open} (m^3/s)	q_{open}^2 (m^3/s)	ΔP_{QF} (Pa)
10	9,4	0,0273	0,0230	0,0005	9,80
20	14,3	0,0396	0,0327	0,0011	20,56
30	17,6	0,0480	0,0390	0,0015	29,82
40	20,5	0,0556	0,0448	0,0020	39,62
50	23,1	0,0626	0,0502	0,0025	50,09
60	25,4	0,0690	0,0548	0,0030	60,11

Power Law

c	n	r
0,0075	0,4806	0,9996

Quadratic Formula

A	B	r
-60	21114	0,9999

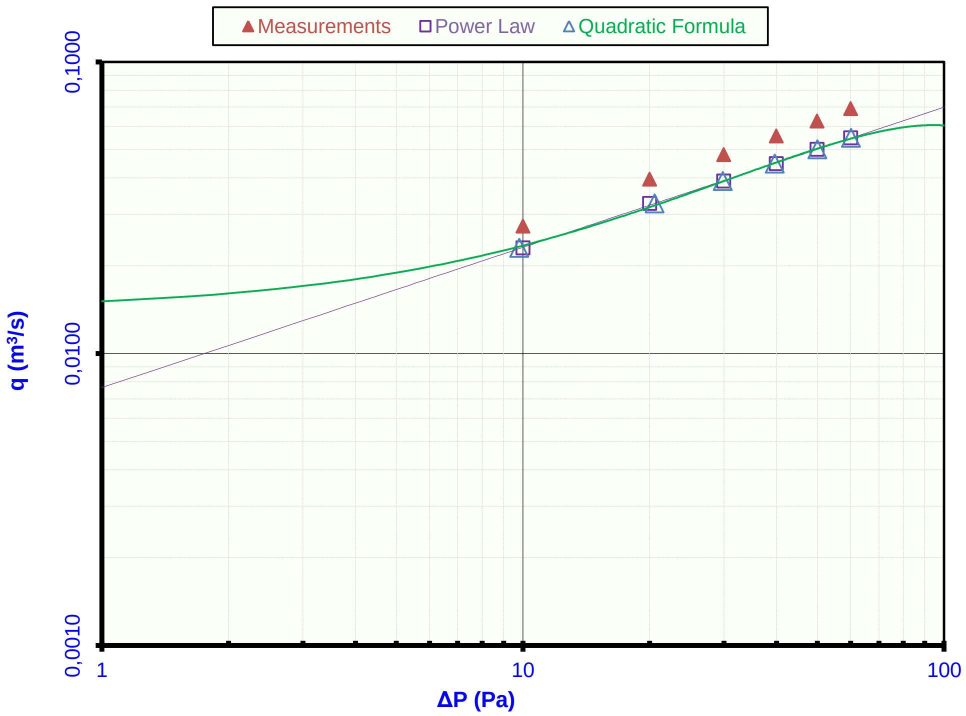

$A_{e;50}$ (m^2)	0,0054	**$u_{v;4}$ (m/s)**	1,53	**Re_4**	9008
ELA_4 (m^2)	0,0093	**$u_{v;50}$ (m/s)**	5,28	**Re_{50}**	31002

Measurement 1.5 L-shape

ΔP_{Bias} (Pa)	0
ΔT_{int} (°C)	27,7
ΔT_e (°C)	25
Flange #	3
μ	0,00002
ρ	1,205

Openings geometrics

L (m)	0,01	**A (m^2)**	0,0095
w (m)	0,03	**Peri (m)**	0,810
d (m)	0,38	**P/A**	85,26
Ø (m)	na	**L/d_h**	0,26
d_h (m)	0,05		

ΔP_m (Pa)	v_r (m/s)	q_m (m^3/s)	q_{open} (m^3/s)	q_{open}^2 (m^3/s)	ΔP_{QF} (Pa)
10	9,6	0,0278	0,0235	0,0006	10,45
20	14,4	0,0398	0,0329	0,0011	20,07
30	18,1	0,0493	0,0403	0,0016	29,85
40	21,1	0,0572	0,0464	0,0022	39,24
50	24	0,0651	0,0526	0,0028	50,33
60	26,4	0,0719	0,0576	0,0033	60,19

Power Law

c	n	r
0,0072	0,5004	0,9996

Quadratic Formula

A	B	r
31	17588	0,9999

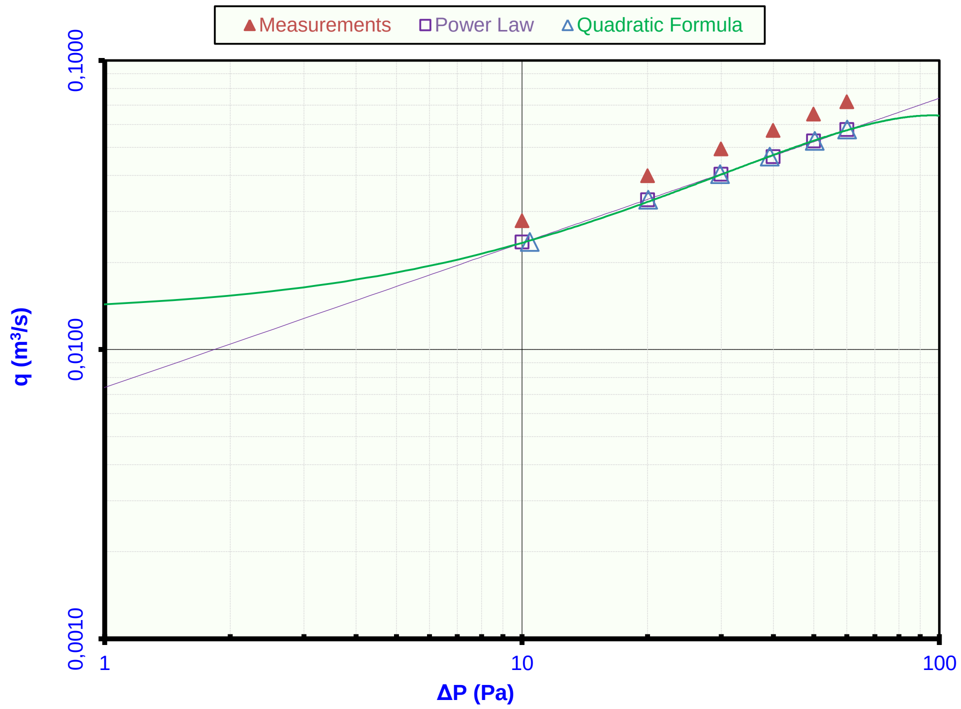

$A_{e;50}$ (m^2)	0,0056	**$u_{v;4}$ (m/s)**	1,52	**Re_4**	4302
ELA_4 (m^2)	0,0092	**$u_{v;50}$ (m/s)**	5,54	**Re_{50}**	15660

Technische Universiteit Delft

Royal HaskoningDHV

Measurement 1.6 Slits

ΔP_{Bias} (Pa)	0
ΔT_{int} (ºC)	27,7
ΔT_e (ºC)	25
Flange #	3
µ	0,00002
ρ	1,205

Openings geometrics

L (m)	0,01	**A (m^2)**	0,0095
w (m)	1,90	**Peri (m)**	3,820
d (m)	0,01	**P/A**	402,11
Ø (m)	na	**L/d_h**	1,21
d_h (m)	0,01		

ΔP_m (Pa)	v_r (m/s)	q_m (m^3/s)	q_{open} (m^3/s)	q_{open}^2 (m^3/s)	ΔP_{QF} (Pa)
10	11	0,0313	0,0270	0,0007	10,25
20	16,3	0,0447	0,0377	0,0014	19,96
30	20,3	0,0551	0,0461	0,0021	29,75
40	23,7	0,0643	0,0534	0,0029	39,91
50	26,6	0,0724	0,0599	0,0036	50,19

Power Law

c	n	r
0,0084	0,4950	0,9998

Quadratic Formula

A	B	r
5	13888	1,0000

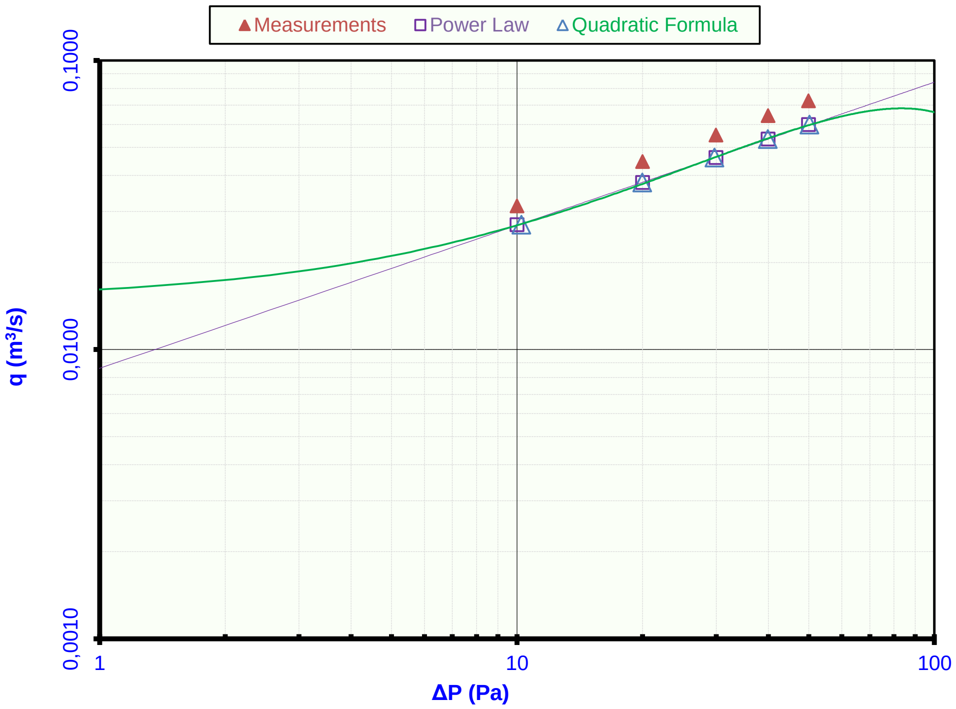

$A_{e;50}$ (m^2)	0,0064	**$u_{v;4}$ (m/s)**	1,76	**Re_4**	1055
ELA_4 (m^2)	0,0106	**$u_{v;50}$ (m/s)**	6,31	**Re_{50}**	3782

Technische Universiteit Delft

Measurement 1.7 Small circle

ΔP_{Bias} (Pa)	0
ΔT_{int} (°C)	27,7
ΔT_e (°C)	25
Flange #	3
μ	0,00002
ρ	1,205

Openings geometrics

L (m)	0,01	**A (m^2)**	0,0010
w (m)	na	**Peri (m)**	0,109
d (m)	na	**P/A**	115,01
Ø (m)	0,03	**L/d_h**	0,35
d_h (m)	0,03		

ΔP_m (Pa)	v_r (m/s)	q_m (m^3/s)	q_{open} (m^3/s)	q_{open}^2 (m^3/s)	ΔP_{QF} (Pa)
10	1,5	0,0072	0,0029	0,0000	6,34
20	2,9	0,0109	0,0040	0,0000	20,07
30	3,9	0,0135	0,0045	0,0000	28,92
40	4,9	0,0161	0,0052	0,0000	42,18
50	5,7	0,0181	0,0056	0,0000	50,83
60	6,6	0,0204	0,0061	0,0000	63,61
70	7,4	0,0224	0,0064	0,0000	71,26
80	8,2	0,0244	0,0050	0,0000	37,74
90	9	0,0263	0,0070	0,0000	87,48
100	9,7	0,0281	0,0073	0,0001	98,25

Power Law

c	n	r
0,0011	0,4019	0,9969

Quadratic Formula

A	B	r
-4925	2493976	0,9989

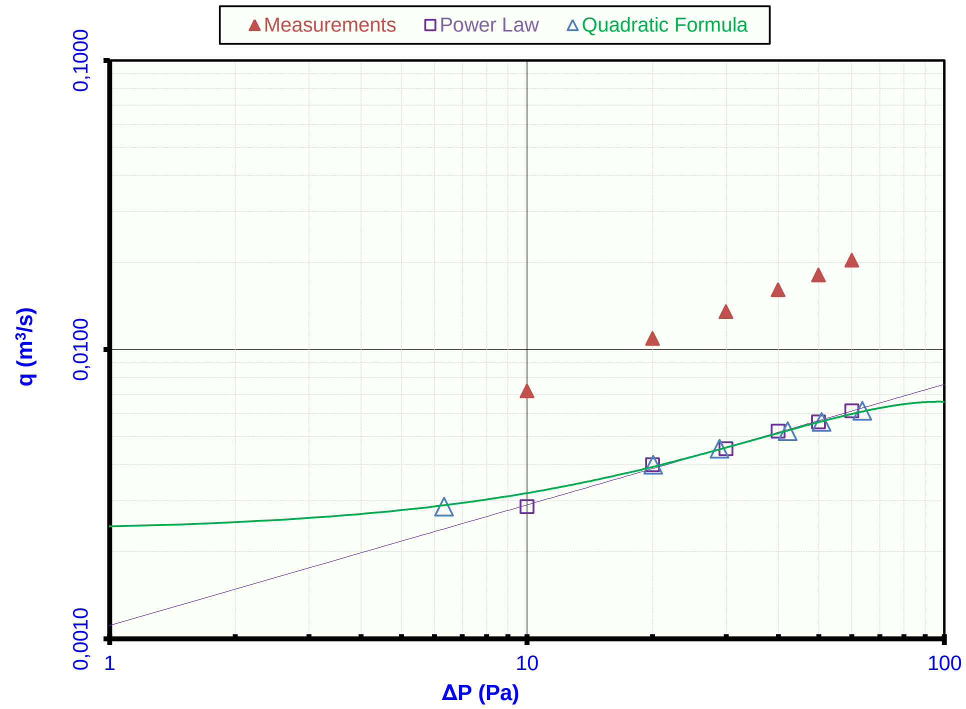

$A_{e;50}$ (m^2)	0,0006	**$u_{v;4}$ (m/s)**	2,10	**Re_4**	4395
ELA_4 (m^2)	0,0013	**$u_{v;50}$ (m/s)**	5,90	**Re_{50}**	12371

Measurement 1.8 Small circles (10)

ΔP_{Bias} (Pa)	0
ΔT_{int} (°C)	27,7
ΔT_e (°C)	25
Flange #	3
µ	0,00002
ρ	1,205

Openings geometrics

L (m)	0,01	**A (m^2)**	0,0095
w (m)	na	**Peri (m)**	1,093
d (m)	na	**P/A**	115,01
Ø (m)	0,03	**L/d_h**	0,35
d_h (m)	0,03		

ΔP_m (Pa)	v_r (m/s)	q_m (m^3/s)	q_{open} (m^3/s)	q_{open}^2 (m^3/s)	ΔP_{QF} (Pa)
10	9,4	0,0273	0,0230	0,0005	9,80
20	14,3	0,0396	0,0327	0,0011	20,56
30	17,6	0,0480	0,0390	0,0015	29,82
40	20,5	0,0556	0,0448	0,0020	39,62
50	23,1	0,0626	0,0502	0,0025	50,09
60	25,4	0,0690	0,0548	0,0030	60,11

Power Law

c	n	r
0,0075	0,4806	0,9996

Quadratic Formula

A	B	r
-60	21114	0,9999

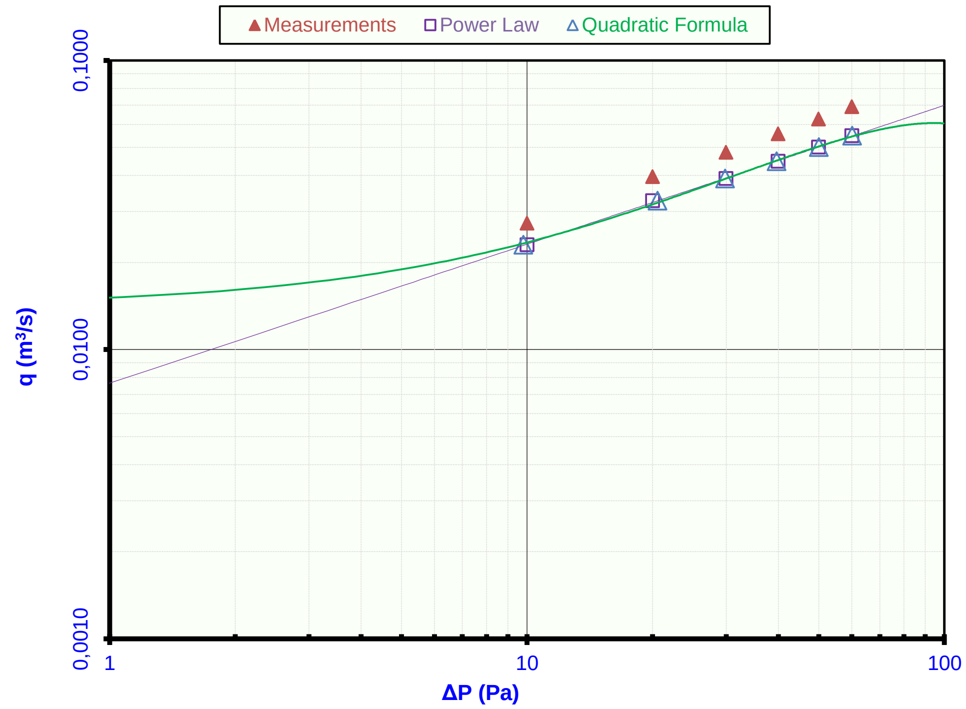

$A_{e;50}$ (m^2)	0,0054	**$u_{v;4}$ (m/s)**	1,53	**Re_4**	3214
ELA_4 (m^2)	0,0093	**$u_{v;50}$ (m/s)**	5,28	**Re_{50}**	11062

Measurement 1.9 Small Circles (4)

ΔP_{Bias} (Pa)	0
ΔT_{int} (°C)	27,4
ΔT_e (°C)	25
Flange #	3
μ	0,00002
ρ	1,205

Openings geometrics

L (m)	0,01	**A (m^2)**	0,0038
w (m)	na	**Peri (m)**	0,437
d (m)	na	**P/A**	115,01
Ø (m)	0,03	**L/d_h**	0,35
d_h (m)	0,03		

ΔP_m (Pa)	v_r (m/s)	q_m (m^3/s)	q_{open} (m^3/s)	q_{open}^2 (m^3/s)	ΔP_{QF} (Pa)
10	4,2	0,0143	0,0100	0,0001	8,74
20	6,6	0,0204	0,0134	0,0002	18,97
30	8,5	0,0251	0,0161	0,0003	29,43
40	10,3	0,0296	0,0187	0,0004	41,68
50	11,7	0,0331	0,0206	0,0004	51,66
60	13	0,0363	0,0221	0,0005	60,58
70	14,3	0,0396	0,0236	0,0006	70,52
80	15,5	0,0426	0,0233	0,0005	68,05
90	16,6	0,0454	0,0261	0,0007	87,54
100	17,8	0,0485	0,0278	0,0008	100,53

Power Law

c	n	r
0,0035	0,4443	0,9993

Quadratic Formula

A	B	r
-654	153751	0,9996

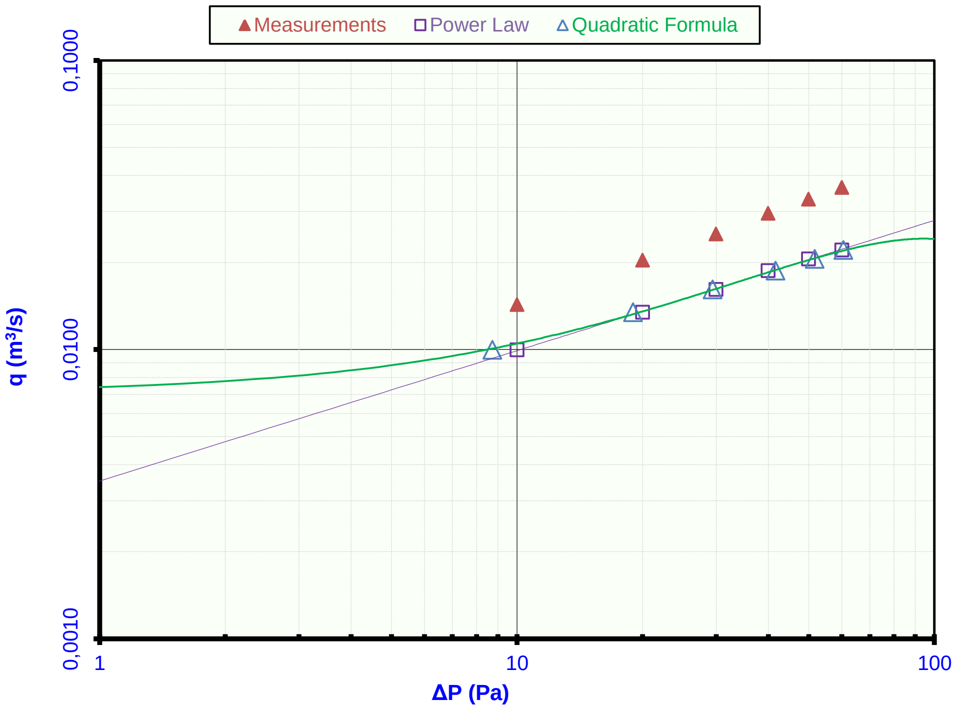

$A_{e;50}$ (m^2)	0,0022	**$u_{v;4}$ (m/s)**	1,71	**Re_4**	3585
ELA_4 (m^2)	0,0041	**$u_{v;50}$ (m/s)**	5,42	**Re_{50}**	11348

Technische Universiteit Delft

2. Slits

Measurement 2.01 Slit 0,5 x 950 mm

ΔP_{Bias} (Pa)	0
ΔT_{int} (°C)	24,3
ΔT_e (°C)	24,1
Flange #	2
μ	0,00002
ρ	1,205

Openings geometrics

L (m)	0,012	**A (m^2)**	0,0005
w (m)	0,950	**Peri (m)**	1,901
d (m)	0,0005	**P/A**	4002,105
Ø (m)	na	**L/d_h**	12,000
d_h (m)	0,001		

ΔP_m (Pa)	v_r (m/s)	q_m (m^3/s)	q_{open} (m^3/s)	q_{open}^2 (m^3/s)	ΔP_{QF} (Pa)
10	3,6	0,0034	0,0002	0,0000	11,40
20	6,7	0,0055	0,0003	0,0000	18,48
30	10,0	0,0077	0,0005	0,0000	29,51
40	12,9	0,0096	0,0007	0,0000	41,09
50	15,4	0,0113	0,0009	0,0000	49,41
60	17,7	0,0128	0,0010	0,0000	58,25
70	20	0,0144	0,0013	0,0000	71,81
80	22,3	0,0161	0,0014	0,0000	82,08
90	24,3	0,0176	0,0015	0,0000	88,42
100	26,2	0,0190	0,0017	0,0000	99,52

Power Law

c	n	r
0,00002	0,9524	0,9953

Quadratic Formula

A	B	r
54801	1737303	0,9995

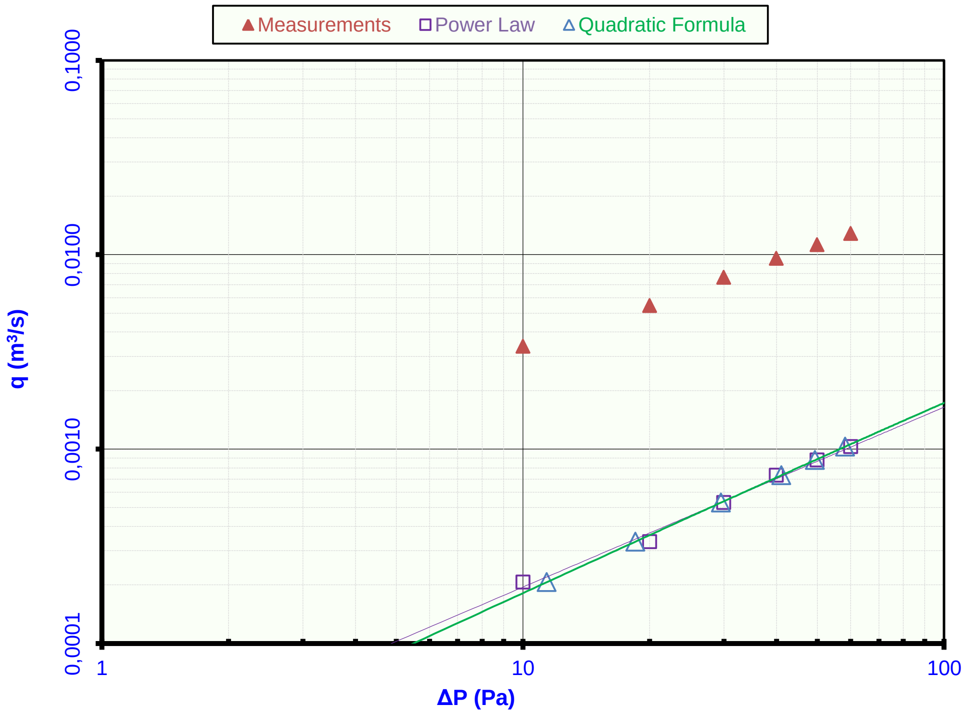

$A_{e;50}$ (m^2)	0,0001	**$u_{v;4}$ (m/s)**	0,17	**Re_4**	10
ELA_4 (m^2)	0,0001	**$u_{v;50}$ (m/s)**	1,85	**Re_{50}**	111

Measurement 2.02 Slit 0,5 x 1900 mm

ΔP_{Bias} (Pa)	0
ΔT_{int} (°C)	24,2
ΔT_e (°C)	24,1
Flange #	2
μ	0,00002
ρ	1,205

Openings geometrics

L (m)	0,012	**A (m^2)**	0,0010
w (m)	1,900	**Peri (m)**	3,802
d (m)	0,0005	**P/A**	4002,105
Ø (m)	na	**L/d_h**	12,000
d_h (m)	0,001		

ΔP_m (Pa)	v_r (m/s)	q_m (m^3/s)	q_{open} (m^3/s)	q_{open}^2 (m^3/s)	ΔP_{QF} (Pa)
10	4	0,0036	0,0005	0,0000	11,22
20	7,6	0,0061	0,0009	0,0000	21,97
30	11,1	0,0084	0,0013	0,0000	29,86
40	14,3	0,0105	0,0017	0,0000	39,98
50	17,1	0,0124	0,0020	0,0000	49,11
60	19,6	0,0142	0,0024	0,0000	57,09
70	22,3	0,0161	0,0029	0,0000	71,26
80	24,8	0,0179	0,0033	0,0000	80,81
90	27,2	0,0197	0,0037	0,0000	92,96
100	29,0	0,0211	0,0039	0,0000	97,20

Power Law

c	n	r
0,00006	0,9170	0,9979

Quadratic Formula

A	B	r
23110	488509	0,9991

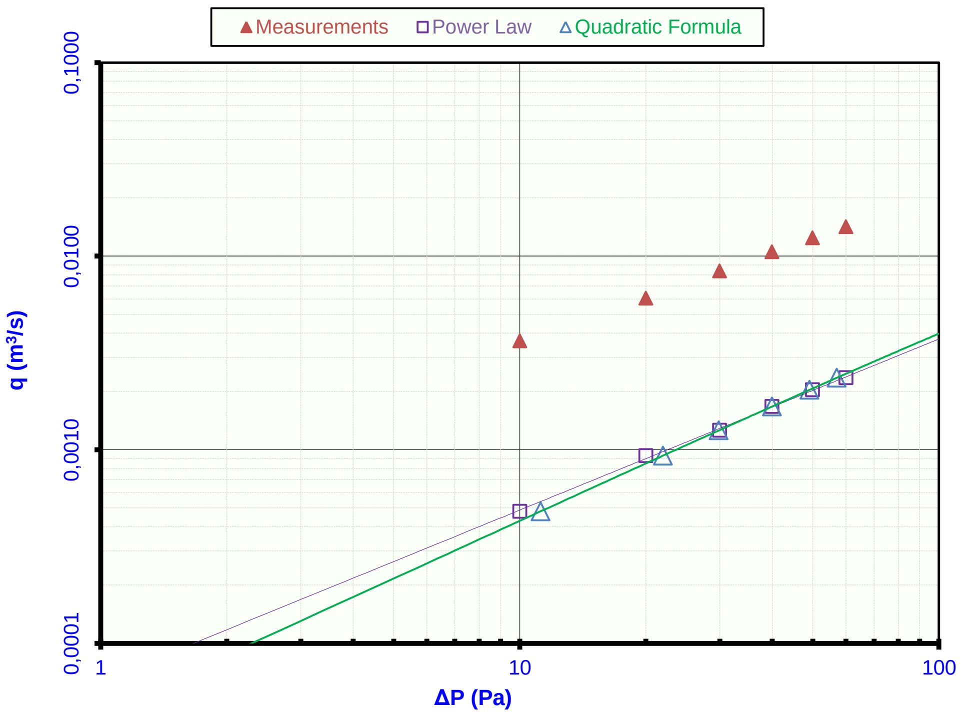

$A_{e;50}$ (m^2)	0,0002	**$u_{v;4}$ (m/s)**	0,21	**Re_4**	13
ELA_4 (m^2)	0,0001	**$u_{v;50}$ (m/s)**	2,14	**Re_{50}**	129

Technische Universiteit Delft

Measurement 2.03 Slit 0,5 x 2850 mm

ΔP_{Bias} (Pa)	0
ΔT_{int} (°C)	24,3
ΔT_e (°C)	24,1
Flange #	2
μ	0,00002
ρ	1,205

Openings geometrics

L (m)	0,012	**A (m^2)**	0,0014
w (m)	2,850	**Peri (m)**	5,704
d (m)	0,0005	**P/A**	4002,807
Ø (m)	na	**L/d_h**	12,000
d_h (m)	0,001		

ΔP_m (Pa)	v_r (m/s)	q_m (m^3/s)	q_{open} (m^3/s)	$q_{open}{}^2$ (m^3/s)	ΔP_{QF} (Pa)
10	4,1	0,0037	0,0005	0,0000	11,45
20	7,9	0,0063	0,0011	0,0000	23,57
30	11,5	0,0086	0,0015	0,0000	31,71
40	14,8	0,0109	0,0020	0,0000	41,72
50	17,6	0,0128	0,0024	0,0000	49,43
60	20,7	0,0149	0,0031	0,0000	64,87
70	23,1	0,0167	0,0035	0,0000	72,16
80	25,8	0,0187	0,0040	0,0000	83,09
90	28,5	0,0207	0,0047	0,0000	97,66
100	28,9	0,0211	0,0038	0,0000	78,72

Power Law

c	n	r
0,00006	0,9565	0,9962

Quadratic Formula

A	B	r
20896	-58773	0,9852

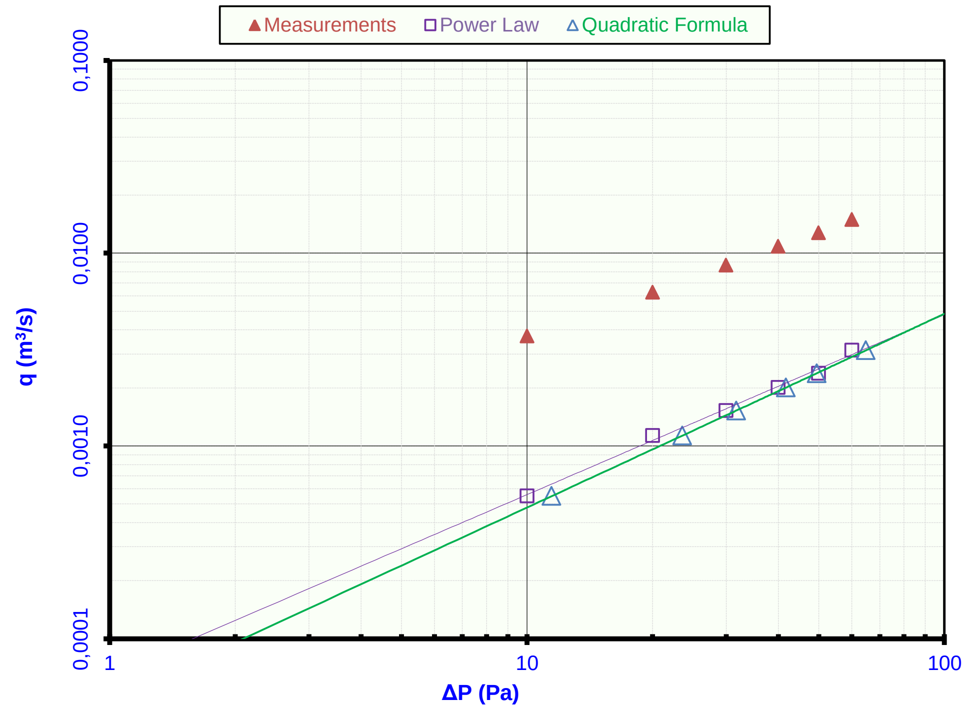

$A_{e;50}$ (m^2)	0,0003	**$u_{v;4}$ (m/s)**	0,16	**Re_4**	10
ELA_4 (m^2)	0,0001	**$u_{v;50}$ (m/s)**	1,67	**Re_{50}**	101

Measurement 2.04 Slit 1 x 950 mm

ΔP_{Bias} (Pa)	0
ΔT_{int} (°C)	24,3
ΔT_e (°C)	24,1
Flange #	2 / 3
μ	0,00002
ρ	1,205

Openings geometrics

L (m)	0,012	**A (m^2)**	0,0010
w (m)	0,950	**Peri (m)**	1,908
d (m)	0,0010	**P/A**	2008,421
Ø (m)	na	**L/d_h**	6,025
d_h (m)	0,002		

ΔP_m (Pa)	v_r (m/s)	q_m (m^3/s)	q_{open} (m^3/s)	q_{open}^2 (m^3/s)	ΔP_{QF} (Pa)
10	6,2	0,0051	0,0020	0,0000	8,86
20	10,9	0,0082	0,0031	0,0000	19,63
30	15,0	0,0110	0,0039	0,0000	28,81
40	18,7	0,0135	0,0047	0,0000	40,79
50	21,8	0,0157	0,0053	0,0000	51,99
60	24,5	0,0177	0,0059	0,0000	62,45
70	6,2	0,0194	0,0062	0,0000	68,14
80	7	0,0214	0,0067	0,0000	79,57
90	7,7	0,0231	0,0071	0,0001	88,45
100	8,4	0,0249	0,0076	0,0001	100,61

Power Law

c	n	r
0,00053	0,5780	0,9965

Quadratic Formula

A	B	r
1466	1548366	0,9995

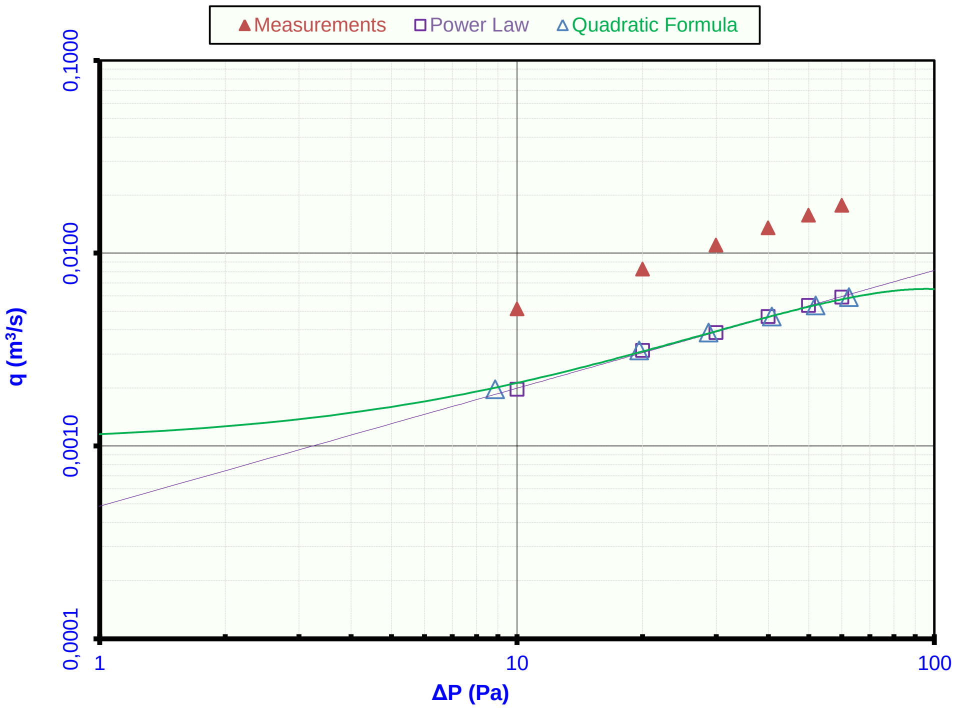

$A_{e;50}$ (m^2)	0,0006	**$u_{v;4}$ (m/s)**	1,25	**Re_4**	151
ELA_4 (m^2)	0,0008	**$u_{v;50}$ (m/s)**	5,62	**Re_{50}**	675

Technische Universiteit Delft

Royal HaskoningDHV

Measurement 2.05 Slit 1,5 x 950 mm

ΔP_{Bias} (Pa)	0
ΔT_{int} (ºC)	24,1
ΔT_{e} (ºC)	24,1
Flange #	2 / 3
µ	0,00002
ρ	1,205

Openings geometrics

L (m)	0,012	**A (m^2)**	0,0014
w (m)	0,950	**Peri (m)**	1,912
d (m)	0,0015	**P/A**	1341,754
Ø (m)	na	**L/d_h**	4,025
d_h (m)	0,003		

ΔP_m (Pa)	v_r (m/s)	q_m (m^3/s)	q_{open} (m^3/s)	q_{open}^2 (m^3/s)	ΔP_{QF} (Pa)
10	8,6	0,0067	0,0036	0,0000	8,35
20	14,3	0,0105	0,0054	0,0000	19,27
30	19,3	0,0139	0,0068	0,0000	31,03
40	23,4	0,0169	0,0080	0,0001	43,16
50	26,5	0,0192	0,0088	0,0001	52,01
60	6,9	0,0211	0,0093	0,0001	57,94
70	7,8	0,0234	0,0102	0,0001	69,37
80	8,6	0,0254	0,0107	0,0001	76,68
90	9,5	0,0276	0,0116	0,0001	89,83
100	10,3	0,0296	0,0123	0,0002	101,84

Power Law

c	n	r
0,00110	0,5232	0,9946

Quadratic Formula

A	B	r
-59	674944	0,9990

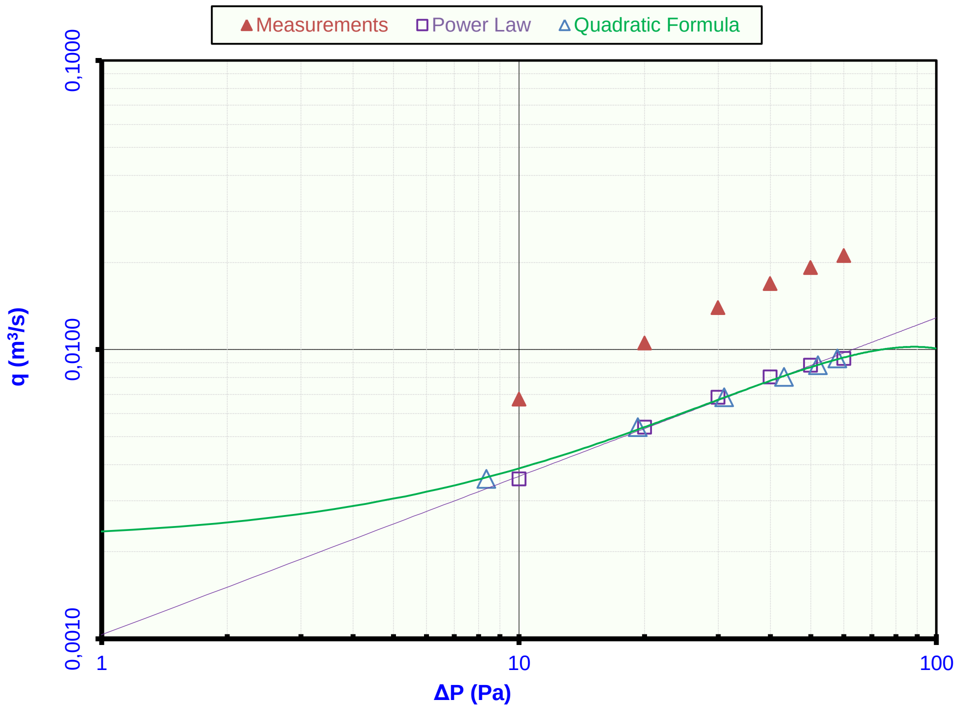

$A_{e;50}$ (m^2)	0,0009	**$u_{v;4}$ (m/s)**	1,60	**Re_4**	288
ELA_4 (m^2)	0,0015	**$u_{v;50}$ (m/s)**	6,19	**Re_{50}**	1112

Measurement 2.06 Slit 2 x 950 mm

ΔP_{Bias} (Pa)	0
ΔT_{int} (°C)	24,1
ΔT_e (°C)	24,1
Flange #	3
μ	0,00002
ρ	1,205

Openings geometrics

L (m)	0,012	**A (m^2)**	0,0019
w (m)	0,950	**Peri (m)**	1,916
d (m)	0,0020	**P/A**	1008,421
Ø (m)	na	**L/d_h**	3,025
d_h (m)	0,004		

ΔP_m (Pa)	v_r (m/s)	q_m (m^3/s)	q_{open} (m^3/s)	q_{open}^2 (m^3/s)	ΔP_{QF} (Pa)
10	2	0,0085	0,0054	0,0000	10,31
20	3,7	0,0130	0,0079	0,0001	21,79
30	5	0,0163	0,0092	0,0001	29,68
40	6,4	0,0199	0,0110	0,0001	42,31
50	7,4	0,0224	0,0120	0,0001	49,97
60	8,4	0,0249	0,0131	0,0002	59,21
70	9,3	0,0271	0,0139	0,0002	67,22
80	10,3	0,0296	0,0149	0,0002	77,28
90	11,3	0,0321	0,0161	0,0003	89,30
100	12,3	0,0346	0,0173	0,0003	103,65

Power Law

c	n	r
0,00174	0,4927	0,9976

Quadratic Formula

A	B	r
91	340592	0,9990

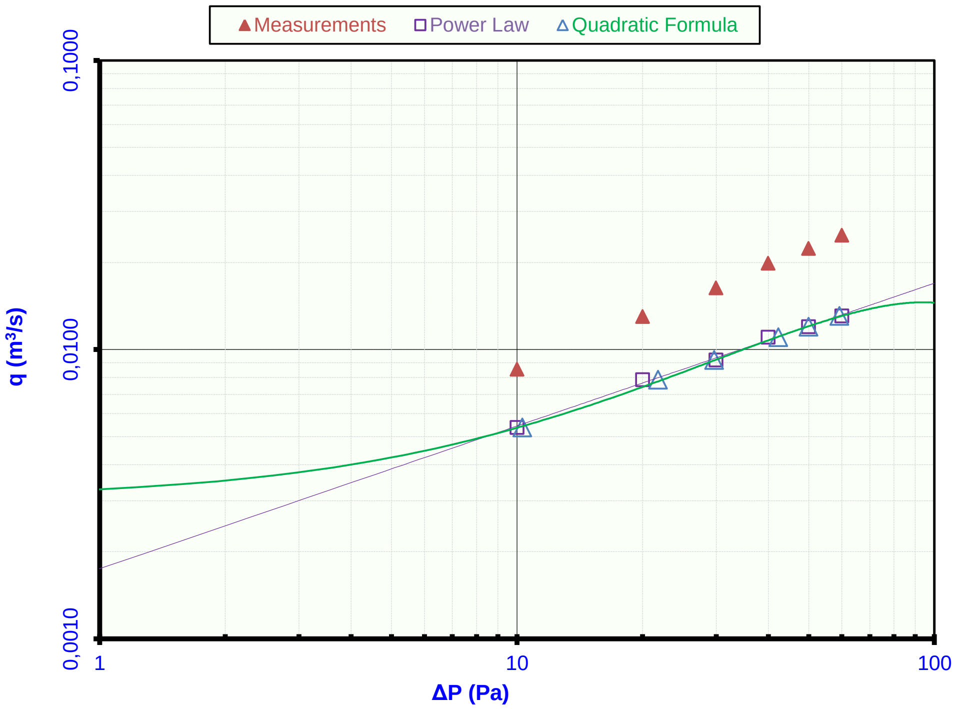

$A_{e;50}$ (m^2)	0,0013	**$u_{v;4}$ (m/s)**	1,81	**Re_4**	433
ELA_4 (m^2)	0,0022	**$u_{v;50}$ (m/s)**	6,31	**Re_{50}**	1507

Technische Universiteit Delft

Measurement 2.07 Slit 2,5 x 950 mm

ΔP_{Bias} (Pa)	0
ΔT_{int} (°C)	24,1
ΔT_e (°C)	24,1
Flange #	3
μ	0,00002
ρ	1,205

Openings geometrics

L (m)	0,012	**A (m^2)**	0,0024
w (m)	0,950	**Peri (m)**	1,920
d (m)	0,0025	**P/A**	808,421
Ø (m)	na	**L/d_h**	2,425
d_h (m)	0,005		

ΔP_m (Pa)	v_r (m/s)	q_m (m^3/s)	q_{open} (m^3/s)	q_{open}^2 (m^3/s)	ΔP_{QF} (Pa)
10	2,7	0,0104	0,0072	0,0001	9,68
20	4,6	0,0153	0,0102	0,0001	20,26
30	6,2	0,0194	0,0122	0,0001	29,91
40	7,6	0,0229	0,0140	0,0002	39,78
50	8,9	0,0261	0,0157	0,0002	50,51
60	10	0,0288	0,0170	0,0003	59,67
70	11,1	0,0316	0,0184	0,0003	69,97
80	12,2	0,0343	0,0197	0,0004	80,32
90	13,2	0,0368	0,0208	0,0004	90,24
100	14,1	0,0391	0,0218	0,0005	99,59

Power Law

c	n	r
0,00239	0,4793	0,9999

Quadratic Formula

A	B	r
-254	220633	1,0000

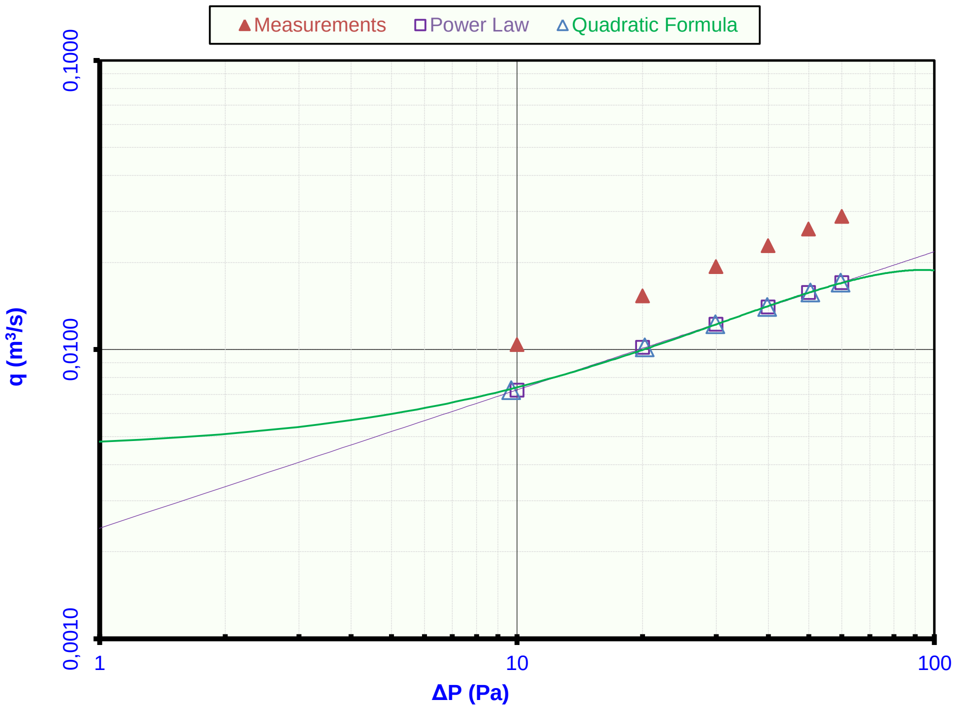

$A_{e;50}$ (m^2)	0,0017	**$u_{v;4}$ (m/s)**	1,95	**Re_4**	582
ELA_4 (m^2)	0,0030	**$u_{v;50}$ (m/s)**	6,62	**Re_{50}**	1973

Technische Universiteit Delft

Royal HaskoningDHV

Measurement 2.08 Slit 3,5 x 950 mm

ΔP_{Bias} (Pa)	0
ΔT_{int} (°C)	24,3
ΔT_e (°C)	24,1
Flange #	3
μ	0,00002
ρ	1,205

Openings geometrics

L (m)	0,012	**A (m^2)**	0,0033
w (m)	0,950	**Peri (m)**	1,928
d (m)	0,0035	**P/A**	579,850
Ø (m)	na	**L/d_h**	1,740
d_h (m)	0,007		

ΔP_m (Pa)	v_r (m/s)	q_m (m^3/s)	q_{open} (m^3/s)	q_{open}^2 (m^3/s)	ΔP_{QF} (Pa)
10	4	0,0138	0,0106	0,0001	10,14
20	6,4	0,0199	0,0147	0,0002	20,37
30	8,4	0,0249	0,0177	0,0003	30,03
40	10,1	0,0291	0,0202	0,0004	39,52
50	11,7	0,0331	0,0227	0,0005	50,05
60	13,1	0,0366	0,0248	0,0006	59,97
70	14,4	0,0398	0,0267	0,0007	69,80
80	15,7	0,0431	0,0285	0,0008	79,96
90	16,9	0,0462	0,0302	0,0009	90,11
100	18,0	0,0491	0,0318	0,0010	100,15

Power Law

c	n	r
0,00349	0,4768	0,9998

Quadratic Formula

A	B	r
-142	103509	1,0000

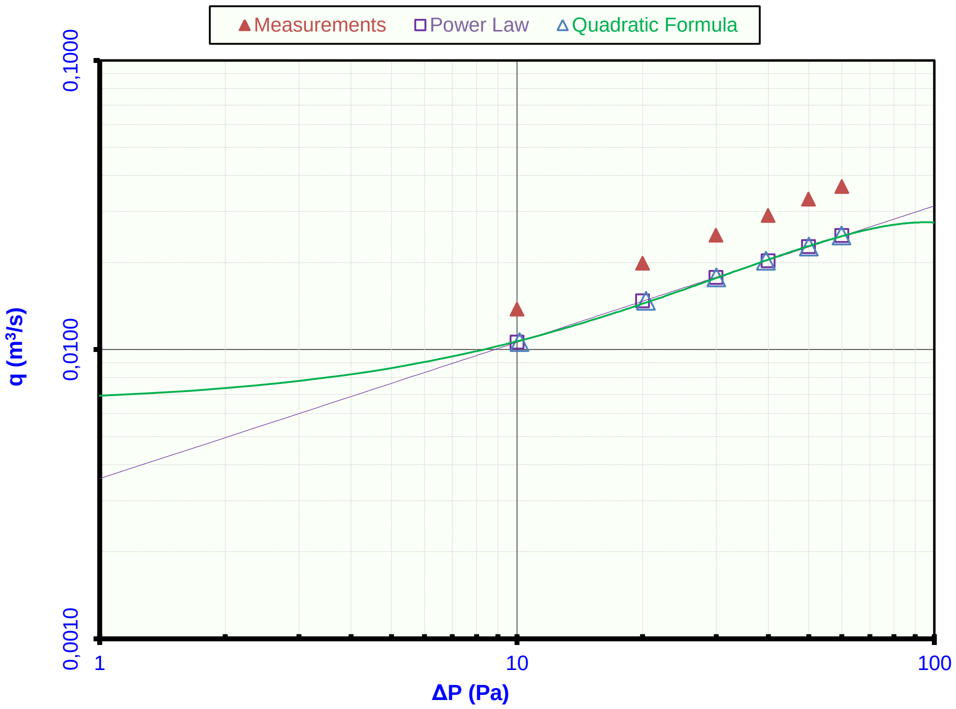

$A_{e;50}$ (m^2)	0,0025	**$u_{v;4}$ (m/s)**	2,03	**Re_4**	846
ELA_4 (m^2)	0,0043	**$u_{v;50}$ (m/s)**	6,82	**Re_{50}**	2836

Technische Universiteit Delft

Measurement 2.09 Slit 4,5 x 950 mm

ΔP_{Bias} (Pa)	0
ΔT_{int} (°C)	24,3
ΔT_e (°C)	24,1
Flange #	3
µ	0,00002
ρ	1,205

Openings geometrics

L (m)	0,012	**A (m^2)**	0,0043
w (m)	0,950	**Peri (m)**	1,936
d (m)	0,0045	**P/A**	452,865
Ø (m)	na	**L/d_h**	1,359
d_h (m)	0,009		

ΔP_m (Pa)	v_r (m/s)	q_m (m^3/s)	q_{open} (m^3/s)	q_{open}^2 (m^3/s)	ΔP_{QF} (Pa)
10	5,3	0,0171	0,0139	0,0002	9,40
20	8,2	0,0244	0,0192	0,0004	19,55
30	10,6	0,0303	0,0232	0,0005	29,55
40	12,8	0,0358	0,0270	0,0007	40,89
50	14,5	0,0401	0,0297	0,0009	50,29
60	16,1	0,0442	0,0324	0,0010	60,28
70	17,6	0,0480	0,0348	0,0012	70,47
80	19,0	0,0517	0,0370	0,0014	80,05
90	20,3	0,0551	0,0391	0,0015	89,74
100	21,5	0,0583	0,0410	0,0017	99,45

Power Law

c	n	r
0,00467	0,4709	0,9999

Quadratic Formula

A	B	r
-222	64453	0,9999

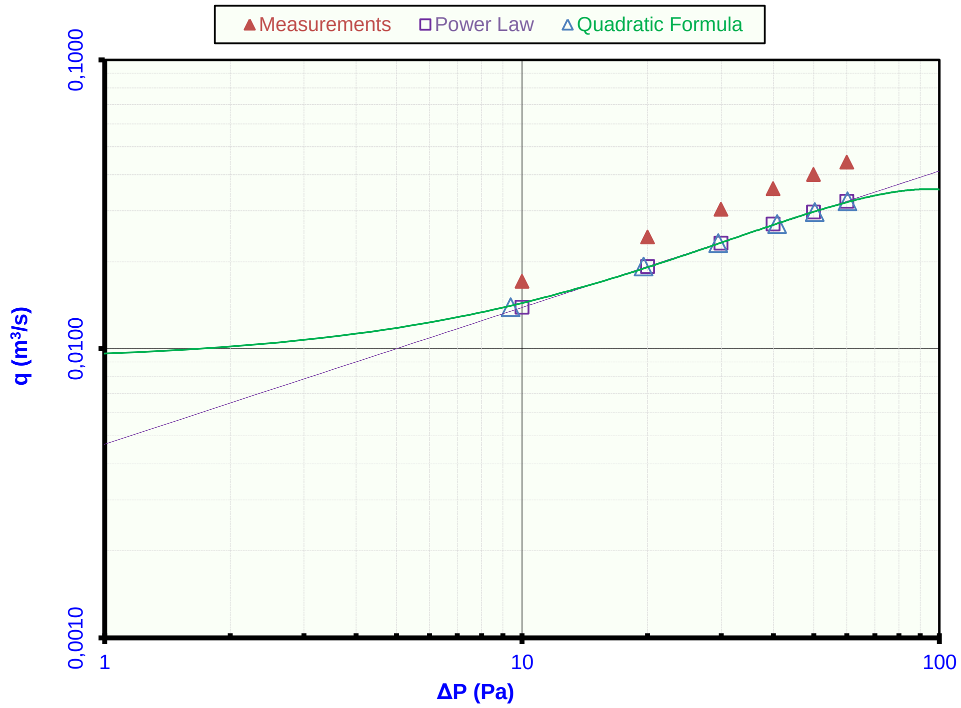

$A_{e;50}$ (m^2)	0,0032	**$u_{v;4}$ (m/s)**	2,10	**Re_4**	1116
ELA_4 (m^2)	0,0057	**$u_{v;50}$ (m/s)**	6,95	**Re_{50}**	3699

3. Openings

Measurement 2.10 1x circle Ø 10 mm

ΔP_{Bias} (Pa)	0
ΔT_{int} (°C)	24,6
ΔT_e (°C)	24,1
Flange #	2
μ	0,00002
ρ	1,205

Openings geometrics

L (m)	0,012	**A (m^2)**	0,0001
w (m)	na	**Peri (m)**	0,031
d (m)	na	**P/A**	400,000
Ø (m)	0,010	**L/d_h**	1,200
d_h (m)	0,010		

ΔP_m (Pa)	v_r (m/s)	q_m (m^3/s)	q_{open} (m^3/s)	q_{open}^2 (m^3/s)	ΔP_{QF} (Pa)
10	3,4	0,0032	0,0001	0,0000	8,82
20	6,4	0,0053	0,0001	0,0000	16,78
30	9,6	0,0074	0,0003	0,0000	32,09
40	12,3	0,0092	0,0003	0,0000	39,55
50	14,8	0,0109	0,0005	0,0000	53,85
60	17,0	0,0124	0,0005	0,0000	61,12
70	19,1	0,0138	0,0006	0,0000	68,35
80	21,3	0,0154	0,0007	0,0000	75,59
90	23,5	0,0170	0,0009	0,0000	93,05
100	25,3	0,0183	0,0010	0,0000	99,01

Power Law

c	n	r
0,00000	1,1835	0,9938

Quadratic Formula

A	B	r
130105	-33690792	0,9983

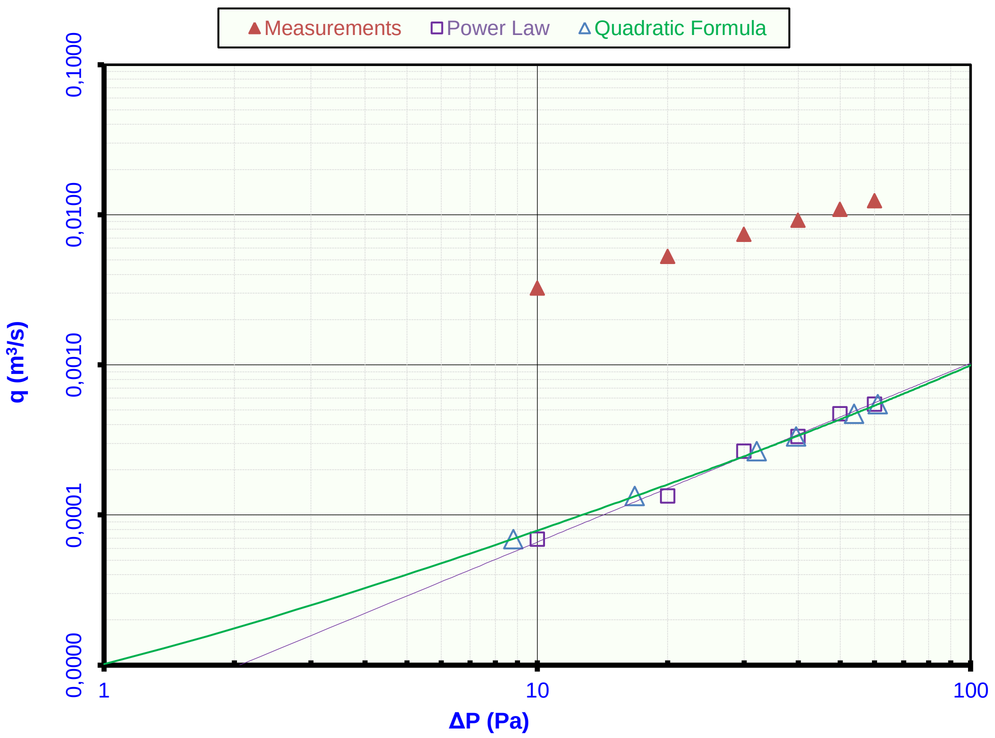

$A_{e;50}$ (m^2)	0,0000	$u_{v;4}$ (m/s)	0,28	Re_4	168
ELA_4 (m^2)	0,0000	$u_{v;50}$ (m/s)	6,00	Re_{50}	3617

Measurement 2.12 1x circle Ø 16 mm

ΔP_{Bias} (Pa)	0
ΔT_{int} (°C)	24,6
ΔT_{e} (°C)	24,1
Flange #	2
μ	0,00002
ρ	1,205

Openings geometrics

L (m)	0,012	**A (m^2)**	0,0002
w (m)	na	**Peri (m)**	0,050
d (m)	na	**P/A**	250,000
Ø (m)	0,016	**L/d_h**	0,750
d_h (m)	0,016		

ΔP_m (Pa)	v_r (m/s)	q_m (m^3/s)	q_{open} (m^3/s)	q_{open}^2 (m^3/s)	ΔP_{QF} (Pa)
10	4,2	0,0038	0,0006	0,0000	13,39
20	7,6	0,0061	0,0009	0,0000	23,37
30	10,9	0,0082	0,0011	0,0000	30,55
40	13,8	0,0102	0,0013	0,0000	39,20
50	16,4	0,0119	0,0016	0,0000	49,44
60	18,7	0,0135	0,0017	0,0000	57,74
70	20,9	0,0151	0,0019	0,0000	67,17
80	23,2	0,0167	0,0021	0,0000	78,10
90	25,3	0,0183	0,0023	0,0000	90,24
100	27,2	0,0197	0,0025	0,0000	103,54

Power Law

c	n	r
0,00015	0,5967	0,9965

Quadratic Formula

A	B	r
15120	10668389	0,9986

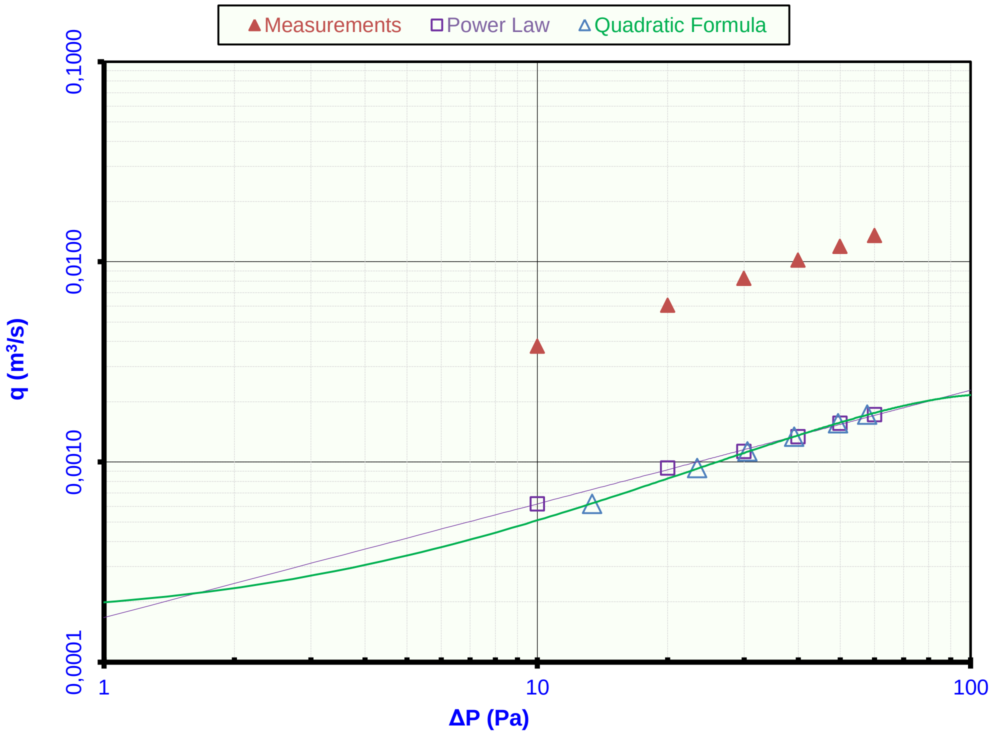

$A_{e;50}$ (m^2)	0,0002	**$u_{v;4}$ (m/s)**	1,72	**Re_4**	1656
ELA_4 (m^2)	0,0002	**$u_{v;50}$ (m/s)**	7,75	**Re_{50}**	7468

Measurement 2.13 1x circle Ø 20 mm

ΔP_{Bias} (Pa)	0
ΔT_{int} (°C)	23,4
ΔT_{e} (°C)	22,8
Flange #	2
μ	0,00002
ρ	1,205

Openings geometrics

L (m)	0,012	**A (m^2)**	0,0003
w (m)	na	**Peri (m)**	0,063
d (m)	na	**P/A**	200,000
Ø (m)	0,020	**L/d_h**	0,600
d_h (m)	0,020		

ΔP_m (Pa)	v_r (m/s)	q_m (m^3/s)	q_{open} (m^3/s)	q_{open}^2 (m^3/s)	ΔP_{QF} (Pa)
10	4,8	0,0042	0,0010	0,0000	12,41
20	8,5	0,0067	0,0015	0,0000	23,09
30	11,9	0,0089	0,0018	0,0000	29,79
40	14,9	0,0109	0,0021	0,0000	38,05
50	17,7	0,0128	0,0025	0,0000	50,36
60	20,1	0,0145	0,0027	0,0000	59,71
70	22,4	0,0162	0,0030	0,0000	70,49
80	24,6	0,0178	0,0031	0,0000	76,56
90	26,7	0,0194	0,0033	0,0000	86,47
100	28,8	0,0210	0,0037	0,0000	104,88

Power Law

c	n	r
0,00028	0,5479	0,9958

Quadratic Formula

A	B	r
6046	5919922	0,9982

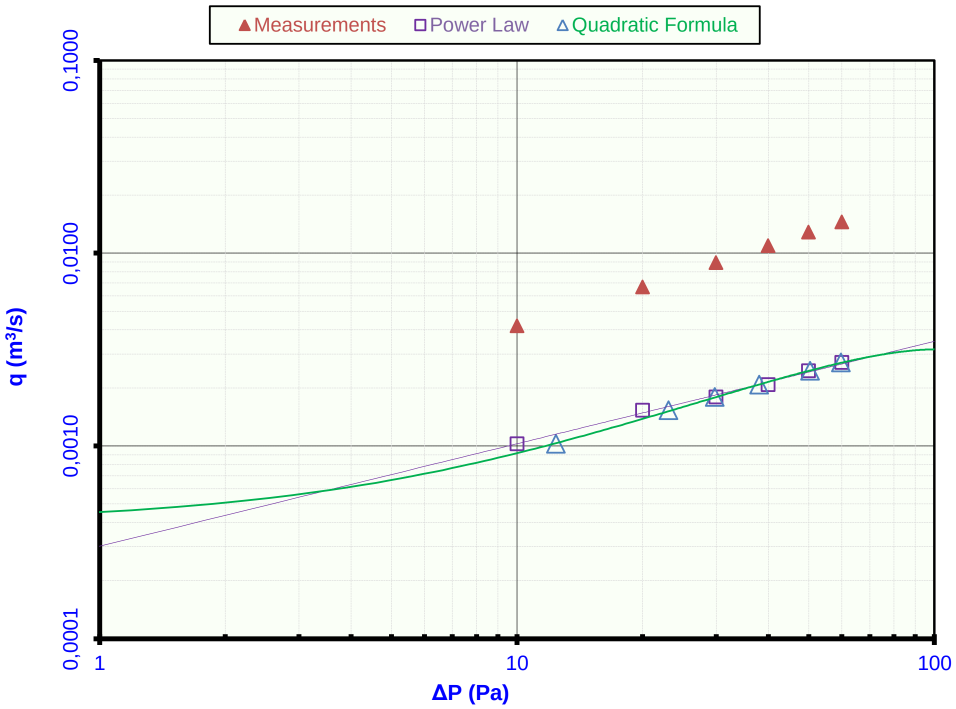

$A_{e;50}$ (m^2)	0,0003	**$u_{v;4}$ (m/s)**	1,94	**Re_4**	2333
ELA_4 (m^2)	0,0004	**$u_{v;50}$ (m/s)**	7,80	**Re_{50}**	9399

Measurement 2.14 1x circle Ø 25 mm

ΔP_{Bias} (Pa)	0
ΔT_{int} (°C)	23,5
ΔT_e (°C)	23,8
Flange #	2
μ	0,00002
ρ	1,205

Openings geometrics

L (m)	0,012	**A (m^2)**	0,0005
w (m)	na	**Peri (m)**	0,079
d (m)	na	**P/A**	160,000
Ø (m)	0,025	**L/d_h**	0,480
d_h (m)	0,025		

ΔP_m (Pa)	v_r (m/s)	q_m (m^3/s)	q_{open} (m^3/s)	q_{open}^2 (m^3/s)	ΔP_{QF} (Pa)
10	5,4	0,0046	0,0014	0,0000	11,70
20	9,5	0,0073	0,0022	0,0000	22,77
30	13,0	0,0096	0,0025	0,0000	28,63
40	16,2	0,0118	0,0030	0,0000	37,29
50	19,2	0,0139	0,0035	0,0000	49,47
60	21,9	0,0158	0,0040	0,0000	62,27
70	24,1	0,0174	0,0042	0,0000	68,71
80	26,5	0,0192	0,0046	0,0000	78,43
90	28,8	0,0210	0,0050	0,0000	91,67

Power Law

c	n	r
0,00039	0,5603	0,9947

Quadratic Formula

A	B	r
4047	2894629	0,9989

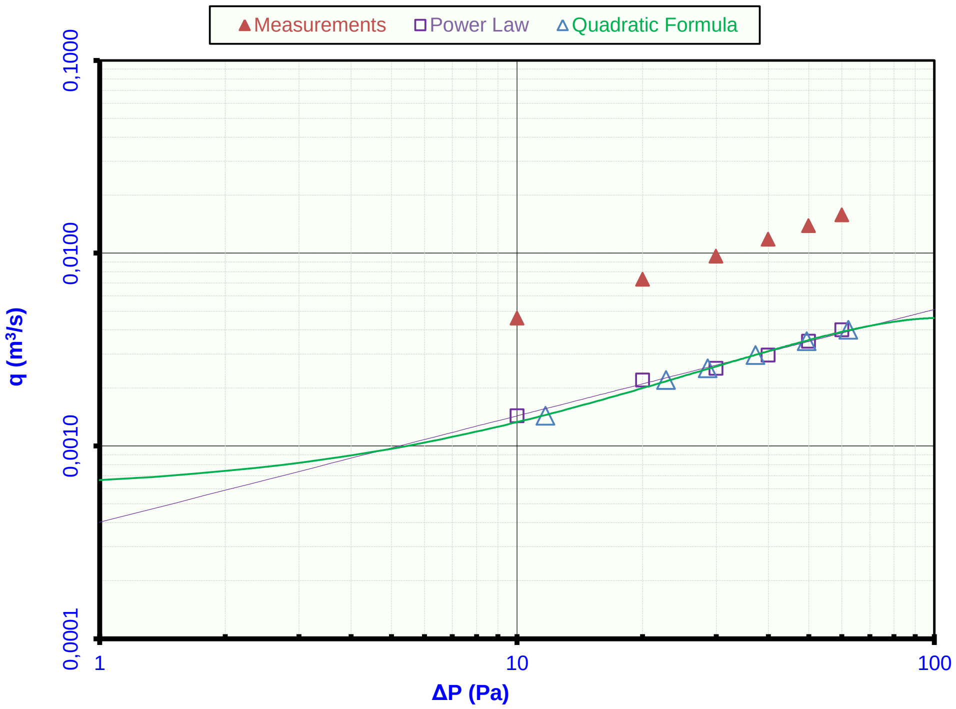

$A_{e;50}$ (m^2)	0,0004	**$u_{v;4}$ (m/s)**	1,73	**Re_4**	2598
ELA_4 (m^2)	0,0005	**$u_{v;50}$ (m/s)**	7,12	**Re_{50}**	10721

Technische Universiteit Delft

Measurement 2.15 1x circle Ø 32 mm

ΔP_{Bias} (Pa)	0
ΔT_{int} (°C)	24,4
ΔT_e (°C)	23,8
Flange #	2
μ	0,00002
ρ	1,205

Openings geometrics

L (m)	0,012	**A (m^2)**	0,0008
w (m)	na	**Peri (m)**	0,101
d (m)	na	**P/A**	125,000
Ø (m)	0,032	**L/d_h**	0,375
d_h (m)	0,032		

ΔP_m (Pa)	v_r (m/s)	q_m (m^3/s)	q_{open} (m^3/s)	q_{open}^2 (m^3/s)	ΔP_{QF} (Pa)
10	6,2	0,0051	0,0020	0,0000	11,20
20	10,6	0,0081	0,0029	0,0000	20,26
30	14,8	0,0109	0,0037	0,0000	29,81
40	18,3	0,0132	0,0044	0,0000	39,00
50	21,4	0,0154	0,0051	0,0000	49,03
60	24,3	0,0176	0,0057	0,0000	60,92
70	26,8	0,0194	0,0063	0,0000	70,42
80	29,3	0,0214	0,0067	0,0000	79,85

Power Law

c	n	r
0,00049	0,5967	0,9995

Quadratic Formula

A	B	r
3152	1296304	0,9998

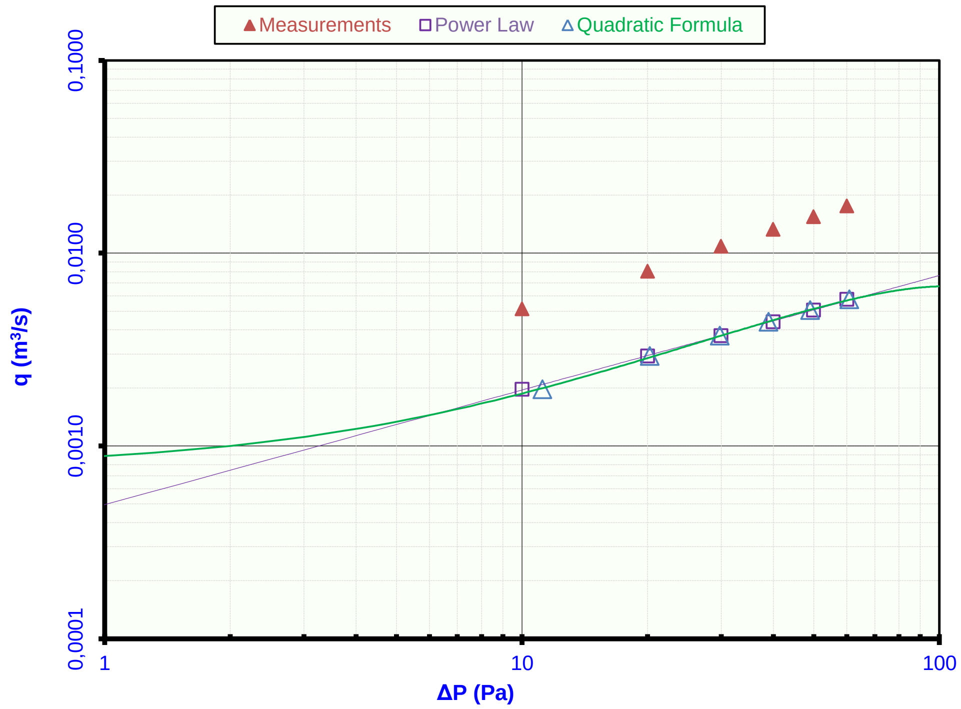

$A_{e;50}$ (m^2)	0,0006	**$u_{v;4}$ (m/s)**	1,39	**Re_4**	2671
ELA_4 (m^2)	0,0007	**$u_{v;50}$ (m/s)**	6,28	**Re_{50}**	12113

Technische Universiteit Delft

Royal HaskoningDHV

Measurement 2.16 6x circle Ø 10 mm

ΔP_{Bias} (Pa)	0
ΔT_{int} (°C)	24,5
ΔT_e (°C)	24,1
Flange #	2 / 3
μ	0,00002
ρ	1,205

Openings geometrics

L (m)	0,012	**A (m^2)**	0,0005
w (m)	na	**Peri (m)**	0,031
d (m)	na	**P/A**	66,667
Ø (m)	0,010	**L/d_h**	0,200
d_h (m)	0,060		

ΔP_m (Pa)	v_r (m/s)	q_m (m^3/s)	q_{open} (m^3/s)	q_{open}^2 (m^3/s)	ΔP_{QF} (Pa)
10	5,6	0,0047	0,0016	0,0000	9,99
20	9,5	0,0073	0,0022	0,0000	19,07
30	13,3	0,0098	0,0027	0,0000	29,05
40	16,5	0,0120	0,0032	0,0000	38,86
50	19,5	0,0141	0,0037	0,0000	52,93
60	21,9	0,0158	0,0040	0,0000	61,26
70	24,3	0,0176	0,0044	0,0000	73,21
80	6,1	0,0191	0,0045	0,0000	75,95
90	6,8	0,0209	0,0049	0,0000	89,81
100	7,4	0,0224	0,0051	0,0000	99,46

Power Law

c	n	r
0,00046	0,5202	0,9977

Quadratic Formula

A	B	r
615	3691301	0,9990

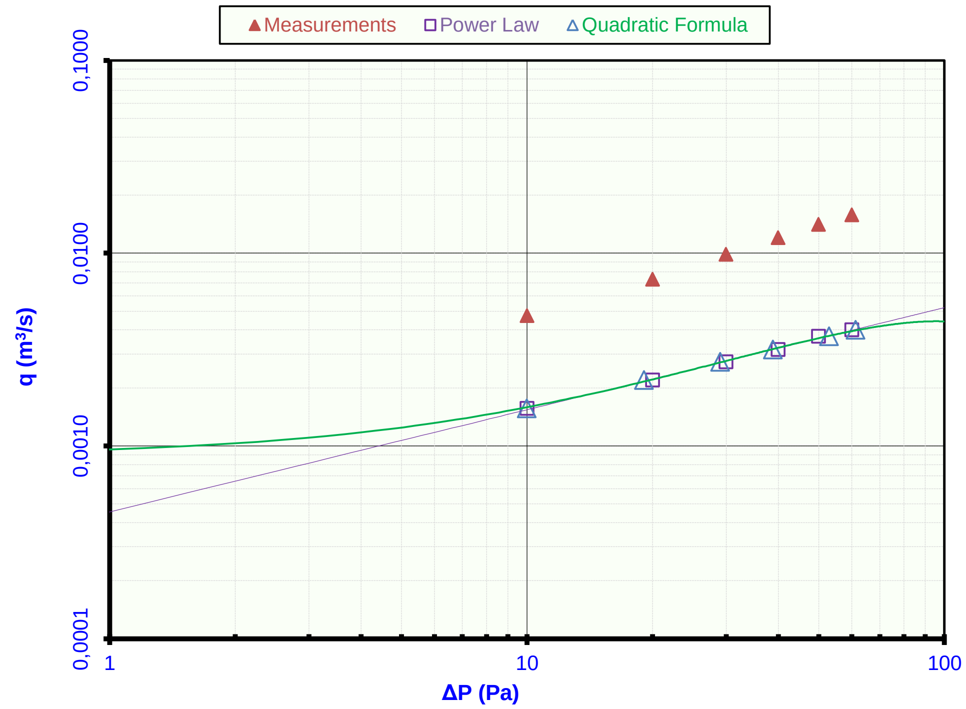

$A_{e;50}$ (m^2)	0,0004	**$u_{v;4}$ (m/s)**	2,03	**Re_4**	7327
ELA_4 (m^2)	0,0006	**$u_{v;50}$ (m/s)**	7,86	**Re_{50}**	28417

Measurement 2.17 6x circle Ø 13 mm

ΔP_{Bias} (Pa)	0
ΔT_{int} (°C)	24,3
ΔT_e (°C)	23,8
Flange #	2 / 3
μ	0,00002
ρ	1,205

Openings geometrics

L (m)	0,012	**A (m^2)**	0,0008
w (m)	na	**Peri (m)**	0,041
d (m)	na	**P/A**	51,282
Ø (m)	0,013	**L/d_h**	0,154
d_h (m)	0,078		

ΔP_m (Pa)	v_r (m/s)	q_m (m^3/s)	q_{open} (m^3/s)	q_{open}^2 (m^3/s)	ΔP_{QF} (Pa)
10	7,5	0,0060	0,0028	0,0000	9,36
20	12,0	0,0090	0,0038	0,0000	18,98
30	16,2	0,0118	0,0047	0,0000	29,30
40	19,7	0,0142	0,0054	0,0000	39,71
50	23,0	0,0166	0,0062	0,0000	54,06
60	5,9	0,0186	0,0068	0,0000	65,54
70	6,5	0,0201	0,0069	0,0000	68,30
80	7,2	0,0219	0,0072	0,0001	74,30
90	8,0	0,0239	0,0078	0,0001	88,83
100	8,7	0,0256	0,0083	0,0001	101,17

Power Law

c	n	r
0,00095	0,4683	0,9956

Quadratic Formula

A	B	r
-1219	1597681	0,9977

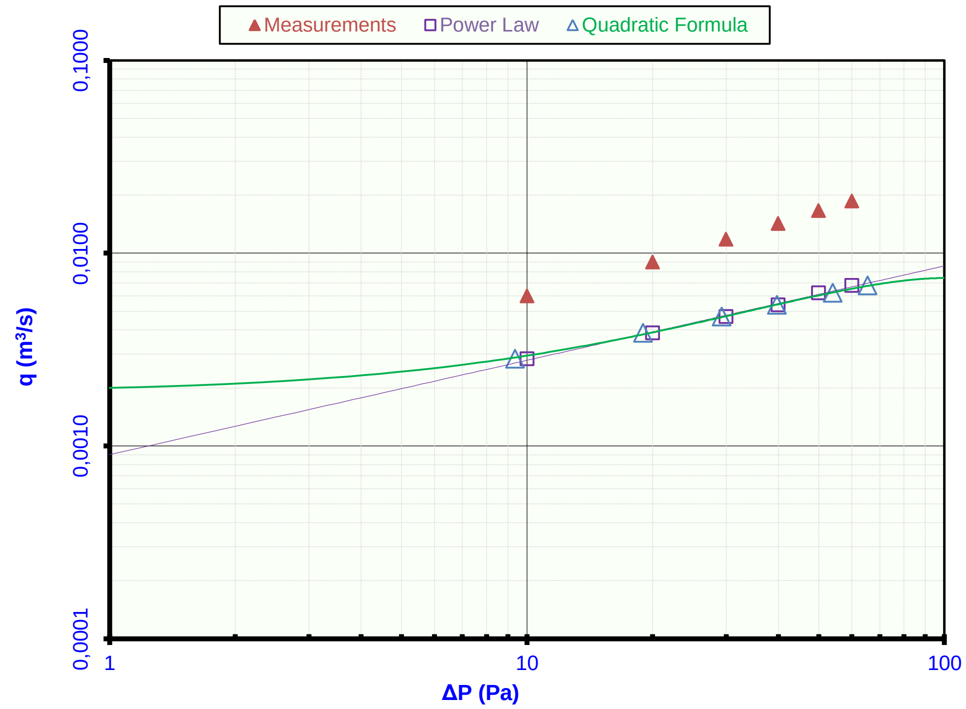

$A_{e;50}$ (m^2)	0,0007	**$u_{v;4}$ (m/s)**	2,29	**Re_4**	10755
ELA_4 (m^2)	0,0012	**$u_{v;50}$ (m/s)**	7,80	**Re_{50}**	36650

Technische Universiteit Delft

Royal HaskoningDHV

Measurement 2.18 6x circle Ø 16 mm

ΔP_{Bias} (Pa)	0
ΔT_{int} (°C)	23,1
ΔT_{e} (°C)	22,8
Flange #	2 / 3
μ	0,00002
ρ	1,205

Openings geometrics

L (m)	0,012	**A (m^2)**	0,0012
w (m)	na	**Peri (m)**	0,050
d (m)	na	**P/A**	41,667
Ø (m)	0,016	**L/d_h**	0,125
d_h (m)	0,096		

ΔP_m (Pa)	v_r (m/s)	q_m (m^3/s)	q_{open} (m^3/s)	q_{open}^2 (m^3/s)	ΔP_{QF} (Pa)
10	9,0	0,0070	0,0038	0,0000	8,51
20	14,3	0,0105	0,0054	0,0000	18,61
30	19,0	0,0137	0,0066	0,0000	29,24
40	23,1	0,0167	0,0078	0,0001	42,02
50	6,1	0,0191	0,0087	0,0001	53,07
60	6,9	0,0211	0,0093	0,0001	60,94
70	7,7	0,0231	0,0099	0,0001	69,91
80	8,5	0,0251	0,0105	0,0001	77,87
90	9,3	0,0271	0,0111	0,0001	88,07
100	10,1	0,0291	0,0118	0,0001	100,97

Power Law

c	n	r
0,00126	0,4859	0,9978

Quadratic Formula

A	B	r
-794	788640	0,9993

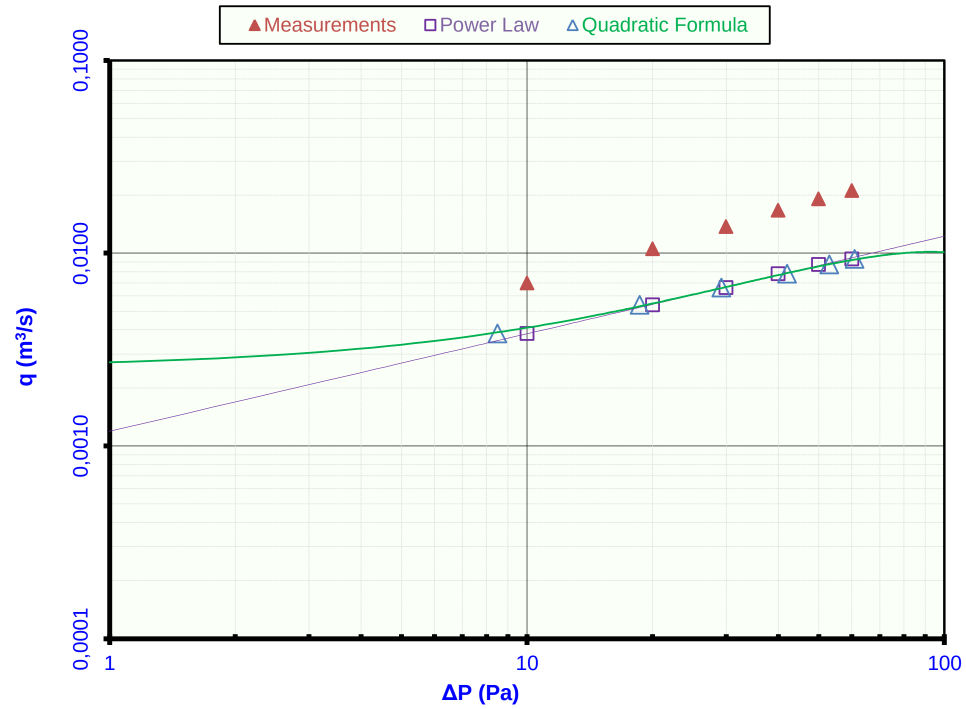

$A_{e;50}$ (m^2)	0,0009	**$u_{v;4}$ (m/s)**	2,05	**Re_4**	11833
ELA_4 (m^2)	0,0016	**$u_{v;50}$ (m/s)**	7,23	**Re_{50}**	41819

TU Delft
Technische Universiteit Delft

Royal HaskoningDHV

Measurement 2.19 6x circle Ø 20 mm

ΔP_{Bias} (Pa)	0
ΔT_{int} (ºC)	24,5
ΔT_e (ºC)	24,1
Flange #	3
μ	0,00002
ρ	1,205

Openings geometrics

L (m)	0,012	**A (m^2)**	0,0019
w (m)	na	**Peri (m)**	0,063
d (m)	na	**P/A**	33,333
Ø (m)	0,020	**L/d_h**	0,100
d_h (m)	0,120		

ΔP_m (Pa)	v_r (m/s)	q_m (m^3/s)	q_{open} (m^3/s)	q_{open}^2 (m^3/s)	ΔP_{QF} (Pa)
10	2,1	0,0088	0,0056	0,0000	8,84
20	3,7	0,0130	0,0079	0,0001	20,15
30	5,1	0,0166	0,0095	0,0001	30,91
40	6,2	0,0194	0,0105	0,0001	39,30
50	7,3	0,0221	0,0117	0,0001	50,23
60	8,3	0,0246	0,0128	0,0002	60,95
70	9,2	0,0268	0,0137	0,0002	70,32
80	10,1	0,0291	0,0144	0,0002	79,18
90	11,0	0,0313	0,0153	0,0002	90,00
100	11,8	0,0333	0,0161	0,0003	99,80

Power Law

c	n	r
0,00200	0,4502	0,9994

Quadratic Formula

A	B	r
-942	445425	0,9999

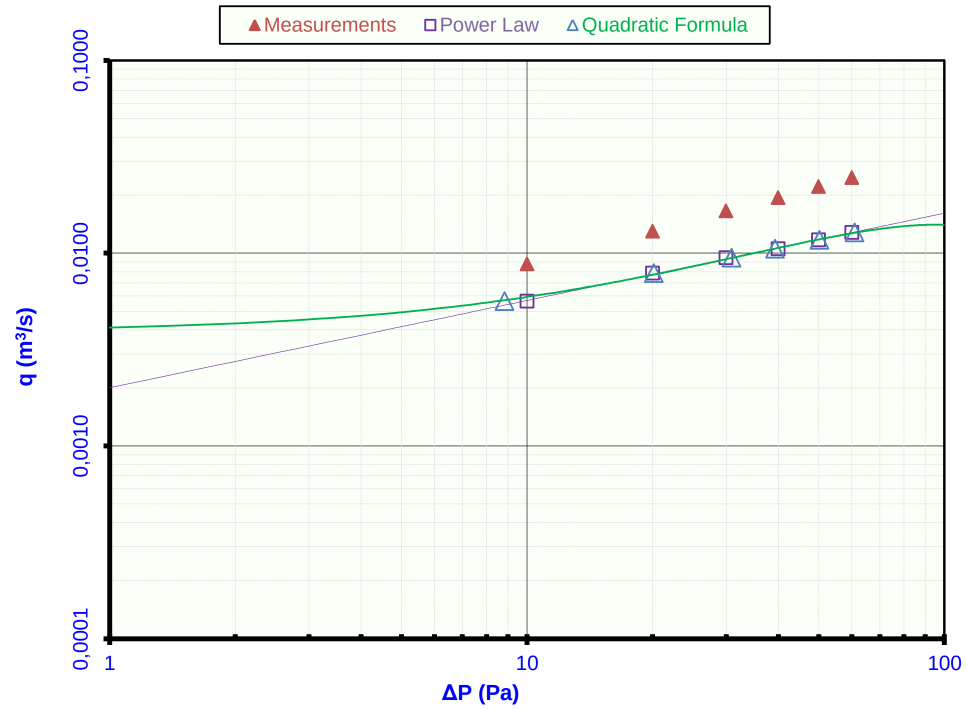

$A_{e;50}$ (m^2)	0,0013	**$u_{v;4}$ (m/s)**	1,98	**Re_4**	14337
ELA_4 (m^2)	0,0024	**$u_{v;50}$ (m/s)**	6,22	**Re_{50}**	44993

Measurement 2.20   6x circle Ø 25 mm

ΔP_{Bias} (Pa)	0
ΔT_{int} (°C)	24,6
ΔT_e (°C)	24,1
Flange #	3
μ	0,00002
ρ	1,205

Openings geometrics

L (m)	0,012	**A (m^2)**	0,0029
w (m)	na	**Peri (m)**	0,079
d (m)	na	**P/A**	26,667
Ø (m)	0,025	**L/d_h**	0,080
d_h (m)	0,150		

ΔP_m (Pa)	v_r (m/s)	q_m (m^3/s)	q_{open} (m^3/s)	q_{open}^2 (m^3/s)	ΔP_{QF} (Pa)
10	3,3	0,0120	0,0088	0,0001	8,72
20	5,3	0,0171	0,0120	0,0001	19,05
30	7,1	0,0216	0,0145	0,0002	30,08
40	8,6	0,0254	0,0165	0,0003	40,61
50	9,9	0,0286	0,0182	0,0003	50,67
60	11,1	0,0316	0,0198	0,0004	60,92
70	12,2	0,0343	0,0211	0,0004	70,64
80	13,3	0,0371	0,0224	0,0005	80,40
90	14,3	0,0396	0,0236	0,0006	89,75
100	15,2	0,0419	0,0246	0,0006	98,55

Power Law

c	n	r
0,00311	0,4491	0,9998

Quadratic Formula

A	B	r
-683	190438	0,9998

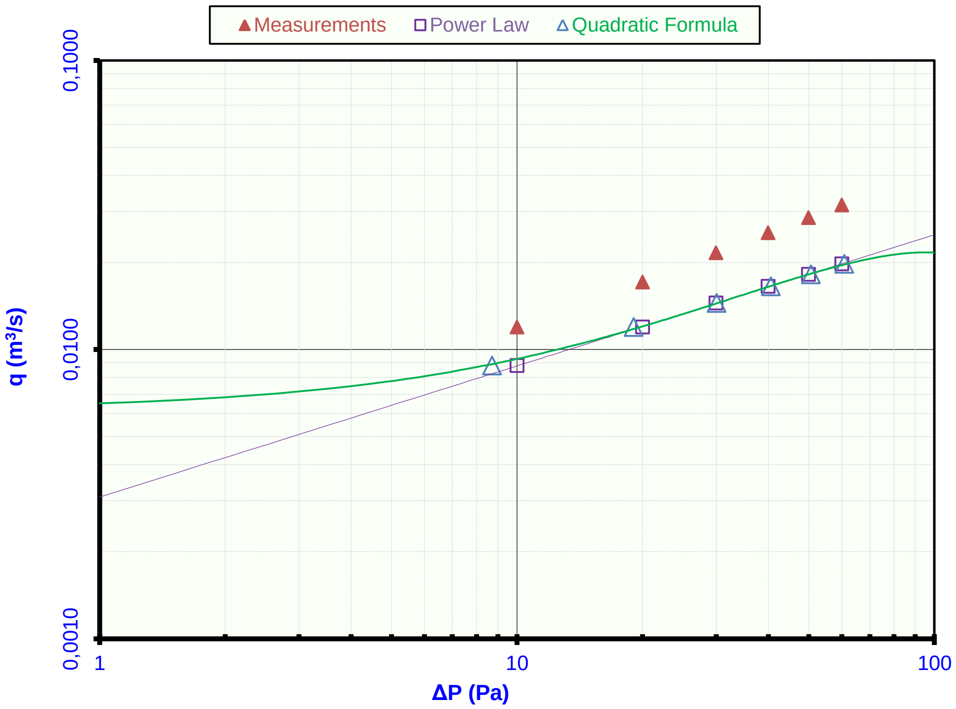

$A_{e;50}$ (m^2)	0,0020	**$u_{v;4}$ (m/s)**	1,97	**Re_4**	17760
ELA_4 (m^2)	0,0037	**$u_{v;50}$ (m/s)**	6,18	**Re_{50}**	55860

Measurement 2.21 6x circle Ø 32 mm

ΔP_{Bias} (Pa)	0
ΔT_{int} (°C)	24,3
ΔT_e (°C)	24,1
Flange #	3
μ	0,00002
ρ	1,205

Openings geometrics

L (m)	0,012	**A (m^2)**	0,0048
w (m)	na	**Peri (m)**	0,101
d (m)	na	**P/A**	20,833
Ø (m)	0,032	**L/d_h**	0,063
d_h (m)	0,192		

ΔP_m (Pa)	v_r (m/s)	q_m (m^3/s)	q_{open} (m^3/s)	q_{open}^2 (m^3/s)	ΔP_{QF} (Pa)
10	4,7	0,0156	0,0124	0,0002	9,85
20	7,3	0,0221	0,0170	0,0003	19,99
30	9,6	0,0278	0,0207	0,0004	30,83
40	11,4	0,0323	0,0235	0,0006	40,33
50	13,0	0,0363	0,0259	0,0007	49,88
60	14,5	0,0401	0,0283	0,0008	59,95
70	15,8	0,0434	0,0302	0,0009	68,88
80	17,2	0,0470	0,0323	0,0010	79,41
90	18,5	0,0504	0,0343	0,0012	90,10
100	19,7	0,0535	0,0362	0,0013	100,86

Power Law

c	n	r
0,00422	0,4633	0,9997

Quadratic Formula

A	B	r
-239	83345	0,9999

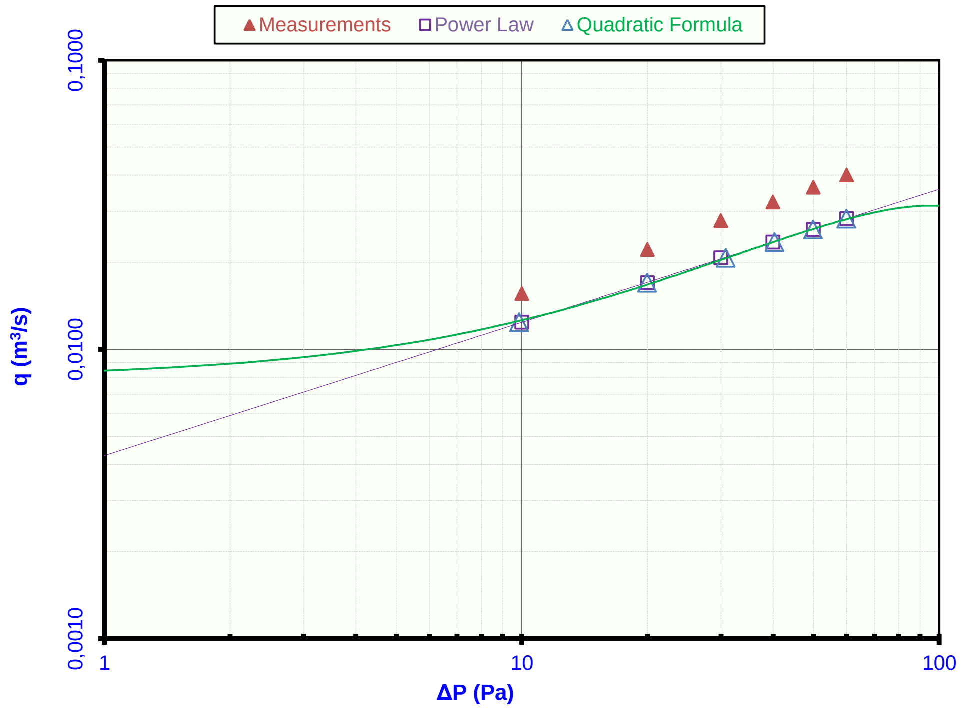

$A_{e;50}$ (m^2)	0,0028	**$u_{v;4}$ (m/s)**	1,66	**Re_4**	19246
ELA_4 (m^2)	0,0051	**$u_{v;50}$ (m/s)**	5,37	**Re_{50}**	62176

Technische Universiteit Delft

4. Pipes

Technische Universiteit Delft

Measurement 2.22 6x 50 cm pipes, Ø 10 mm

ΔP_{Bias} (Pa)	0
ΔT_{int} (°C)	24,5
ΔT_e (°C)	24,1
Flange #	2
μ	0,00002
ρ	1,205

Openings geometrics

L (m)	0,500	**A (m²)**	0,0003
w (m)	na	**Peri (m)**	0,025
d (m)	na	**P/A**	83,333
Ø (m)	0,008	**L/d_h**	10,417
d_h (m)	0,048		

ΔP_m (Pa)	v_r (m/s)	q_m (m³/s)	q_{open} (m³/s)	q_{open}^2 (m³/s)	ΔP_{QF} (Pa)
10	4,0	0,0036	0,0005	0,0000	8,12
20	7,5	0,0060	0,0009	0,0000	20,47
30	10,8	0,0082	0,0011	0,0000	28,64
40	13,7	0,0101	0,0013	0,0000	38,90
50	16,3	0,0119	0,0015	0,0000	51,47
60	18,6	0,0135	0,0017	0,0000	61,90
70	20,8	0,0150	0,0018	0,0000	73,99
80	23,0	0,0166	0,0019	0,0000	82,52
90	25,0	0,0181	0,0021	0,0000	91,78
100	26,9	0,0195	0,0023	0,0000	108,26

Power Law

c	n	r
0,00011	0,6478	0,9940

Quadratic Formula

A	B	r
8464	17521671	0,9986

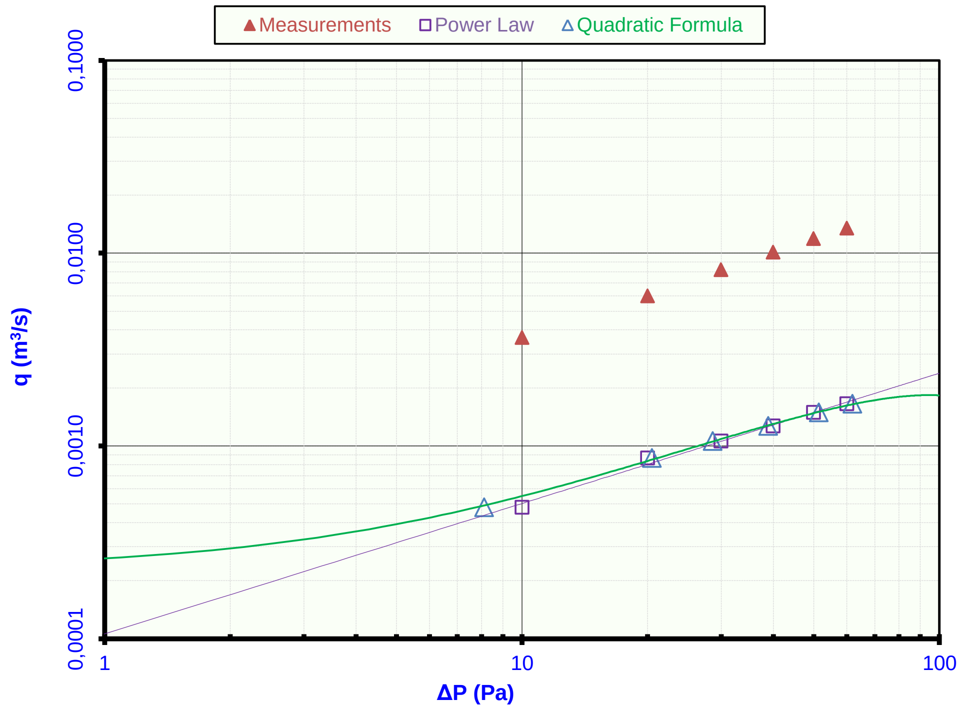

$A_{e;50}$ (m²)	0,0002	**$u_{v;4}$ (m/s)**	0,93	**Re_4**	2691
ELA_4 (m²)	0,0002	**$u_{v;50}$ (m/s)**	4,94	**Re_{50}**	14282

Measurement 2.23 6x 50 cm pipes, Ø 13 mm

ΔP_{Bias} (Pa)	0
ΔT_{int} (°C)	24,2
ΔT_e (°C)	23,8
Flange #	2
μ	0,00002
ρ	1,205

Openings geometrics

L (m)	0,500	**A (m^2)**	0,0006
w (m)	na	**Peri (m)**	0,035
d (m)	na	**P/A**	60,606
Ø (m)	0,011	**L/d_h**	7,576
d_h (m)	0,066		

ΔP_m (Pa)	v_r (m/s)	q_m (m^3/s)	q_{open} (m^3/s)	q_{open}^2 (m^3/s)	ΔP_{QF} (Pa)
10	4,9	0,0043	0,0011	0,0000	13,64
20	8,7	0,0068	0,0017	0,0000	23,04
30	12,3	0,0092	0,0021	0,0000	30,46
40	15,5	0,0113	0,0025	0,0000	39,30
50	18,2	0,0132	0,0028	0,0000	46,41
60	21,0	0,0152	0,0033	0,0000	59,94
70	23,4	0,0169	0,0037	0,0000	69,64
80	25,9	0,0187	0,0041	0,0000	80,82
90	28,0	0,0204	0,0043	0,0000	88,35

Power Law

c	n	r
0,00024	0,6349	0,9956

Quadratic Formula

A	B	r
9866	2405969	0,9991

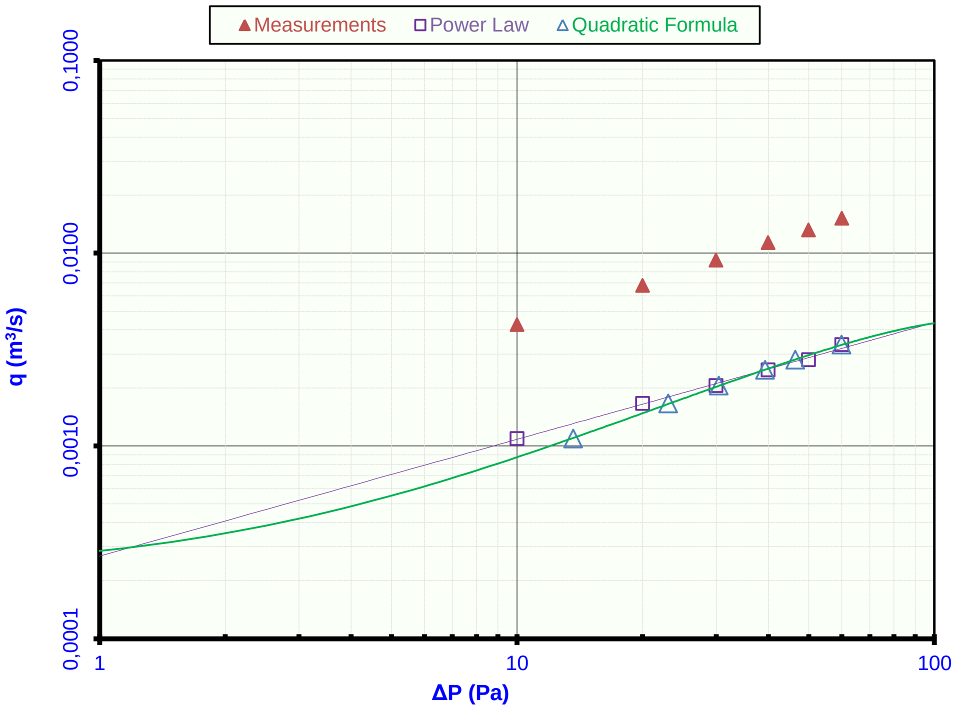

$A_{e;50}$ (m^2)	0,0003	**$u_{v;4}$ (m/s)**	1,03	**Re_4**	4089
ELA_4 (m^2)	0,0004	**$u_{v;50}$ (m/s)**	4,90	**Re_{50}**	19503

TU Delft
Technische Universiteit Delft

Royal HaskoningDHV

Measurement 2.24 6x 50 cm pipes, Ø 16 mm

ΔP_{Bias} (Pa)	0
ΔT_{int} (°C)	24,2
ΔT_e (°C)	23,8
Flange #	2 / 3
μ	0,00002
ρ	1,205

Openings geometrics

L (m)	0,500	**A (m^2)**	0,0007
w (m)	na	**Peri (m)**	0,038
d (m)	na	**P/A**	55,556
Ø (m)	0,012	**L/d_h**	6,944
d_h (m)	0,072		

ΔP_m (Pa)	v_r (m/s)	q_m (m^3/s)	q_{open} (m^3/s)	q_{open}^2 (m^3/s)	ΔP_{QF} (Pa)
10	5,5	0,0047	0,0015	0,0000	9,54
20	9,5	0,0073	0,0022	0,0000	19,79
30	13,3	0,0098	0,0027	0,0000	30,14
40	16,4	0,0119	0,0031	0,0000	38,63
50	19,4	0,0140	0,0036	0,0000	52,88
60	4,8	0,0158	0,0040	0,0000	64,18
70	5,4	0,0173	0,0042	0,0000	68,88
80	6,1	0,0191	0,0045	0,0000	78,75
90	6,7	0,0206	0,0046	0,0000	83,91
100	7,4	0,0224	0,0051	0,0000	103,13

Power Law

c	n	r
0,00045	0,5224	0,9965

Quadratic Formula

A	B	r
648	3825424	0,9980

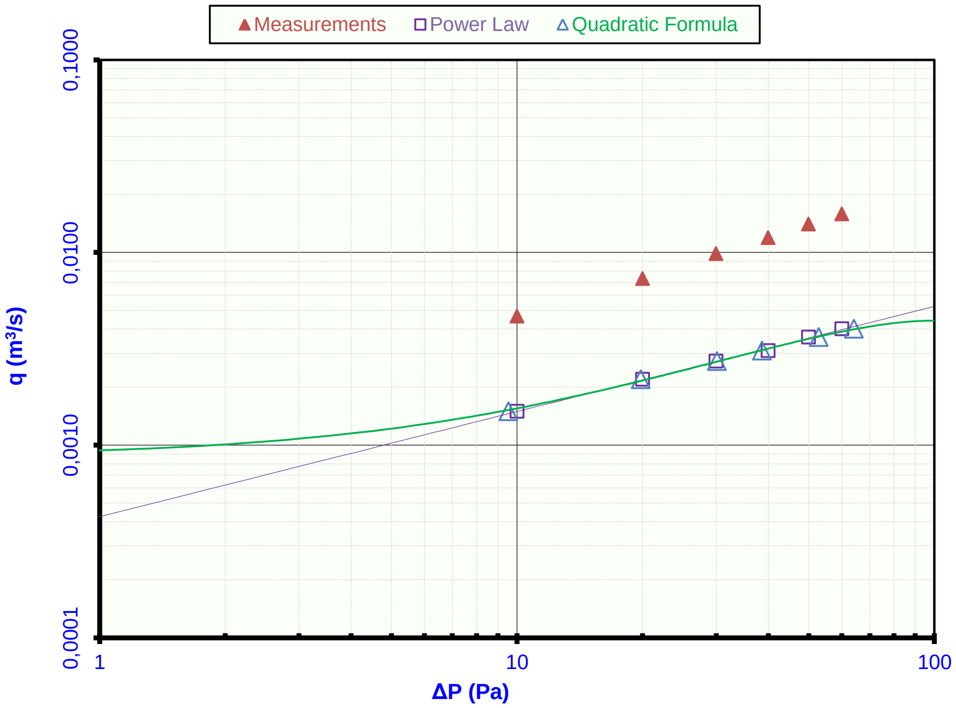

$A_{e;50}$ (m^2)	0,0004	**$u_{v;4}$ (m/s)**	1,38	**Re_4**	5967
ELA_4 (m^2)	0,0006	**$u_{v;50}$ (m/s)**	5,36	**Re_{50}**	23232

Technische Universiteit Delft

Measurement 2.25 6x 50 cm pipes, Ø 20 mm

ΔP_{Bias} (Pa)	0
ΔT_{int} (°C)	24,2
ΔT_e (°C)	23,8
Flange #	2 / 3
μ	0,00002
ρ	1,205

Openings geometrics

L (m)	0,500	**A (m^2)**	0,0012
w (m)	na	**Peri (m)**	0,050
d (m)	na	**P/A**	41,667
Ø (m)	0,016	**L/d_h**	5,208
d_h (m)	0,096		

ΔP_m (Pa)	v_r (m/s)	q_m (m^3/s)	q_{open} (m^3/s)	q_{open}^2 (m^3/s)	ΔP_{QF} (Pa)
10	7,8	0,0062	0,0030	0,0000	9,52
20	12,9	0,0096	0,0044	0,0000	21,12
30	3,5	0,0125	0,0054	0,0000	30,92
40	4,5	0,0151	0,0062	0,0000	41,78
50	5,3	0,0171	0,0067	0,0000	48,92
60	6,1	0,0191	0,0073	0,0001	58,22
70	6,9	0,0211	0,0079	0,0001	68,93
80	7,7	0,0231	0,0085	0,0001	78,55
90	8,5	0,0251	0,0091	0,0001	90,94
100	9,2	0,0268	0,0096	0,0001	101,35

Power Law

c	n	r
0,00100	0,4878	0,9981

Quadratic Formula

A	B	r
-287	1131416	0,9996

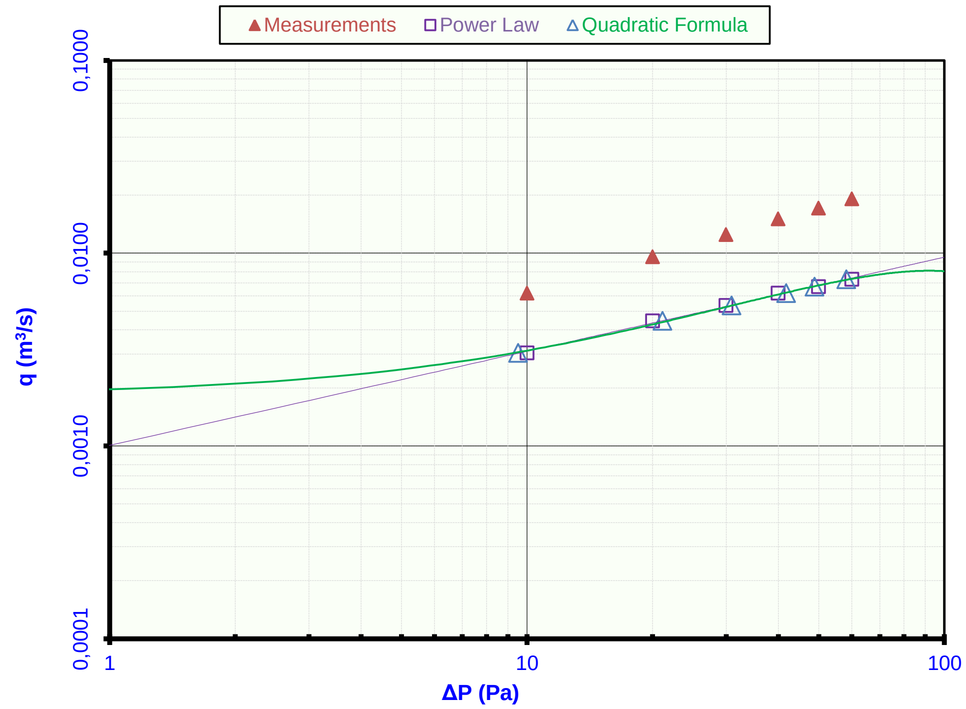

$A_{e;50}$ (m^2)	0,0007	**$u_{v;4}$ (m/s)**	1,63	**Re_4**	9416
ELA_4 (m^2)	0,0012	**$u_{v;50}$ (m/s)**	5,56	**Re_{50}**	32138

Measurement 2.26 6x 34 cm pipes, Ø 10 mm

ΔP_{Bias} (Pa)	0
ΔT_{int} (°C)	24,3
ΔT_e (°C)	24,1
Flange #	2
μ	0,00002
ρ	1,205

Openings geometrics

L (m)	0,340	**A (m^2)**	0,0003
w (m)	na	**Peri (m)**	0,025
d (m)	na	**P/A**	83,333
Ø (m)	0,008	**L/d_h**	7,083
d_h (m)	0,048		

ΔP_m (Pa)	v_r (m/s)	q_m (m^3/s)	q_{open} (m^3/s)	q_{open}^2 (m^3/s)	ΔP_{QF} (Pa)
10	4,3	0,0039	0,0007	0,0000	13,28
20	7,8	0,0062	0,0011	0,0000	24,64
30	11,1	0,0084	0,0013	0,0000	31,52
40	14,0	0,0103	0,0015	0,0000	39,86
50	16,6	0,0121	0,0017	0,0000	49,74
60	18,9	0,0137	0,0019	0,0000	57,78
70	21,1	0,0152	0,0020	0,0000	66,94
80	23,4	0,0169	0,0022	0,0000	77,54
90	25,4	0,0184	0,0024	0,0000	84,80
100	27,5	0,0200	0,0027	0,0000	107,25

Power Law

c	n	r
0,00018	0,5695	0,9945

Quadratic Formula

A	B	r
12597	9889080	0,9965

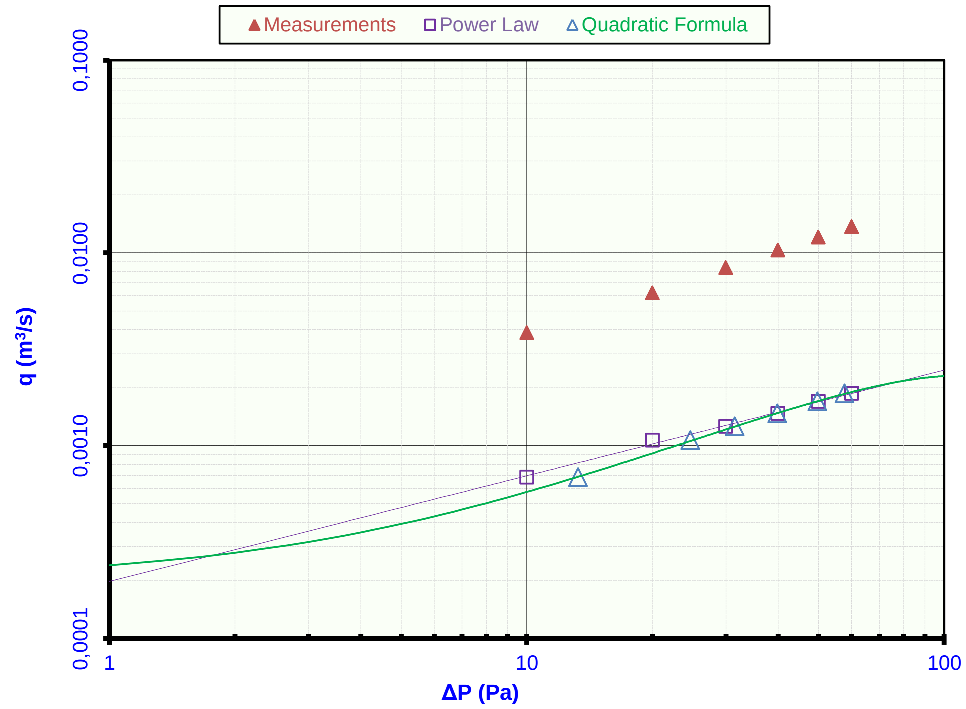

$A_{e;50}$ (m^2)	0,0002	**$u_{v;4}$ (m/s)**	1,34	**Re_4**	3866
ELA_4 (m^2)	0,0003	**$u_{v;50}$ (m/s)**	5,62	**Re_{50}**	16248

Measurement 2.27 6x 34 cm pipes, Ø 13 mm

ΔP_{Bias} (Pa)	0
ΔT_{int} (°C)	24,2
ΔT_{e} (°C)	23,8
Flange #	2
μ	0,00002
ρ	1,205

Openings geometrics

L (m)	0,340	**A (m^2)**	0,0006
w (m)	na	**Peri (m)**	0,035
d (m)	na	**P/A**	60,606
Ø (m)	0,011	**L/d_h**	5,152
d_h (m)	0,066		

ΔP_m (Pa)	v_r (m/s)	q_m (m^3/s)	q_{open} (m^3/s)	q_{open}^2 (m^3/s)	ΔP_{QF} (Pa)
10	5,5	0,0047	0,0015	0,0000	13,89
20	9,5	0,0073	0,0022	0,0000	23,67
30	13,2	0,0098	0,0027	0,0000	31,40
40	16,4	0,0119	0,0031	0,0000	39,54
50	19,2	0,0139	0,0035	0,0000	47,70
60	21,8	0,0157	0,0039	0,0000	57,17
70	24,3	0,0176	0,0044	0,0000	68,08
80	26,7	0,0194	0,0047	0,0000	76,74
90	29,2	0,0213	0,0053	0,0000	92,94

Power Law

c	n	r
0,00040	0,5595	0,9953

Quadratic Formula

A	B	r
6004	2189657	0,7382

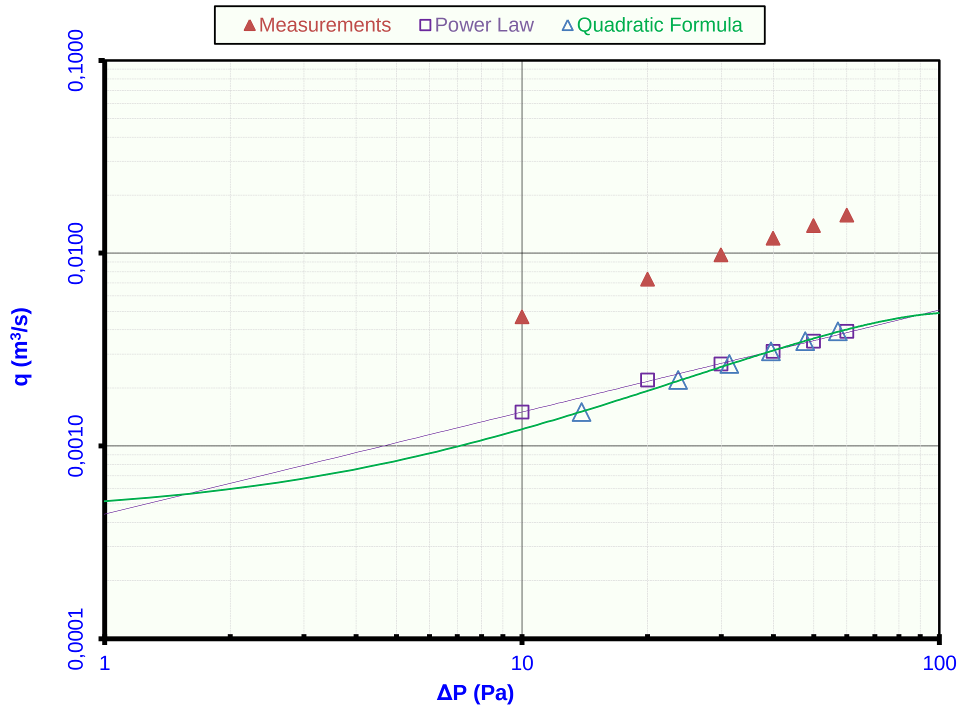

$A_{e;50}$ (m^2)	0,0004	**$u_{v;4}$ (m/s)**	1,52	**Re_4**	6063
ELA_4 (m^2)	0,0006	**$u_{v;50}$ (m/s)**	6,13	**Re_{50}**	24366

Measurement 2.28 6x 34 cm pipes, Ø 16 mm

ΔP_{Bias} (Pa)	0
ΔT_{int} (°C)	23,1
ΔT_e (°C)	22,8
Flange #	2 / 3
μ	0,00002
ρ	1,205

Openings geometrics

L (m)	0,340	**A (m^2)**	0,0007
w (m)	na	**Peri (m)**	0,038
d (m)	na	**P/A**	55,556
Ø (m)	0,012	**L/d_h**	4,722
d_h (m)	0,072		

ΔP_m (Pa)	v_r (m/s)	q_m (m^3/s)	q_{open} (m^3/s)	q_{open}^2 (m^3/s)	ΔP_{QF} (Pa)
10	6,1	0,0051	0,0019	0,0000	8,57
20	10,4	0,0079	0,0028	0,0000	19,26
30	14,2	0,0105	0,0033	0,0000	27,82
40	17,6	0,0128	0,0039	0,0000	39,00
50	20,6	0,0149	0,0045	0,0000	51,42
60	23,4	0,0169	0,0051	0,0000	66,54
70	25,6	0,0185	0,0053	0,0000	73,70
80	6,5	0,0201	0,0055	0,0000	76,99
90	7,2	0,0219	0,0059	0,0000	88,72
100	7,8	0,0234	0,0061	0,0000	96,80

Power Law

c	n	r
0,00059	0,5122	0,9955

Quadratic Formula

A	B	r
-601	2694195	0,9977

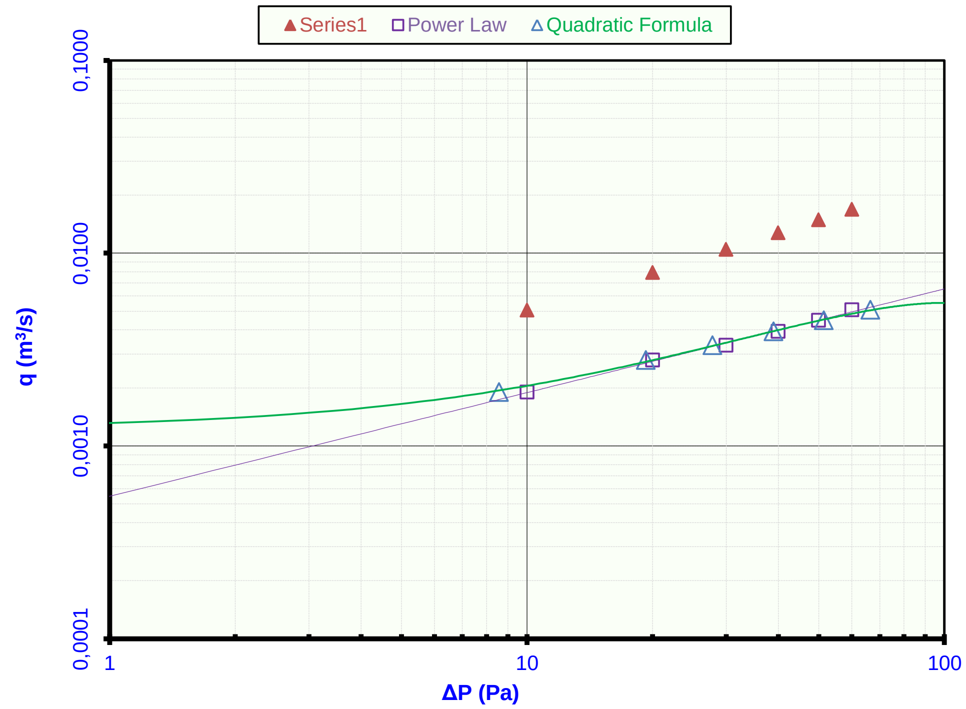

$A_{e;50}$ (m^2)	0,0005	**$u_{v;4}$ (m/s)**	1,77	**Re_4**	7665
ELA_4 (m^2)	0,0008	**$u_{v;50}$ (m/s)**	6,60	**Re_{50}**	28651

Technische Universiteit Delft

Royal HaskoningDHV

Measurement 2.29 6x 34 cm pipes, Ø 20 mm

ΔP_{Bias} (Pa)	0
ΔT_{int} (°C)	24,2
ΔT_e (°C)	23,8
Flange #	2 / 3
μ	0,00002
ρ	1,205

Openings geometrics

L (m)	0,340	**A (m^2)**	0,0012
w (m)	na	**Peri (m)**	0,050
d (m)	na	**P/A**	41,667
Ø (m)	0,016	**L/d_h**	3,542
d_h (m)	0,096		

ΔP_m (Pa)	v_r (m/s)	q_m (m^3/s)	q_{open} (m^3/s)	q_{open}^2 (m^3/s)	ΔP_{QF} (Pa)
10	8,2	0,0065	0,0033	0,0000	8,48
20	13,6	0,0100	0,0049	0,0000	20,77
30	17,9	0,0130	0,0058	0,0000	30,25
40	21,4	0,0154	0,0066	0,0000	39,06
50	5,6	0,0178	0,0075	0,0001	50,86
60	6,4	0,0199	0,0081	0,0001	59,77
70	7,3	0,0221	0,0089	0,0001	74,28
80	8,0	0,0239	0,0092	0,0001	79,14
90	8,7	0,0256	0,0096	0,0001	86,17
100	9,5	0,0276	0,0103	0,0001	100,75

Power Law

c	n	r
0,00111	0,4841	0,9967

Quadratic Formula

A	B	r
-786	1018778	0,9990

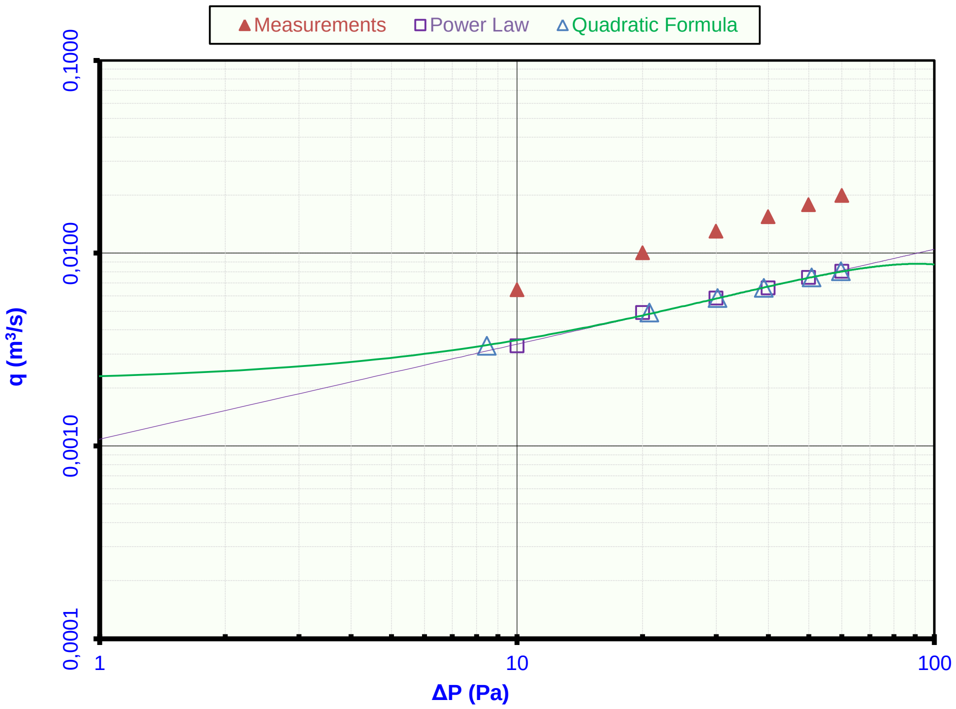

$A_{e;50}$ (m^2)	0,0008	**$u_{v;4}$ (m/s)**	1,79	**Re_4**	10366
ELA_4 (m^2)	0,0014	**$u_{v;50}$ (m/s)**	6,19	**Re_{50}**	35776

Technische Universiteit Delft

Measurement 2.30 6x 16 cm pipes, Ø 10 mm

ΔP_{Bias} (Pa)	0
ΔT_{int} (°C)	24,3
ΔT_e (°C)	24,1
Flange #	2
μ	0,00002
ρ	1,205

Openings geometrics

L (m)	0,160	**A (m^2)**	0,0003
w (m)	na	**Peri (m)**	0,025
d (m)	na	**P/A**	83,333
Ø (m)	0,008	**L/d_h**	3,333
d_h (m)	0,048		

ΔP_m (Pa)	v_r (m/s)	q_m (m^3/s)	q_{open} (m^3/s)	q_{open}^2 (m^3/s)	ΔP_{QF} (Pa)
10	4,3	0,0039	0,0007	0,0000	11,94
20	7,9	0,0063	0,0011	0,0000	23,07
30	11,3	0,0085	0,0014	0,0000	30,77
40	14,3	0,0105	0,0017	0,0000	40,05
50	17,0	0,0124	0,0020	0,0000	51,07
60	19,2	0,0139	0,0021	0,0000	55,21
70	21,6	0,0156	0,0024	0,0000	69,14
80	24,0	0,0173	0,0027	0,0000	82,02
90	25,9	0,0187	0,0027	0,0000	84,97
100	28,0	0,0204	0,0031	0,0000	103,95

Power Law

c	n	r
0,00016	0,6354	0,9963

Quadratic Formula

A	B	r
12884	6634974	0,9978

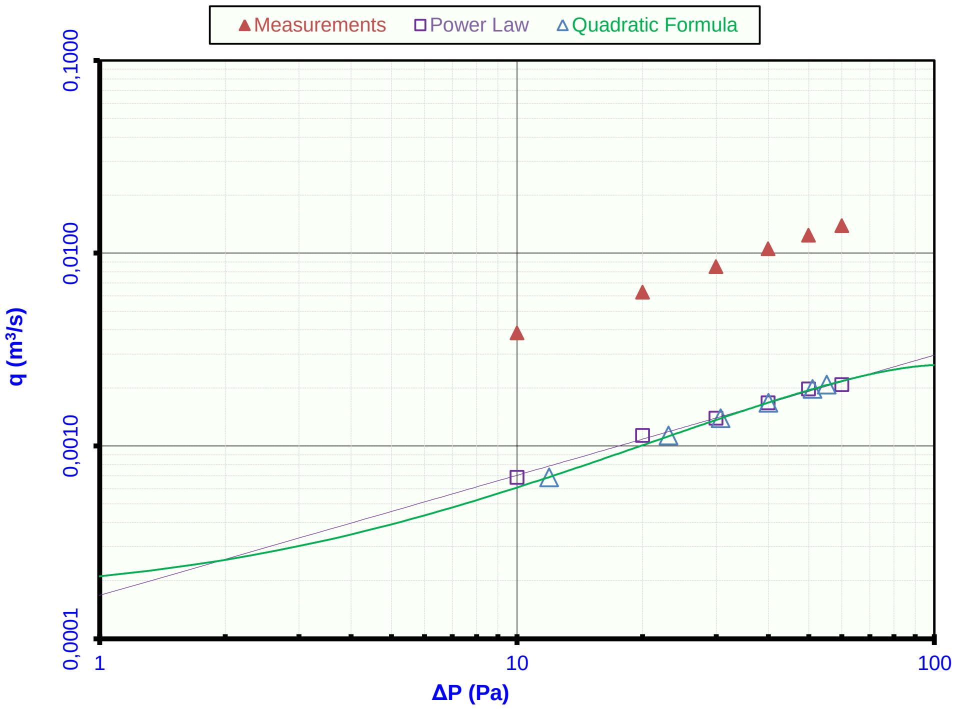

$A_{e;50}$ (m^2)	0,0002	**$u_{v;4}$ (m/s)**	1,28	**Re_4**	3700
ELA_4 (m^2)	0,0002	**$u_{v;50}$ (m/s)**	6,53	**Re_{50}**	18876

Measurement 2.31 — 6x 16 cm pipes, Ø 13 mm

ΔP_{Bias} (Pa)	0
ΔT_{int} (°C)	24,2
ΔT_e (°C)	23,8
Flange #	2
μ	0,00002
ρ	1,205

Openings geometrics

L (m)	0,160	**A (m^2)**	0,0006
w (m)	na	**Peri (m)**	0,035
d (m)	na	**P/A**	60,606
Ø (m)	0,011	**L/d_h**	2,424
d_h (m)	0,066		

ΔP_m (Pa)	v_r (m/s)	q_m (m^3/s)	q_{open} (m^3/s)	q_{open}^2 (m^3/s)	ΔP_{QF} (Pa)
10	5,6	0,0047	0,0016	0,0000	9,58
20	9,8	0,0075	0,0024	0,0000	20,41
30	13,5	0,0100	0,0029	0,0000	28,29
40	16,9	0,0123	0,0034	0,0000	39,83
50	19,8	0,0143	0,0039	0,0000	50,85
60	22,4	0,0162	0,0044	0,0000	62,08
70	24,9	0,0180	0,0048	0,0000	75,24
80	27,2	0,0197	0,0051	0,0000	83,50
90	28,8	0,0210	0,0050	0,0000	79,88

Power Law

c	n	r
0,00042	0,5683	0,9985

Quadratic Formula

A	B	r
1571	2915632	0,7364

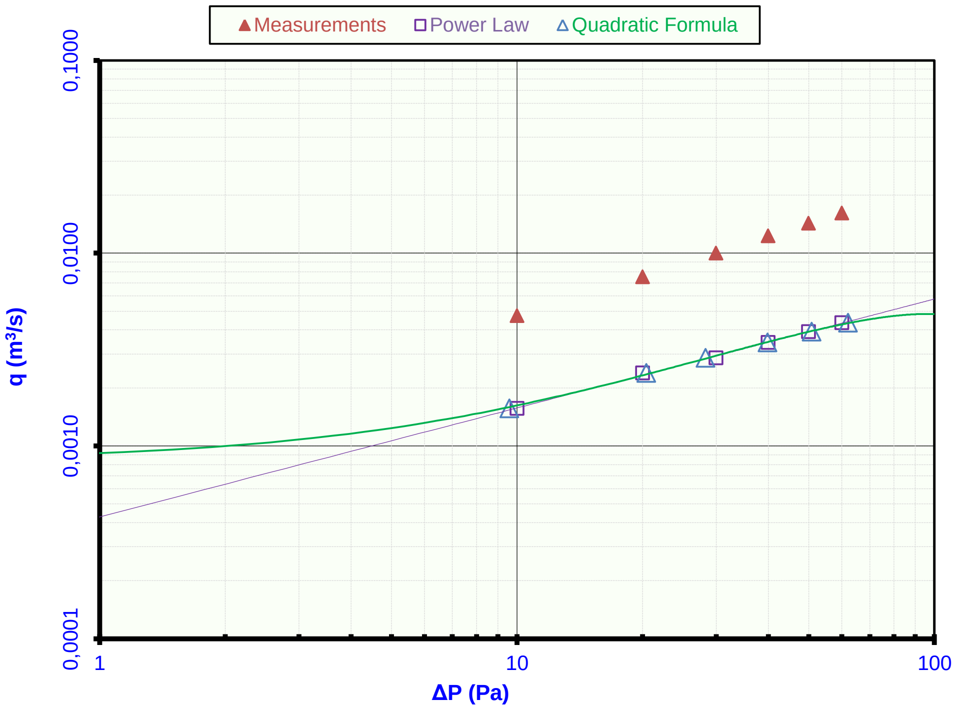

$A_{e;50}$ (m^2)	0,0004	**$u_{v;4}$ (m/s)**	1,62	**Re_4**	6446
ELA_4 (m^2)	0,0006	**$u_{v;50}$ (m/s)**	6,87	**Re_{50}**	27306

Measurement 2.32 6x 16 cm pipes, Ø 16 mm

ΔP_{Bias} (Pa)	0
ΔT_{int} (°C)	23,5
ΔT_e (°C)	22,8
Flange #	2 / 3
μ	0,00002
ρ	1,205

Openings geometrics

L (m)	0,160	**A (m^2)**	0,0007
w (m)	na	**Peri (m)**	0,038
d (m)	na	**P/A**	55,556
Ø (m)	0,012	**L/d_h**	2,222
d_h (m)	0,072		

ΔP_m (Pa)	v_r (m/s)	q_m (m^3/s)	q_{open} (m^3/s)	q_{open}^2 (m^3/s)	ΔP_{QF} (Pa)
10	6,4	0,0053	0,0021	0,0000	8,10
20	10,6	0,0081	0,0029	0,0000	18,05
30	14,5	0,0107	0,0035	0,0000	27,91
40	17,7	0,0128	0,0040	0,0000	36,70
50	20,8	0,0150	0,0046	0,0000	50,91
60	23,6	0,0170	0,0052	0,0000	66,53
70	6,0	0,0189	0,0057	0,0000	79,33
80	6,6	0,0204	0,0057	0,0000	80,39
90	7,3	0,0221	0,0061	0,0000	92,67
100	7,9	0,0236	0,0064	0,0000	101,13

Power Law

c	n	r
0,00066	0,4930	0,9954

Quadratic Formula

A	B	r
-2084	2831417	0,9943

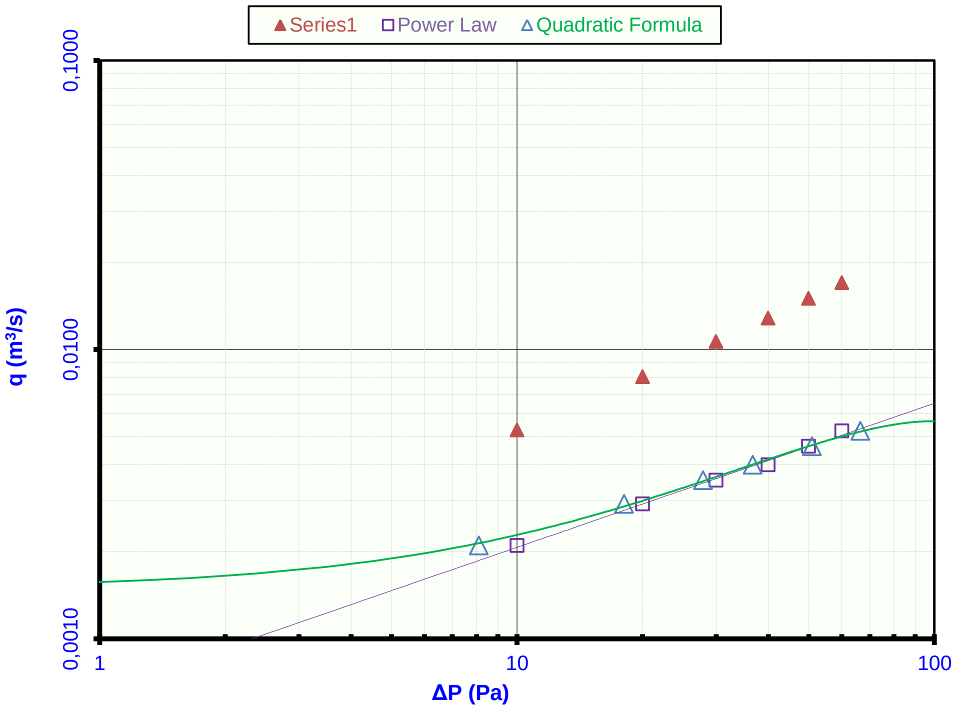

$A_{e;50}$ (m^2)	0,0005	**$u_{v;4}$ (m/s)**	1,94	**Re_4**	8401
ELA_4 (m^2)	0,0008	**$u_{v;50}$ (m/s)**	6,81	**Re_{50}**	29561

Measurement 2.33 6x 16 cm pipes, Ø 20 mm

ΔP_{Bias} (Pa)	0
ΔT_{int} (°C)	24,3
ΔT_e (°C)	23,8
Flange #	2 / 3
μ	0,00002
ρ	1,205

Openings geometrics

L (m)	0,160	**A (m^2)**	0,0012
w (m)	na	**Peri (m)**	0,050
d (m)	na	**P/A**	41,667
Ø (m)	0,016	**L/d_h**	1,667
d_h (m)	0,096		

ΔP_m (Pa)	v_r (m/s)	q_m (m^3/s)	q_{open} (m^3/s)	q_{open}^2 (m^3/s)	ΔP_{QF} (Pa)
10	8,9	0,0069	0,0038	0,0000	7,73
20	14,0	0,0103	0,0052	0,0000	17,60
30	18,9	0,0137	0,0065	0,0000	30,54
40	4,9	0,0161	0,0072	0,0001	38,33
50	6,0	0,0189	0,0085	0,0001	54,84
60	6,8	0,0209	0,0091	0,0001	63,64
70	7,6	0,0229	0,0097	0,0001	73,69
80	8,3	0,0246	0,0100	0,0001	78,32
90	9,0	0,0263	0,0103	0,0001	85,02
100	9,8	0,0283	0,0111	0,0001	98,93

Power Law

c	n	r
0,00128	0,4700	0,9948

Quadratic Formula

A	B	r
-1470	937879	0,9976

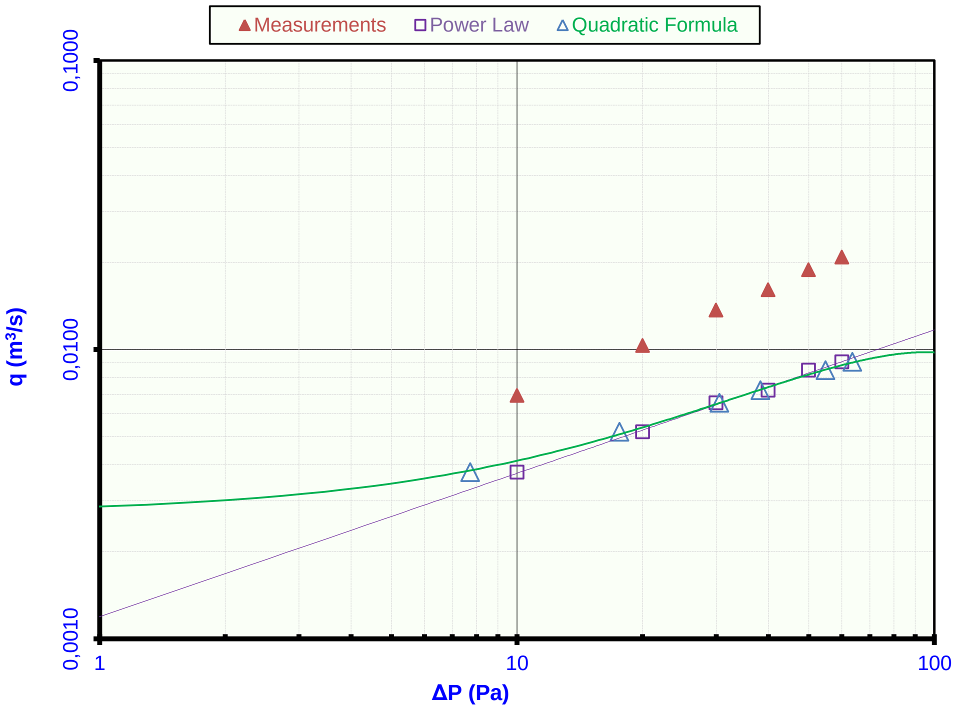

$A_{e;50}$ (m^2)	0,0009	**$u_{v;4}$ (m/s)**	2,04	**Re_4**	11776
ELA_4 (m^2)	0,0016	**$u_{v;50}$ (m/s)**	7,02	**Re_{50}**	40613

Measurement 2.34 — 6x 16 cm pipes, Ø 10 mm

perpendicular to exit pane

ΔP_{Bias} (Pa)	0
ΔT_{int} (°C)	24,3
ΔT_e (°C)	24,1
Flange #	2
μ	0,00002
ρ	1,205

Openings geometrics

L (m)	0,160	**A (m^2)**	0,0003
w (m)	na	**Peri (m)**	0,025
d (m)	na	**P/A**	83,333
Ø (m)	0,008	**L/d_h**	3,333
d_h (m)	0,048		

ΔP_m (Pa)	v_r (m/s)	q_m (m^3/s)	q_{open} (m^3/s)	q_{open}^2 (m^3/s)	ΔP_{QF} (Pa)
10	4,3	0,0039	0,0007	0,0000	11,65
20	7,9	0,0063	0,0011	0,0000	22,11
30	11,3	0,0085	0,0014	0,0000	29,24
40	14,3	0,0105	0,0017	0,0000	37,78
50	17,1	0,0124	0,0020	0,0000	50,31
60	19,6	0,0142	0,0024	0,0000	62,36
70	21,8	0,0157	0,0025	0,0000	70,17
80	24,1	0,0174	0,0028	0,0000	79,11
90	26,1	0,0189	0,0029	0,0000	85,34
100	28,2	0,0205	0,0033	0,0000	103,23

Power Law

c	n	r
0,00015	0,6676	0,9971

Quadratic Formula

A	B	r
13093	5695885	0,9987

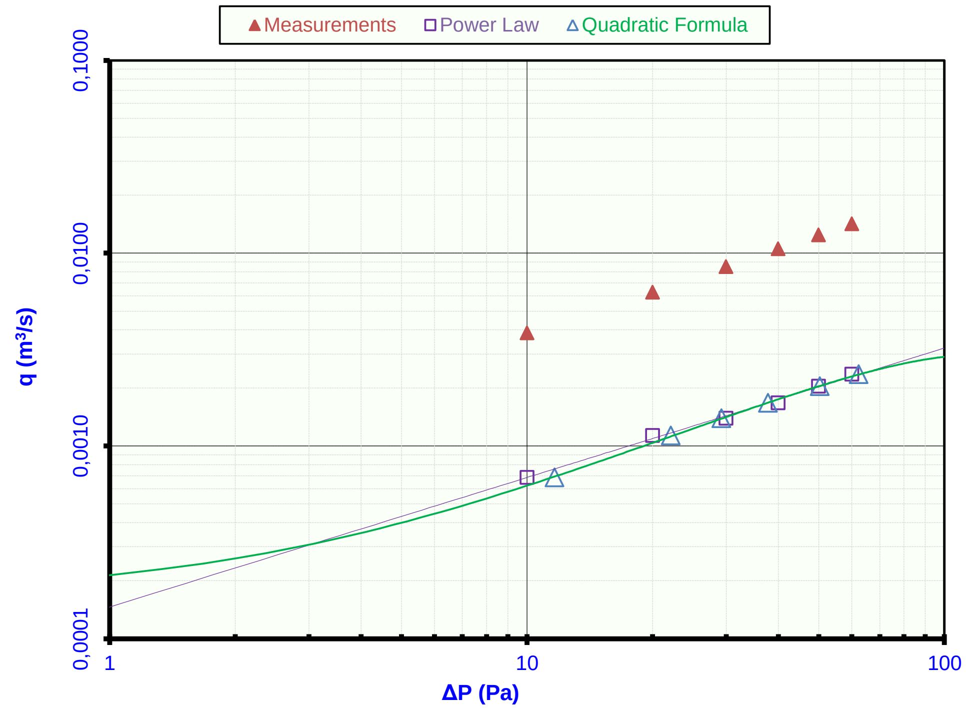

$A_{e;50}$ (m^2)	0,0002	$u_{v;4}$ (m/s)	1,22	Re_4	3542
ELA_4 (m^2)	0,0002	$u_{v;50}$ (m/s)	6,75	Re_{50}	19535

Technische Universiteit Delft

Royal HaskoningDHV

Measurement 2.35

6x 16 cm pipes, Ø 13 mm

perpendicular to exit pane

ΔP_{Bias} (Pa)	0
ΔT_{int} (°C)	24,2
ΔT_e (°C)	23,8
Flange #	2
μ	0,00002
ρ	1,205

Openings geometrics

L (m)	0,160	**A (m^2)**	0,0006
w (m)	na	**Peri (m)**	0,035
d (m)	na	**P/A**	60,606
Ø (m)	0,011	**L/d_h**	2,424
d_h (m)	0,066		

ΔP_m (Pa)	v_r (m/s)	q_m (m^3/s)	q_{open} (m^3/s)	q_{open}^2 (m^3/s)	ΔP_{QF} (Pa)
10	5,6	0,0047	0,0016	0,0000	10,16
20	9,9	0,0076	0,0025	0,0000	21,18
30	13,6	0,0100	0,0029	0,0000	28,48
40	16,9	0,0123	0,0034	0,0000	37,66
50	20,1	0,0145	0,0041	0,0000	52,03
60	22,7	0,0164	0,0046	0,0000	62,46
70	25,2	0,0182	0,0050	0,0000	74,56
80	27,6	0,0200	0,0054	0,0000	84,38

Power Law

c	n	r
0,00040	0,5936	0,9967

Quadratic Formula

A	B	r
2768	2383782	0,9937

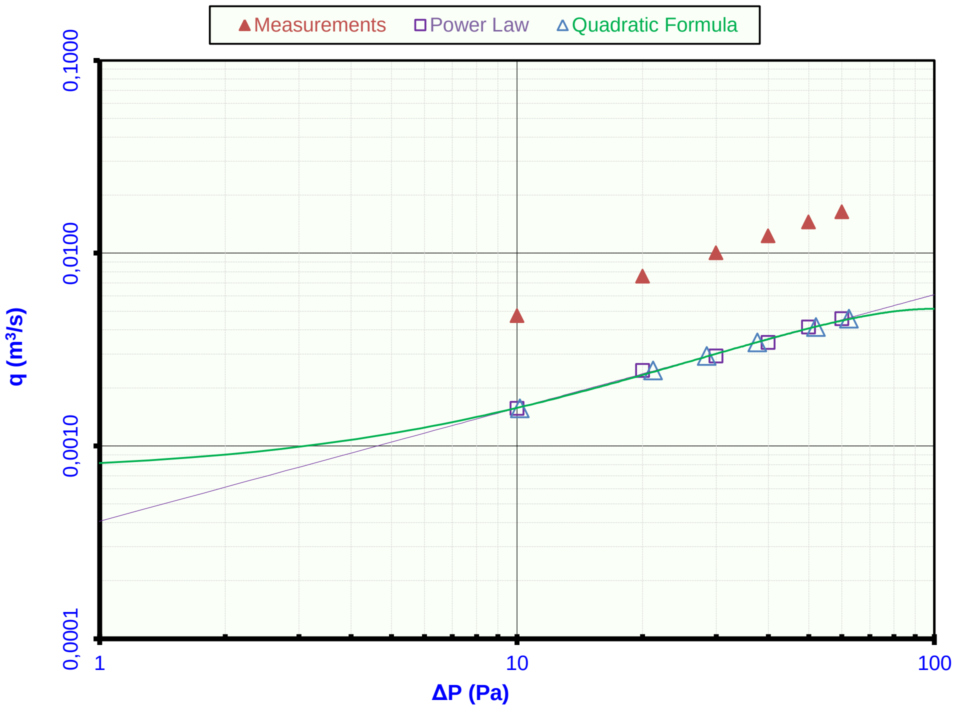

$A_{e;50}$ (m^2)	0,0004	**$u_{v;4}$ (m/s)**	1,58	**Re_4**	6286
ELA_4 (m^2)	0,0006	**$u_{v;50}$ (m/s)**	7,24	**Re_{50}**	28783

Measurement 2.36 — 6x 16 cm pipes, Ø 16 mm

perpendicular to exit pane

ΔP_{Bias} (Pa)	0
ΔT_{int} (°C)	23,5
ΔT_e (°C)	22,8
Flange #	2 / 3
μ	0,00002
ρ	1,205

Openings geometrics

L (m)	0,160	**A (m^2)**	0,0007
w (m)	na	**Peri (m)**	0,038
d (m)	na	**P/A**	55,556
Ø (m)	0,012	**L/d_h**	2,222
d_h (m)	0,072		

ΔP_m (Pa)	v_r (m/s)	q_m (m^3/s)	q_{open} (m^3/s)	q_{open}^2 (m^3/s)	ΔP_{QF} (Pa)
10	6,4	0,0053	0,0021	0,0000	9,82
20	10,6	0,0081	0,0029	0,0000	18,98
30	14,6	0,0107	0,0036	0,0000	28,79
40	18,1	0,0131	0,0043	0,0000	40,46
50	21,1	0,0152	0,0048	0,0000	52,09
60	23,8	0,0172	0,0054	0,0000	64,33
70	26,6	0,0193	0,0061	0,0000	82,84
80	6,7	0,0206	0,0060	0,0000	79,04
90	7,2	0,0219	0,0059	0,0000	76,17
100	8,0	0,0239	0,0066	0,0000	97,07

Power Law

c	n	r
0,00065	0,5042	0,9863

Quadratic Formula

A	B	r
7	2223898	0,9898

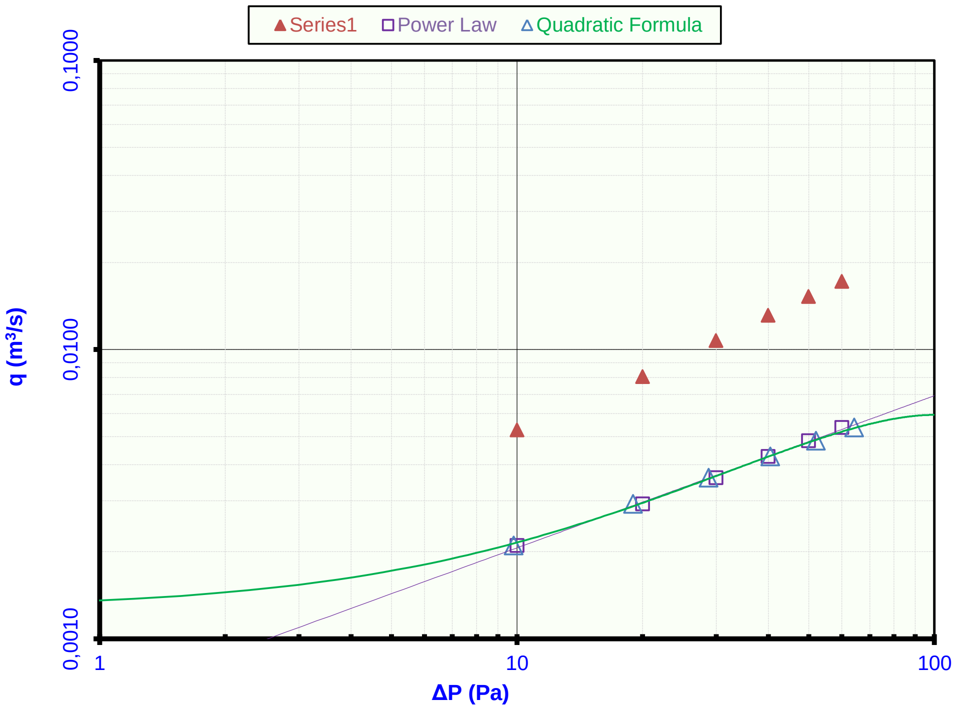

$A_{e;50}$ (m^2)	0,0005	**$u_{v;4}$ (m/s)**	1,94	**Re_4**	8400
ELA_4 (m^2)	0,0008	**$u_{v;50}$ (m/s)**	7,13	**Re_{50}**	30929

TU Delft — Technische Universiteit Delft

Royal HaskoningDHV

Measurement 2.37

6x 16 cm pipes, Ø 20 mm

perpendicular to exit pane

ΔP_{Bias} (Pa)	0
ΔT_{int} (°C)	24,3
ΔT_e (°C)	23,8
Flange #	2 / 3
μ	0,00002
ρ	1,205

Openings geometrics

L (m)	0,160	**A (m^2)**	0,0012
w (m)	na	**Peri (m)**	0,050
d (m)	na	**P/A**	41,667
Ø (m)	0,016	**L/d_h**	1,667
d_h (m)	0,096		

ΔP_m (Pa)	v_r (m/s)	q_m (m^3/s)	q_{open} (m^3/s)	q_{open}^2 (m^3/s)	ΔP_{QF} (Pa)
10	8,8	0,0069	0,0037	0,0000	7,62
20	14,1	0,0104	0,0053	0,0000	18,42
30	18,8	0,0136	0,0065	0,0000	30,04
40	22,6	0,0163	0,0075	0,0001	41,38
50	5,9	0,0186	0,0082	0,0001	51,43
60	6,8	0,0209	0,0091	0,0001	63,73
70	7,5	0,0226	0,0094	0,0001	69,65
80	8,3	0,0246	0,0100	0,0001	78,32
90	9,1	0,0266	0,0106	0,0001	89,47
100	9,8	0,0283	0,0111	0,0001	98,80

Power Law

c	n	r
0,00126	0,4738	0,9974

Quadratic Formula

A	B	r
-1362	927125	0,9992

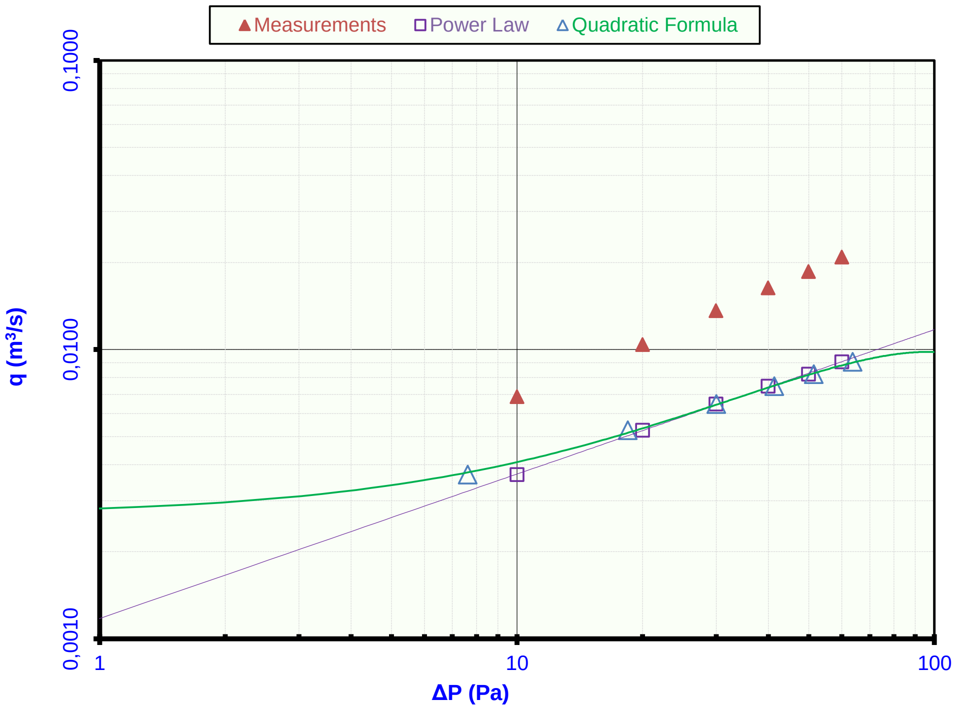

$A_{e;50}$ (m^2)	0,0009	**$u_{v;4}$ (m/s)**	2,01	**Re_4**	11646
ELA_4 (m^2)	0,0015	**$u_{v;50}$ (m/s)**	6,81	**Re_{50}**	39405

B. Calibration certificates

1. Measuring flanges

The flanges are used to reduce the section of the tube and thus increase the velocity of the air inside the tube, at equal pressure difference. The air flow volume through the flanges is calibrated for the air velocity at the centre of each flange. It is proven that there is an exponential relationship for the known surface area of each flanges cross-section as coefficient, and an exponent over the air velocity that is mathematically determined:

$$q_v = A \cdot v^c$$

Where:

q_v	air flow volume	m^3/s
A	open area of flange	m^2
v	air velocity	m/s
c	exponent	-

Table 17 - Cross sections and exponents calibrated flanges

Flange	A (m^2)	Exponent
1	0,07296	1,147
2	0,01557	0,92915
3	0,003526	0,92616
4	0,0009295	0,92153
5	0,00012829	1

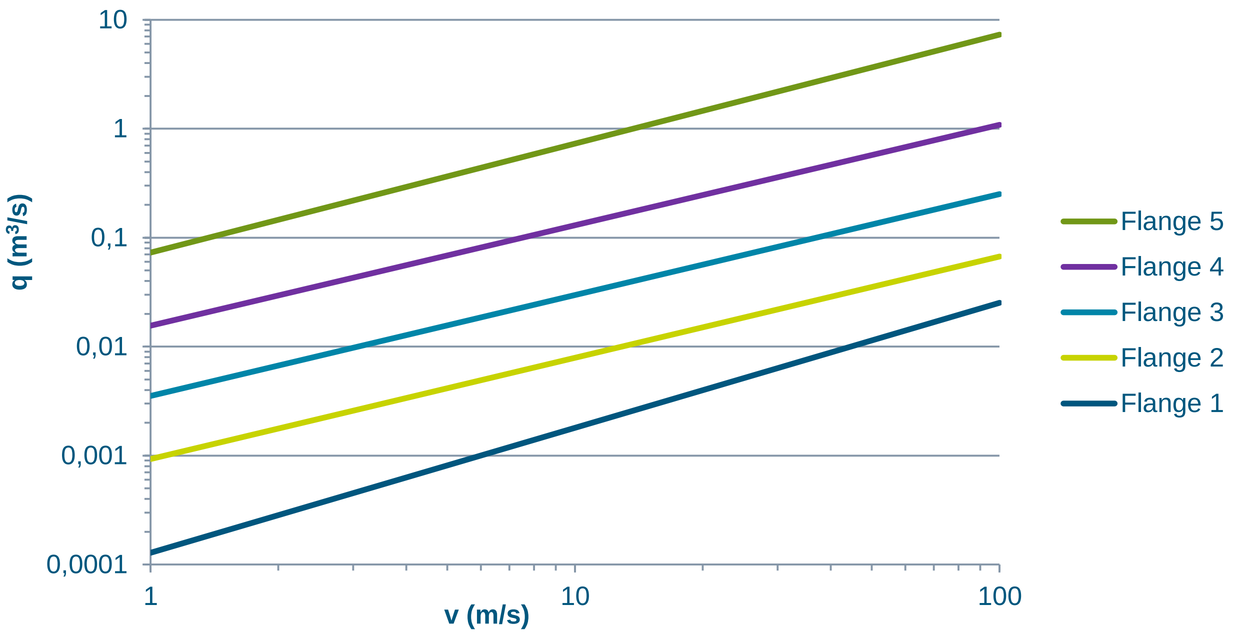

Figure A. 1 - Calibration Flanges

2. Digital micro fan-wheel anemometer

Brand Thies Clima
Serial number 0101121

CERTIFICATE OF CALIBRATION

Dutch Metrology Institute

Applicant	Meetbureau Bijleveld Harmenkokslaan 60 2611 TS DELFT The Netherlands
Submitted	An anemometer Manufacturer : Thies Clima Type : 4.3405.20.002 Working principle: Vane anemometer Serial number : 0902122 Identification : Ø 15 mm
Calibration method	The error of the anemometer is determined by comparison with the primary standard for air velocity measurement. The calibration is carried out with air under atmospheric pressure, at an ambient temperature of (20 ± 0.5) °C and a relative humidity of (45 ± 5) %. During calibration, the arrow on the anemometer was pointing downstream.
Date of calibration	1 October 2015
Result	The results of the calibration are shown on page 2 of this certificate. The reported uncertainty of measurement is based on the standard uncertainty multiplied by a coverage factor $k = 2$, which for a normal distribution corresponds to a coverage probability of approximately 95 %. The standard uncertainty of measurement has been determined in accordance with the GUM 'Evaluation of measurement data - Guide to the expression of uncertainty in measurement'.
Traceability	The results of the calibration services of VSL are traceable to primary and/or (inter)nationally accepted measurement standards.

Delft, 1 October 2015
VSL B.V.

S.K. Hagendoorn BSc
Senior Metrologist

VSL
Dutch Metrology Institute

VSL B.V.
Thijsseweg 11, 2629 JA Delft (NL)
P.O. Box 654, 2600 AR Delft (NL)
T +31 15 269 15 00
F +31 15 261 29 71
I www.vsl.nl

CERTIFICATE OF CALIBRATION

Instrument	Manufacturer	: Thies Clima
	Serial number	: 0902122
	Identification	: Ø 15 mm
	Type	: 4.3405.20.002
	Tested range	: 1 - 25 m/s

Results

Indicated velocity (averaged) (m/s)	Reference velocity (m/s)	Error (%)	Uncertainty (%)
25.13	24.47	2.7	2.1
20.03	19.18	4.5	2.2
14.97	14.34	4.3	2.3
10.07	9.73	3.5	2.6
5.00	5.26	-5.0	2.9
1.00	1.67	-40	10

The stated uncertainty is the uncertainty in the determination of the error. The uncertainty in the determination of the reference velocity does not exceed 2 % at a reference velocity equal or above 1 m/s and does not exceed 0.05 m/s at reference velocities below 1 m/s.

The error is determined by:

$$\text{Error} = \frac{\text{Indicated velocity} - \text{Reference velocity}}{\text{Reference velocity}} \times 100\ \%$$

VSL
Dutch Metrology Institute

CERTIFICATE OF CALIBRATION

VSL is het Nationaal Metrologisch Instituut (NMI) van Nederland en levert in die hoedanigheid herleidbaarheid van meetresultaten naar internationaal geaccepteerde meetstandaarden. Het bestaan van een gezamenlijk vertrouwen in juiste productspecificaties en productcontrole is van fundamenteel belang om aan internationale, geharmoniseerde wetgeving op het gebied van handel, kwaliteit, gezondheid, veiligheid en milieu te kunnen voldoen. Gestandaardiseerde en gelijkwaardige metingen die herleidbaar zijn naar internationaal geaccepteerde standaarden zijn hierbij essentieel.

Dit certificaat is in overeenstemming met de kalibratie- en meetmogelijkheden (CMC's) die opgenomen zijn in Appendix C van de wederzijdse erkenningsovereenkomst (MRA), opgesteld door het Internationaal Comité voor Maten en Gewichten (CIPM). In het kader van de MRA, erkennen alle deelnemende instituten de geldigheid van elkaars kalibratie- en meetcertificaten voor de grootheden, bereiken en meetonzekerheden zoals gespecificeerd in Appendix C (details op http://www.bipm.org).

VSL is geaccrediteerd door de RvA (Raad voor Accreditatie) voor kalibraties tegen de vereisten vastgelegd in de ISO/IEC 17025 (accreditatiescope K999), voor het organiseren van interlaboratoriumonderzoeken tegen de vereisten vastgelegd in de ISO/IEC 17043 (accreditatiescope R006) en voor het produceren van referentiematerialen tegen de vereisten vastgelegd in ISO Guide 34 alsmede tegen de relevante vereisten vastgelegd in de ISO/IEC 17025 (accreditatiescope P002). De accreditaties verzekeren dat aan alle eisen van de betrokken norm(en) is voldaan en dat er op regelmatige basis audits plaatsvinden.

CIPM MRA

CALIBRATION
RvA K 999

PROF. TESTING
RvA R 006

Reference Mat.
RvA P 002

VSL is the National Metrology Institute (NMI) of the Netherlands. As such, it provides direct traceability of measurement results to internationally accepted measurement standards. The existence of mutual confidence in product specifications and product control is of fundamental importance in order to fulfill international, harmonized legislation on trade, quality, health, safety and environment. In this respect, standardized and equivalent measurement units and traceability to internationally accepted standards are essential.

This certificate is consistent with the calibration and measurement capabilities (CMCs) that are included in Appendix C of the Mutual Recognition Arrangement (MRA) drawn up by the International Committee for Weights and Measures (CIPM). Under the MRA, all participating institutes recognize the validity of each other's calibration and measurement certificates for the quantities, ranges and measurement uncertainties specified in Appendix C (for details see http://www.bipm.org).

VSL is accredited by the RvA (Dutch Accreditation Council) for calibrations against the requirements as laid down in ISO/IEC 17025 (accreditation scope K999), for organizing proficiency tests against the requirements as laid down in ISO/IEC 17043 (accreditation scope R006) and for producing reference materials against the requirements as laid down in ISO Guide 34 and the relevant requirements of the ISO/IEC 17025 (accreditations scope P002). The accreditations ensure that all requirements of the standard(s) involved are met and that audits conducted are on a regular basis.

3. Inclined well-type manometer

Brand Airflow
Type 5
Serial number 99905

KALIBRATIECERTIFICAAT

Aanvrager	Meetbureau Bijleveld Harmenkokslaan 60 2611 TS DELFT Nederland
Aangeboden	Schuinebuis manometer voor overdruk Fabrikant : Airflow Type : 5 Serienummer : 99905
Wijze van onderzoek	De schuinebuis manometer voor overdruk is met behulp van referentiemanometer voor verschildruk met droge lucht als medium op 8 punten gekalibreerd, hierbij is een cyclus van toenemende en afnemende drukken doorlopen. De manometer is in horizontale positie gekalibreerd, als referentieniveau is de drukaansluiting aangehouden. Voorafgaand aan de kalibratie is het nulpunt van de manometer ingesteld. Tijdens de kalibratie bevond de schuinebuis zich in de onderste positie. De schuinebuismanometer is gejusteerd,de 'as found' waarden zijn weergegeven op blad 2, de 'as left'waarden zijn weergegeven op blad 4. De manometer is afgelezen door aan de onderkant van de meniscus te nemen als referentie, zie blad 4. De metingen zijn verricht bij een omgevingstemperatuur van (20,0 ± 0,5) °C en een relatieve luchtvochtigheid van (50 ± 5) %.
Datum van onderzoek	4 december 2015 tot en met 7 december 2015
Resultaat	De meetresultaten zijn weergegeven op blad 2 van dit certificaat. De gerapporteerde meetonzekerheid is de standaardonzekerheid vermenigvuldigd met een dekkingsfactor $k = 2$, welke voor een normale verdeling overeenkomt met een dekkingswaarschijnlijkheid van ongeveer 95 %. De standaardonzekerheid is bepaald overeenkomstig de GUM 'Evaluation of measurement data - Guide to the expression of uncertainty in measurement'.
Herleidbaarheid	De resultaten van de uitgevoerde kalibraties zijn herleidbaar naar primaire en/of (inter)nationaal erkende meetstandaarden.

Delft, 9 december 2015
VSL B.V.

J.L.W.A. van Geel
Allround metroloog

VSL B.V.
Thijsseweg 11, 2629 JA Delft (NL)
Postbus 654, 2600 AR Delft (NL)
T 015 269 15 00
F 015 261 29 71
I www.vsl.nl

KALIBRATIECERTIFICAAT

Resultaat
Hieronder wordt het as found resultaat van de kalibratie, de bijbehorende onzekerheid en de afwijking weergegeven.

Instrument
Schuinebuismanometer

Schaaldeel	:	0,5 Pa
Bereik	:	(-10 ÷ 125) Pa d
Gekalibreerd bereik	:	(0 ÷ 60) Pa d
Omgevingsdruk	:	(1024,7 ± 0,5) hPa a

	Instrument as found						
Aangeboden waarde	Afgelezen waarde	Berekende waarde	Onzekerheid in de gemeten waarde	Verschil			Hysterese
Pa d	kPa d	Pa d	Pa	Pa	% R.	% F.S.	% F.S.
0,0	0,0	0,0	1,0	0,0	-	0,00	0,00
5,1	0,1	5,0	1,0	-0,1	-2,76	-0,11	-0,16
15,3	0,3	15,0	1,0	-0,3	-2,25	-0,28	-0,16
26,0	0,5	25,0	1,0	-0,9	-3,66	-0,76	-0,56
36,2	0,7	35,0	1,0	-1,2	-3,19	-0,92	-0,16
46,7	0,9	45,0	1,0	-1,7	-3,56	-1,33	-0,40
52,2	1,0	50,0	1,0	-2,2	-4,14	-1,73	-0,32
63,0	1,2	60,0	1,0	-3,0	-4,71	-2,37	-
51,8	1,0	50,0	1,0	-1,8	-3,40	-1,41	-
46,2	0,9	45,0	1,0	-1,2	-2,51	-0,93	-
36,0	0,7	35,0	1,0	-1,0	-2,65	-0,76	-
25,2	0,5	25,0	1,0	-0,3	-0,99	-0,20	-
15,1	0,3	15,0	1,0	-0,1	-0,96	-0,12	-
4,9	0,1	5,0	1,0	0,1	1,19	0,05	-
0,0	0,0	0,0	1,0	0,0	-	0,00	-
Absolute maximale waarde voor verschil en hysterese:				3,0	4,71	2,37	0,56

Opmerkingen
Het verschil (Pa) = Gemeten waarde – Aangeboden waarde.
Het verschil (%R.) = (verschil / Aangeboden waarde) × 100 %.
Het verschil (%F.S.) is gebaseerd op F.S. 125 Pa d.
De berekende waarde is de afgelezen waarde × 50.

De onzekerheid van de aangeboden waarde is opgenomen in de onzekerheid van de gemeten waarde.

KALIBRATIECERTIFICAAT

Resultaat

Hieronder wordt het as left resultaat van de kalibratie, de bijbehorende onzekerheid en de afwijking weergegeven.

Instrument

Schuinebuis manometer voor overdruk

Schaaldeel	:	0,5 Pa
Bereik	:	(-10 ÷ 125) Pa g
Gekalibreerd bereik	:	(0 ÷ 60) Pa g
Omgevingsdruk	:	(1028,1 ± 0,5) hPa a

	Instrument as left						
Aangeboden waarde	Afgelezen waarde	Berekende waarde	Onzekerheid in de gemeten waarde	Verschil			Hysterese
Pa d	Pa d	Pa d	Pa	Pa	% R.	% F.S.	% F.S.
0,0	0,0	0,0	0,7	0,0	-	0,00	0,00
5,0	0,1	5,0	0,7	0,0	0,00	0,00	0,00
15,0	0,3	15,0	0,7	0,0	0,00	0,00	0,00
25,0	0,5	25,0	0,7	0,0	0,00	0,00	0,00
35,0	0,7	35,0	0,7	0,0	0,00	0,00	0,00
45,0	0,9	45,0	0,7	0,0	0,00	0,00	0,00
50,1	1,0	50,0	0,7	-0,1	-0,20	-0,08	-0,08
60,1	1,2	60,0	0,7	-0,1	-0,17	-0,08	-
50,0	1,0	50,0	0,7	0,0	0,00	0,00	-
45,0	0,9	45,0	0,7	0,0	0,00	0,00	-
35,0	0,7	35,0	0,7	0,0	0,00	0,00	-
25,0	0,5	25,0	0,7	0,0	0,00	0,00	-
15,0	0,3	15,0	0,7	0,0	0,00	0,00	-
5,0	0,1	5,0	0,7	0,0	0,00	0,00	-
0,0	0,0	0,0	0,7	0,0	-	0,00	-
Absolute maximale waarde voor verschil en hysterese:				0,1	0,20	0,08	0,08

Opmerkingen

Het verschil (Pa) = Gemeten waarde – Aangeboden waarde.
Het verschil (%R.) = (verschil / Aangeboden waarde) × 100 %.
Het verschil (%F.S.) is gebaseerd op F.S. 125 Pa g.

De onzekerheid van de aangeboden waarde is opgenomen in de onzekerheid van de gemeten waarde.

KALIBRATIECERTIFICAAT

Extra opmerkingen

De metingen zijn uitgevoerd bij een omgevingstemperatuur van (20,0 ± 0,5) °C en een zwaarteveldsterkte g = (9,812 ± 0,000 1) N/kg.

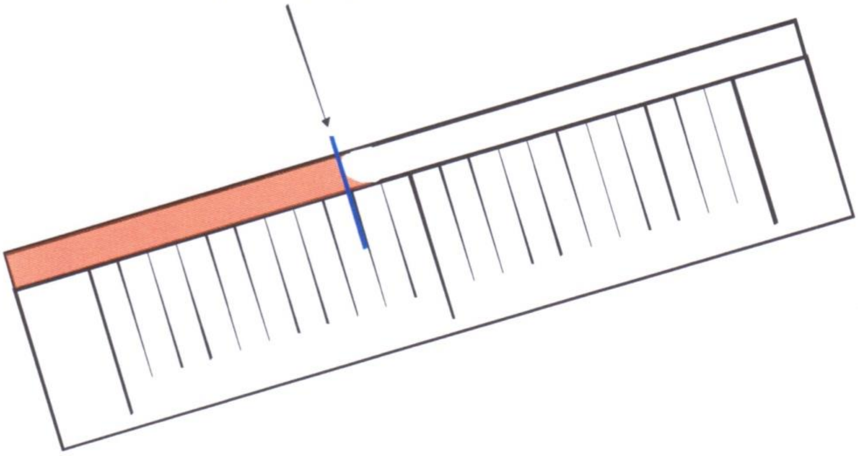

VSL is het Nationaal Metrologisch Instituut (NMI) van Nederland en levert in die hoedanigheid herleidbaarheid van meetresultaten naar internationaal geaccepteerde meetstandaarden. Het bestaan van een gezamenlijk vertrouwen in juiste productspecificaties en productcontrole is van fundamenteel belang om aan internationale, geharmoniseerde wetgeving op het gebied van handel, kwaliteit, gezondheid, veiligheid en milieu te kunnen voldoen. Gestandaardiseerde en gelijkwaardige metingen die herleidbaar zijn naar internationaal geaccepteerde standaarden zijn hierbij essentieel.

Dit certificaat is in overeenstemming met de kalibratie- en meetmogelijkheden (CMC's) die opgenomen zijn in Appendix C van de wederzijdse erkenningsovereenkomst (MRA), opgesteld door het Internationaal Comité voor Maten en Gewichten (CIPM). In het kader van de MRA, erkennen alle deelnemende instituten de geldigheid van elkaars kalibratie- en meetcertificaten voor de grootheden, bereiken en meetonzekerheden zoals gespecificeerd in Appendix C (details op http://www.bipm.org).

VSL is geaccrediteerd door de RvA (Raad voor Accreditatie) voor kalibraties tegen de vereisten vastgelegd in de ISO/IEC 17025 (accreditatiescope K999), voor het organiseren van interlaboratoriumonderzoeken tegen de vereisten vastgelegd in de ISO/IEC 17043 (accreditatiescope R006) en voor het produceren van referentiematerialen tegen de vereisten vastgelegd in ISO Guide 34 alsmede tegen de relevante vereisten vastgelegd in de ISO/IEC 17025 (accreditatiescope P002). De accreditaties verzekeren dat aan alle eisen van de betrokken norm(en) is voldaan en dat er op regelmatige basis audits plaatsvinden.

CIPM MRA

KALIBRATIE RvA K 999

PROF. TESTING RvA R 006

Referentie Mat. RvA P 002

VSL is the National Metrology Institute (NMI) of the Netherlands. As such, it provides direct traceability of measurement results to internationally accepted measurement standards. The existence of mutual confidence in product specifications and product control is of fundamental importance in order to fulfill international, harmonized legislation on trade, quality, health, safety and environment. In this respect, standardized and equivalent measurement units and traceability to internationally accepted standards are essential.

This certificate is consistent with the calibration and measurement capabilities (CMCs) that are included in Appendix C of the Mutual Recognition Arrangement (MRA) drawn up by the International Committee for Weights and Measures (CIPM). Under the MRA, all participating institutes recognize the validity of each other's calibration and measurement certificates for the quantities, ranges and measurement uncertainties specified in Appendix C (for details see http://www.bipm.org).

VSL is accredited by the RvA (Dutch Accreditation Council) for calibrations against the requirements as laid down in ISO/IEC 17025 (accreditation scope K999), for organizing proficiency tests against the requirements as laid down in ISO/IEC 17043 (accreditation scope R006) and for producing reference materials against the requirements as laid down in ISO Guide 34 and the relevant requirements of the ISO/IEC 17025 (accreditations scope P002). The accreditations ensure that all requirements of the standard(s) involved are met and that audits conducted are on a regular basis.

4. Field calibration check

Conform NEN-EN 15004-1, section E.2.7.5
Performed by MbB

FIELD CALIBRATION CHECK

Doel van het onderzoek

Beoordeling van de nauwkeurigheid van de luchtdoorlatendheidstestmethode overeenkomstig paragraaf E.2.7.5 van NEN-EN 15004-1.

Algemene gegevens

Datum onderzoek: 14 juni 2013
Datum rapport : 18 juni 2013

De opzet

De luchtdoorlatendheid van de ruimte is tweemaal gemeten, eenmaal zonder extra lekoppervlak en eenmaal met toevoeging van een rond lekoppervlak van 322,58 cm^2 (50 $inch^2$) in een vlakke plaat. Het statisch drukverschil was -0,5 Pa.

Testresultaat

Het equivalente lekoppervlak (ELA) van de ruimte bij een drukverschil van 10 Pa is 1.121,29 cm^2 en het equivalent lekoppervlak van de ruimte onder toevoeging van 322,58 cm^2 extra lekoppervlak is, bij een drukverschil van 10 Pa, 1.438,51 cm^2. Het equivalent lekoppervlak neemt dus toe met 317,22 cm^2. Het verschil tussen het toegevoegde oppervlak en de berekende toename van het equivalent lekoppervlak is -5,36 cm^2. Dit betekent een afwijking van -1,66 % ten opzichte van het toegevoegde lekoppervlak.

Conclusie

De nauwkeurigheid van de testmethode is **voldoende** hoog om aan de eis van NEN-EN 15004-1, paragraaf E.2.7.5.6 te voldoen. In NEN-EN 15004-1, paragraaf E.2.7.5.6 wordt een nauwkeurigheid geëist van ±15%.

Gebruikte meetinstrumenten

Anemometer: Thies Clima type 4.3405.20.002, serienummer: 0902122
Schuinebuismanometer: Airflow type 5, serienummer: 99905

Rapporteur

Ir. J.H. Bijleveld

MEETBUREAU Bijleveld